



# Durham E-Theses

---

## *Biochemical studies on plant glycerol-3- phosphate acyltransferase*

Hayman, Matthew William

### How to cite:

---

Hayman, Matthew William (2003) *Biochemical studies on plant glycerol-3- phosphate acyltransferase*, Durham theses, Durham University. Available at Durham E-Theses Online: <http://etheses.dur.ac.uk/4056/>

### Use policy

---

The full-text may be used and/or reproduced, and given to third parties in any format or medium, without prior permission or charge, for personal research or study, educational, or not-for-profit purposes provided that:

- a full bibliographic reference is made to the original source
- a [link](#) is made to the metadata record in Durham E-Theses
- the full-text is not changed in any way

The full-text must not be sold in any format or medium without the formal permission of the copyright holders.

Please consult the [full Durham E-Theses policy](#) for further details.

# **Biochemical studies on plant glycerol-3-phosphate acyltransferase**

**Matthew William Hayman**

**PhD Thesis**

**Department of Biological Sciences**

**University of Durham**



**2003**

**18 JUN 2003**

The copyright of this thesis rests with the author.  
No quotation from it should be published without  
his prior written consent and information derived  
from it should be acknowledged.

Thesis

2003/

HAY

# Biochemical studies on plant Glycerol-3-phosphate acyltransferase

Matthew William Hayman

*sn*-Glycerol-3-phosphate acyltransferase [G3PAT, *PlsB* (*E.coli*), EC 2.3.1.15] is an enzyme involved in glycerolipid biosynthesis, catalysing the acylation of glycerol-3-phosphate (G3P) to produce lysophosphatidic acid (LPA). Chilling tolerance in plants is linked to the acyl-group composition of membranes, which is linked to acyltransferases with a higher selectivity for unsaturated acyl-substrates. Plant soluble G3PAT is located in the chloroplast and uses acyl-acyl carrier protein (acyl-ACP) as substrate. Soluble G3PAT exhibits strong substrate selectivity for acyl-ACP, the plastidial substrate *in vivo*, over acyl-CoA. cDNAs encoding soluble G3PATs have previously been cloned from several plant species and both oleate-selective and non-selective forms identified. The purpose of this thesis is to study the mechanism of plastidial G3PAT and attempt to identify factors important in determining substrate selectivity.

An *in vitro* assay has been optimised to distinguish selective and non-selective enzyme forms under physiologically relevant conditions. The assay has been adapted to determine enzyme activity with a range of acyl-ACP and acyl-CoA substrates and to measure the kinetic constants  $K_m$  and  $V_{max}$ . Kinetic measurements have been made on a G3PAT protein from the chilling sensitive plant squash (*Cucurbita moschata*) and the L261F mutant protein containing a single amino acid substitution that significantly alters substrate selectivity. The mutation was found to increase selectivity by raising  $K_m$  for unsaturated acyl-substrate.

Mutant squash G3PAT proteins have been investigated to determine the importance of particular regions or amino acid residues. The mutations E142A, K193S, R235S and R237S resulted in enzymes that were completely inactive. The mutations H194S and L261F altered catalytic or substrate binding characteristics without enzyme inactivation. The catalytic mechanism and order of substrate binding for squash G3PAT have been determined, the reaction was found to proceed via a compulsory-ordered ternary complex with acyl-ACP binding before glycerol-3-phosphate.

# Acknowledgements

I would like to thank my PhD supervisors Dr. Tony Fawcett and Professor Antoni Slabas for their direction, support and encouragement throughout the past four years. I am also very grateful to Bill Simon for continual technical guidance, support and advice. Thanks must also go to John Gilroy for providing an inexhaustible supply of precious protein for me to throw down the sink/on the floor. I also wish to thank my laboratory colleagues for making my time in Durham an enjoyable and rewarding one, particularly Johan 'Krooner' Kroon, Clare Young, Adrian 'Wizard' Brown, Dan 'Protalein' Maltman and John 'Hallo' Hall.

Last, but certainly not least, I would like to say a huge thank you to my family, who have provided me with unconditional support and encouragement and been there for me every step of the way. Thank you.

# Contents

<b>Contents</b>	<b>1</b>
<b>Tables and Figures</b>	<b>4</b>
<b>Declaration</b>	<b>6</b>
<b>Statement of Copyright</b>	<b>7</b>
<b>Publications</b>	<b>8</b>
<b>Abbreviations</b>	<b>9</b>
<b>Chapter 1 Introduction</b>	<b>11</b>
1.1 General Introduction	12
1.2 Lipids	13
1.3 Fatty acid biosynthesis	20
1.3.1 Acetyl-CoA Carboxylase (ACCase)	20
1.3.2 The reactions of fatty acid synthesis	22
1.3.3 Acyl carrier protein (ACP)	24
1.3.4 Fatty Acid Synthase (FAS)	28
1.3.5 The Kennedy pathway	28
1.3.6 Oil body formation	29
1.3.7 Prokaryotic and Eukaryotic pathways	31
1.4 Chilling sensitivity in plants	36
1.4.1 Membrane phosphatidylglycerol (PG) acyl-group composition - thioesterases and acyltransferases	36
1.4.2 Desaturases	37
1.4.3 Other factors affecting plant chilling sensitivity	39
1.5 Glycerol-3-phosphate acyltransferases in plants	40
1.5.1 Mitochondrial G3PAT	40
1.5.2 Microsomal G3PAT	41
1.5.3 Plastidial G3PAT	41
1.6 Aims and objectives of Thesis	42
<b>Chapter 2 Materials and Methods</b>	<b>44</b>
2.1 Materials	45
2.2 Production and purification of recombinant Acyl-ACP Synthetase (AAS)	46
2.2.1 Growth of the Acyl-ACP synthetase	46
2.2.2 Preparation of membranes containing AAS activity	47
2.2.3 Purification of Acyl-ACP Synthetase using Blue-Sepharose chromatography	47
2.3 Assay of Acyl-ACP Synthetase activity	49
2.3.1 Low volume assay (for Blue-Sepharose column fractions)	49
2.3.2 Large volume assay (for acyl-ACP synthesis mixture)	50
2.4 Synthesis and isolation of radiolabelled acyl-ACP substrates	51
2.4.1 Acyl-ACP synthesis	51
2.4.2 Isolation of acyl-ACP substrates using ion-exchange and hydrophobic interaction chromatography	52
2.5 Production and purification of recombinant G3PAT proteins	53
2.5.1 Production of squash G3PAT	53
2.5.2 Preparation of crude cell-free protein extracts (CFEs) of squash G3PAT	53

2.5.3 Preparation of purified G3PAT	55
2.6 SDS PAGE	58
2.6.1 12% SDS PAGE electrophoresis	58
2.6.2 18% Urea gel electrophoresis	58
2.7 Quantification of G3PAT in crude cell-free and purified protein extracts via densitometric scanning	59
2.8 Standard lysophosphatidic acid (LPA) extraction and quantification from reaction mixtures	60
2.9 Assay for G3PAT activity	61
2.9.1 Reaction mixtures	61
2.9.2 Substrate quality	61
2.9.3 Reaction initiation	62
2.10 Assay for G3PAT selectivity	62
2.11 G3PAT assay using short chain substrates	64
2.12 Assay to determine binding of acyl-ACP and G3P substrates to G3PAT	64
2.13 Microdialysis of BSA/acyl-ACP mixtures	65
2.14 Measurement of standard error values	66
<b>Chapter 3 Development of an assay for G3PAT activity</b>	<b>67</b>
3.1 Introduction	68
3.2 Standard assays for G3PAT activity and selectivity	78
3.3 Effect of a range of BSA concentrations on the dual substrate G3PAT assay	81
3.4 Assessment of differential BSA-binding of 18:1-ACP and 16:0-ACP substrates under competitive conditions	83
3.5 Investigation of the effects of 2,6-dimethyl $\beta$ -cyclodextrin, lysozyme and cytochrome C on the dual substrate G3PAT assay	85
3.6 Investigation of substrate selectivity under a range of conditions using G3PAT from squash and Arabidopsis	92
3.7 Investigation of the range of acceptable acyl-CoA and acyl-ACP for the G3PAT reaction	94
3.8 Squash G3PAT uses 12-Azido oleoyl-ACP and 12-Azido oleoyl-CoA as substrates	95
<b>Chapter 4 Substrate binding, activity and selectivity assays of G3PAT mutants</b>	<b>102</b>
4.1 Introduction	103
4.2 Site-directed mutagenesis and the study of acyltransferases	105
4.3 Functional regions/motifs in plant plastidial G3PAT proteins	108
4.4 Analysis of mutant G3PAT proteins - G3P binding pocket	116
4.5 Analysis of mutant G3PAT proteins - can a single residue substitution in the H(X) <sub>4</sub> D box result in alteration of substrate selectivity?	119
4.6 Analysis of mutant G3PAT proteins - acyl-ACP binding pocket	121
4.7 Discussion	124
<b>Chapter 5 Kinetic analysis of wild type and mutant G3PAT proteins</b>	<b>127</b>
5.1 Introduction	128
5.2 Cloning of selective and non-selective G3PAT enzymes and creation of the L261F mutant	133
5.3 Preparation and assay of wild type and mutant recombinant squash G3PATs produced in <i>E. coli</i>	135
5.4 Creation of oil palm G3PAT mutant L352F and determination of its substrate	137

selectivity	
5.5 Determination of kinetic constants for Q24a and Q24a L261F	140
5.6 G3PAT product-inhibition assays	143
5.7 Determination of G3PAT reaction mechanism and binding order	146
5.8 Substrate binding studies on squash G3PAT	151
5.9 Discussion	154
<b>Chapter 6 General Discussion</b>	<b>159</b>
6.1 Discussion	160
6.2 Future work	166
<b>Appendices</b>	<b>169</b>
Appendix 1 Paper in press - Journal of Biological Chemistry	169
Appendix 2 Joint assays on squash and <i>Arabidopsis</i> G3PAT	200
<b>References start</b>	<b>202</b>
<b>References end</b>	<b>225</b>



# Tables and Figures

Table 1.1	Some important fatty acids and their formulae	15
Figure 1.1	Schematic diagrams of palmitic acid, glycerol-3-phosphate and tri-palmitin	16
Figure 1.2	Schematic diagram illustrating the compartmentalisation and overall organisation of lipid biosynthesis in higher plants	23
Figure 1.3	The chemical steps involved in fatty acid synthesis	25
Figure 1.4	ACP is a central component of <i>de novo</i> fatty acid synthesis	26
Figure 1.5	Simplified schematic of the pathways of fatty acid incorporation into cellular components in the plant cell	32
Figure 1.6	Schematic of the two-pathway system of membrane glycerolipid synthesis in <i>Arabidopsis</i> leaves	35
Table 2.1	Acyl-ACP synthesis reaction components	51
Figure 2.1	SDS PAGE gel of <i>E. coli</i> cell lysates demonstrating production of the squash G3PAT protein	54
Figure 2.2	SDS PAGE gel of <i>E. coli</i> cell-free extracts (CFEs) to demonstrate the presence of the squash G3PAT protein	56
Figure 2.3	SDS PAGE gel of squash G3PAT CFEs and purified protein	57
Table 3.1	Summary of the reaction conditions used in acyl-CoA:sn-glycerol-3-phosphate acyltransferase assays by Bertrams and Heinz, 1976.	69
Table 3.2	Summary of the reaction conditions used in acyl-CoA:sn-glycerol-3-phosphate acyltransferase assays by Bertrams and Heinz, 1981.	71
Table 3.3	Summary of the reaction conditions used in G3PAT assays by Frentzen <i>et al</i> , 1983	73
Table 3.4	Summary of the reaction conditions used in G3PAT assays by Frentzen <i>et al</i> , 1987	74
Figure 3.1	Typical results format of G3PAT selectivity assays	80
Table 3.5	Standard conditions for G3PAT assays types	81
Figure 3.2	Selectivity assays with squash G3PAT over a range of BSA concentrations	82
Figure 3.3	Determination of binding of 18:1-ACP and 16:0-ACPs to BSA under competitive conditions	84
Table 3.6	Differential binding of 18:1-ACP and 16:0-ACP substrates to BSA	86
Figure 3.4	Effects of the proteins lysozyme and cytochrome C and the compound 2,6-dimethyl $\beta$ -cyclodextrin on the substrate selectivity of squash G3PAT	88
Table 3.7	Differential binding of 18:1-ACP and 16:0-ACP substrates to 2,6-dimethyl $\beta$ -cyclodextrin	91
Figure 3.5	Alignment of the N-termini of constructs ARA 1AT, AR1, SQU 1AT and NA4	92
Figure 3.6	Authoradiograph of TLC analysis of G3PAT assays using short chain acyl-CoA substrates	96
Figure 3.7	Single substrate assays using acyl-ACP and acyl-CoA substrates	97
Table 3.8	G3PAT reaction velocities with various acyl-CoA and -ACP substrates	98
Figure 3.8	Squash G3PAT uses azidoacyl-CoA and -ACP as substrates	100
Figure 3.9	MALDI TOF mass spectra of squash G3PAT before and after incubation with 12-azidooleoyl-ACP	101
Figure 4.1	N-terminal amino acid alignment of squash plastidial G3PATs	109
Figure 4.2	Multiple sequence alignment of plant G3PATs	110
Figure 4.3	(Top) Structural diagram of the glycerol-3-phosphate (G3P) binding site of	114

	squash G3PAT with modelled.	
Figure 4.3	(Bottom) Structural diagram of the acyl- and glycerol-3-phosphate binding site with modelled G3P and palmitoyl-pantotheine substrate	114
Figure 4.4	Schematic diagram of amino acid residues histidine, lysine, arginine and serine	117
Figure 4.5	Dual substrate assays on mutant squash G3PAT proteins K193S, R235S, R237S and H194S	118
Table 4.1	The mutant G3PAT enzymes K193S, R235S and R237S retain their ability to bind acyl-ACP substrate	119
Table 4.2	Mutants C20S, C177S, C188S and C278S have activity and substrate selectivity similar to wild type	121
Table 4.3	The activity and selectivity of acyl-binding pocket mutant G3PATs	122
Figure 4.6	Substrate selectivity assay on Q24a and mutant R170S	123
Table 5.1	Plastidial G3PATs cloned from various species and their substrate selectivity (if determined)	129
Table 5.2	Membrane-bound G3PATs cloned or purified from various species	130
Figure 5.1	Amino acid sequence alignment schematic of Q24a and mutants Q24a L261F, Q24a P331S and Q24a L261F P331S	134
Figure 5.2	Selectivity assays on Q24a, Q24a L261F, Q24a P331S and Q24a L261F P331S G3PAT proteins	136
Figure 5.3	Selectivity assays on oil palm wild type G3PAT and oil palm L352F G3PAT	139
Figure 5.4	Lineweaver-Burke plots of Q24a and Q24a L261F G3PAT activities	141
Table 5.3	Summary of the kinetic constants for Q24a and Q24a L261F	142
Figure 5.5	Schematic diagram of a ternary complex/sequential reaction mechanism	145
Figure 5.6	Schematic diagram of a ping-pong/substituted enzyme reaction mechanism	145
Figure 5.7 a)	Determination of squash G3PAT kinetic mechanism	147
Figure 5.7 b)	Determination of squash G3PAT kinetic mechanism	148
Figure 5.8	Determination of the order of substrate binding by product inhibition studies	149
Table 5.4	Differential binding of acyl-ACP and G3P substrates to G3PAT	152
Figure 5.9	Schematic diagram of the amino acids leucine and phenylalanine	156
Figure 6.1	Schematic of the proposed mechanism for the squash G3PAT reaction	165

## Declaration

I confirm that no part of the material offered has previously been submitted by me for a degree in this or any other university. Material generated through joint work has been acknowledged and the appropriate publications cited. In all other cases material from the work of others has been acknowledged and quotations and paraphrases suitably indicated.

Signed:

.....

Date:

.....

# **Statement of Copyright**

The copyright of this thesis rests with the author. No quotation from it should be published without prior written consent and information derived from it should be acknowledged.

# Publications

Squash glycerol-3-phosphate (1)-acyltransferase – alteration of substrate selectivity and identification of arginine and lysine residues important in catalytic activity.

Slabas AR, Kroon JTM, Scheirer TP, Gilroy JS, Hayman MW, Rice DW, Turnbull AP, Rafferty JB, Fawcett T and Simon WJ.

Accepted by Journal of Biological Chemistry, September 2002.

Kinetic mechanism and order of substrate binding for *sn*-glycerol-3-phosphate acyltransferase from squash (*Cucurbita moschata*).

Hayman MW, Fawcett T and Slabas AR.

FEBS Letters, 2002, vol. 514, pp. 281-284.

Mutagenesis of squash (*Cucurbita moschata*) glycerol-3-phosphate acyltransferase (GPAT) to produce an enzyme with altered substrate selectivity.

Hayman MW, Fawcett T, Scheirer TF, Simon WJ, Kroon JTM, Gilroy JS, Rice DW, Rafferty JB, Turnbull AP, Sedelnikova SE and Slabas AR.

Biochemical Society Transactions, 2000, vol. 28, pp. 680-681.

Plant glycerol-3-phosphate acyltransferase (GPAT) structure/selectivity studies

Slabas AR, Simon WJ, Scheirer TF, Kroon JTM, Fawcett T, Hayman MW, Gilroy JS, Nishida I, Murata N, Rafferty JB, Turnbull AP and Rice DW.

Biochemical Society Transactions, 2000, vol. 28, pp. 677-679.

# Abbreviations

AAS	acyl-(acyl carrier protein) synthase
ACP	acyl carrier protein
APS	ammonium persulphate
ATP	adenosine triphosphate
BSA	bovine serum albumin
cDNA	copy deoxyribonucleic acid
CMC	critical micelle concentration
CoA	co-enzyme A
Ci	Curie
DAGAT	diacylglycerol acyltransferase
DEPC	Diethyl cyanophosphonate
dpm	radioactive decays per minute
DNA	deoxyribonucleic acid
DTT	dithiothreitol
E. coli	Escherichia coli
FAS	fatty acid synthase
FF	fast flow
g	gram/ unit of gravitational force (centrifugation)
G3P	glycerol-3-phosphate
G3PAT	glycerol-3-phosphate acyltransferase
HEPES	N-(2-Hydroxyethyl)piperazine-N-(2-ethanesulfonic acid)
IPA	iso-propyl alcohol
IPTG	isopropyl $\beta$ -D-thiogalactopyranoside
kDa	kilodalton
Km	Michaelis constant (in $\mu$ M)
KSCN	Potassium thiocyanate
l	litre
LPA	lysophosphatidic acid
LPAAT	lysophosphatidic acid acyltransferase
mg	milligram
MGLP	lipopolysaccharide containing 6-O-methylglucose and glucose
min	minute
ml	millilitre
mM	millimolar
mmole	millimole
MMP	3-O-methylmannose containing polysaccharide
MOPS	3-(N-Morpholino)propanesulfonic acid
M. phlei	mycobacterium phlei
NEMAc	N-ethyl morpholine acetate buffer
ng	nanogram
nmole	nanomole
PCR	polymerase chain reaction
PlsB	glycerol-3-phosphate acyltransferase from <i>E.coli</i> (membrane bound)
pmole	picomole
psi	pounds per square inch
RNA	ribonucleic acid

rpm	revolutions per minute
S.E.M.	standard error measurement
SDS PAGE	sodium dodecyl sulphate polyacrylamide gel electrophoresis
$S_0$	initial substrate concentration
$T_0$	time = zero
TEMED	N,N,N',N'-Tetramethylethylenediamine
Tris	tris (hydroxymethyl) aminoethane buffer
U	Unit (enzyme activity)
UV	ultraviolet
v	volts
$V_0$	initial reaction velocity
$V_{max}$	maximum reaction velocity constant/ $K_{cat}$
v/v	volume/volume
w/v	weight/volume
w/w	weight/weight
$\mu\text{Ci}$	microCurie
$\mu\text{g}$	microgram
$\mu\text{l}$	microlitre
$\mu\text{M}$	micromolar

**Fatty acid nomenclature is  $C_{i:ii}$**

Where  $i$  = acyl-chain length in carbons

$ii$  = number of desaturations in molecule

For instance  $C_{16:0}$ -ACP is palmitoyl-ACP and

$C_{18:1}$ -ACP is an acyl chain of 18 carbons one double or triple bond (oleoyl-ACP unless otherwise stated).

# **Chapter 1**

## **Introduction**



## 1.1 General Introduction

Plants and their products form the vast majority of the world's food supply. Plants provide food chains with essential sources of energy, minerals and fundamental food groups. Mankind has been continually adapting crop plants to its needs for many centuries using traditional breeding techniques. More recent advances in the field of biotechnology have enabled the creation of transgenic plants. These plants have specifically enhanced qualities, known as either input or output traits.

*Input traits.* Crops world-wide are subject to environmental stresses such as invasion by pathogens and parasites, salt stress, water-logging, drought and extremes of temperature. Enhancement of input traits involves increasing plant resistance to these stresses to improve crop performance 'in the field', for example, increasing pest and disease resistance or low temperature (chilling) tolerance.

*Output traits.* Crop plants produce a wide variety of fruits, grains and seeds that may be harvested for use by humans. Each may contain a complex mix of proteins, carbohydrates and lipids. Enhancement of output traits involves increasing the overall quantity of the harvest, or increasing the specific yield of a particular product or range of products to improve the harvest quality. Proteins, lipids or other products may also be expressed at high levels for use in the pharmaceutical industry (Briggs and Koziel, 1998; Napier and Michaelson, 2001).

The bulk of the world's lipids are supplied by plants, most accessibly in the form of seed oils. Major seed oil crops include oilseed rape, soybean, sunflower and oil palm. These plants have been selected by man for oil production as they exhibit several favourable characteristics which facilitate their farming:

- 1 They have a high yield
- 2 They perform well as crops
- 3 The seed oils have no specific requirements for extensive processing

Seed oils are an especially valuable crop as they are a concentrated, easy to harvest resource. The oil produced is used to feed humans and animals and is the primary resource for the production of lubricants, paints and plastics. As a result, the production of plant oils and derived products is an important industry. Thus, the study of the biochemical pathways for lipid biosynthesis and storage has been keenly undertaken.

## **1.2 Lipids**

The group of biological molecules known as lipids is an important and diverse one. All living organisms contain lipids, functioning in various roles such as protection from pathogens and disruption of water balance (e.g. waxes), signalling molecules (e.g. steroids, glycolipids) and as an energy and carbon source, facilitating the production of other classes of molecules and the giving potential for cells to safely store large amounts of chemical energy (e.g. triacylglycerols, glycerolipids). In addition, lipid bilayers form intracellular membranes for the maintenance of physical barriers and sub-cellular compartments, anchoring of proteins to specific localisations, and the establishment of specialised micro-environments for certain metabolic processes, for example

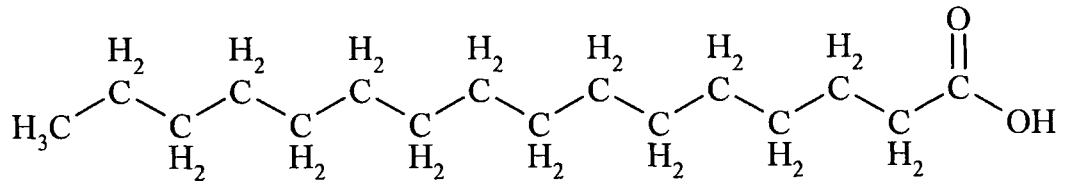
photosynthesis. The physical properties of different membranes vastly affect their function, in turn affecting many other biological systems within the cell. As such, the study of the production of membrane lipids is an important one. Understanding the enzymes responsible and how the functional properties of these enzymes directly influence the composition and types of membrane lipids produced is also of considerable interest. Some important fatty acids and their formulae are shown in Table 1.1.

Lipids are a highly heterogeneous group of chemical compounds, broadly defined by their insolubility in polar solvents, being most readily soluble in polar solvents such as acetone, benzene and chloroform. Lipids consist of a carbon backbone, with side groups which are chiefly non-polar. This is an important characteristic as it enables lipids to associate into non-polar groups and barriers, an example is the phospholipids that form cell membranes. Lipids can also provide a hydrophobic micro-environment that favour reactions which proceed most readily in non-aqueous surroundings, for example some reactions of photosynthetic photosystems I and II and cellular oxidations. Lipids are also a source of both energy and carbon for cellular reactions. In seeds they are most commonly stored as triglycerides (or triacylglycerol; TAGs, figure 1.1), where they may represent up to 80% of the dry weight of storage tissues. Some lipids have regulatory roles and may also form composite molecular groups, eg lipoproteins and glycoproteins. These compounds may also have a variety of functional and structural roles.

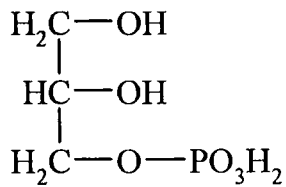
Saturated fatty acids			Unsaturated fatty acids		
Name	No. carbons	Formula	Name	No. carbons	Formula
Butyric acid	4:0	$\text{CH}_3(\text{CH}_2)_2\text{CO}_2\text{H}$	Crotonic acid	4:1	$\text{CH}_3\text{CH}=\text{CHCO}_2\text{H}$
Caproic acid	6:0	$\text{CH}_3(\text{CH}_2)_4\text{CO}_2\text{H}$	Palmitoleic acid	16:1	$\text{CH}_3(\text{CH}_2)_5\text{CH}=\text{CH}(\text{CH}_2)_7\text{CO}_2\text{H}$
Caprylic acid	8:0	$\text{CH}_3(\text{CH}_2)_6\text{CO}_2\text{H}$	Oleic acid	18:1	$\text{CH}_3(\text{CH}_2)_7\text{CH}=\text{CH}(\text{CH}_2)_7\text{CO}_2\text{H}$
Capric acid	10:0	$\text{CH}_3(\text{CH}_2)_8\text{CO}_2\text{H}$	Petroselenic acid	18:1	$\text{CH}_3(\text{CH}_2)_{10}\text{CH}=\text{CH}(\text{CH}_2)_4\text{CO}_2\text{H}$
Lauric acid	12:0	$\text{CH}_3(\text{CH}_2)_{10}\text{CO}_2\text{H}$	Ricinoleic acid	18:1	$\text{CH}_3(\text{CH}_2)_5\text{CH}(\text{OH})\text{CH}_2\text{CH}=\text{CH}(\text{CH}_2)_7\text{CO}_2\text{H}$
Myristic acid	14:0	$\text{CH}_3(\text{CH}_2)_{12}\text{CO}_2\text{H}$	Linoleic acid	18:2	$\text{CH}_3(\text{CH}_2)_3(\text{CH}_2\text{CH}=\text{CH})_2(\text{CH}_2)_7\text{CO}_2\text{H}$
Palmitic acid	16:0	$\text{CH}_3(\text{CH}_2)_{14}\text{CO}_2\text{H}$	$\alpha$ -Linolenic acid	18:3	$\text{CH}_3(\text{CH}_2\text{CH}=\text{CH})_3(\text{CH}_2)_7\text{CO}_2\text{H}$
Stearic acid	18:0	$\text{CH}_3(\text{CH}_2)_{16}\text{CO}_2\text{H}$	Arachidonic acid	20:4	$\text{CH}_3(\text{CH}_2)_3(\text{CH}_2\text{CH}=\text{CH})_4(\text{CH}_2)_3\text{CO}_2\text{H}$
Arachidic acid	20:0	$\text{CH}_3(\text{CH}_2)_{18}\text{CO}_2\text{H}$	Erucic acid	22:1	$\text{CH}_3(\text{CH}_2)_7\text{CH}=\text{CH}(\text{CH}_2)_{11}\text{CO}_2\text{H}$
Lignoceric acid	22:0	$\text{CH}_3(\text{CH}_2)_{20}\text{CO}_2\text{H}$	Nervonic acid	24:1	$\text{CH}_3(\text{CH}_2)_7\text{CH}=\text{CH}(\text{CH}_2)_{13}\text{CO}_2\text{H}$

Table 1.1 Some important fatty acids and their formulae.

a) Palmitic acid



b) Glycerol-3-phosphate



c) Tri-palmitin

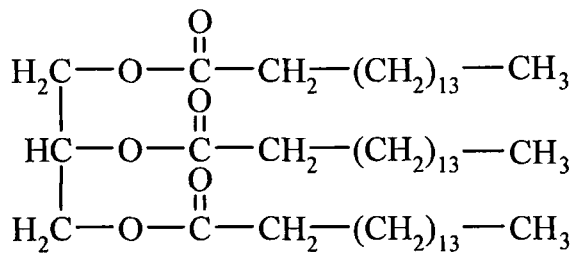


**Figure 1.1** Schematic diagrams of a) palmitic acid, a fatty acid; b) glycerol-3-phosphate and c) tri-palmitin, a triacylglyceride (TAG).

Lipids can be broadly divided into three main functional groups: Neutral lipids, phospholipids and steroids. Glycolipids and sphingolipids are important additional groups.

*Neutral lipids.* At the cellular pH these lipids bear no charge, making the side groups entirely hydrophobic. These are rarely found free in the cell (due to toxic effects) and are usually complexed with glycerol to form triglycerides, the main constituent of fats and oils. The properties of the fats/oils depend almost entirely on the acyl chain length and level of desaturation. As a general rule, triglycerides containing longer, more saturated acyl chains are more gel-like with less fluid properties.

*Phospholipids.* This class of lipids forms the majority of biological membranes. These phosphate containing molecules have a structure related to triglycerides, with one acyl chain replaced by a phosphate containing polar group at position *sn*-3. On the other side of the bridging phosphate group can be a variety of polar chemical groups of varying levels of size and complexity including choline, ethanolamine, glycerol, inositol, glycosides, serine or threonine. This means that this is a highly diverse group of compounds, a useful characteristic as it often correlates with advantageous functional diversity. Phospholipids are amphipathic and have a “dual-solubility” in both polar and apolar solvents. In fact, this property is of fundamental importance to their interactions in membranes. Phospholipids at the interface formed by a layer of polar solvent over the top of a layer of non-polar solvent take up a 2D sheet-like arrangement to satisfy their dual solubility properties. In an aqueous solution phospholipids form a bilayer, an

organisation which is favourable to both the hydrophobic and hydrophilic chemical domains. Phospholipid bilayers, held together by a combination of polar and non-polar associations are the primary framework of biological membranes.

*Steroids and sterols.* This class of compounds consists of a framework of (usually) four interconnected 5 or 6 carbon rings with a further one or more attached lipid groups. The most common steroids are the sterols, which have a hydroxy group at one end of the framework and a complex, non-polar carbon chain at the opposite end. Of the sterols, cholesterol is the most common in animal cell plasma membranes. Sterols are synthesised by the mevalonate pathway of isoprenoid metabolism (Lichtenhaler, 1987) in which acetyl-CoA and acetoacetyl-CoA condense to form 3-HMG CoA, the precursor of mevalonate. Mevalonate is converted into isopentenyl pyrophosphate, a 5 carbon intermediate for many subsequent reactions. Various condensations, cyclisations and isomerisations are used to produce further intermediates such as geranyl and farnesyl pyrophosphate and eventually C<sub>27-30</sub> compounds such as squalene, lanosterol and cholesterol. Plants produce little cholesterol, instead cyclising 2,3-oxidosqualene into cycloartenol (Benveniste, 1986) which is further metabolised into 24-ethyl sterols, the major sterol in higher plants. Common plant sterols include sitosterol, campesterol, episterol and stigmasterol. Hormones with steroid-based structures are known to have considerable effects on biochemical functions of a number of organisms; in plants brassinosteroids are important in the regulation of growth and development. Plant sterols have limited uptake in the gut of mammals and, together with stanols and sterolins, have

been demonstrated to have beneficial effects by lowering blood cholesterol when included in the diet of humans (reviewed by Jones, 1999).

*Glycolipids.* These are amphipathic lipids with carbohydrate groups anchored to their polar segments. They are present in the highest proportions in bacterial plasma membranes and the thylakoid membranes of chloroplasts. They lend varied structural and functional properties to membranes. The simple or branched carbohydrate regions can form many hydrogen bonds and reinforce the bilayer structure. For these reason they are present in the highest levels in membranes which are subject to higher than normal physical or chemical stress. The carbohydrate chains can also form external recognition markers, for example blood group recognition factors on the external surface of red blood cells.

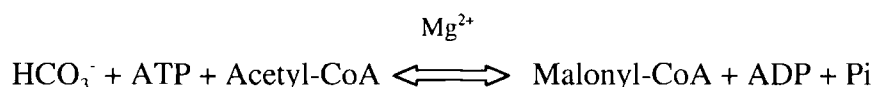
*Sphingolipids.* These membrane lipids are structurally similar to phospholipids, but the 'backbone' is sphingosine, rather than glycerol. Sphingosine is an amino alcohol that contains a long, unsaturated hydrocarbon chain. In all sphingolipids, the amino group of sphingosine is acylated (to form ceramide). The terminal hydroxyl group may also be substituted, often for phosphorylcholine or glucose/galactose to form sphingomyelin or cercerebrosides/gangliosides respectively.



## 1.3 Fatty acid biosynthesis

### 1.3.1 Acetyl-CoA Carboxylase (ACCase)

ACCase catalyses the carboxylation of acetyl-CoA to yield malonyl-CoA. The reaction is:



ACCase, together with malonyl-CoA:ACP transacylase (figure 1.2), is responsible for the production of malonyl-ACP extender units for fatty acid synthesis. The ACCase reaction has two distinct steps, catalysed at two separate active sites on the protein. The first involves an ATP dependant carboxylation of the biotin prosthetic group of biotin carboxyl carrier protein (BCCP) using bicarbonate (dissolved from atmospheric  $\text{CO}_2$ ), proceeding via a carboxylphosphate intermediate. The second occurs as BCCP moves from the biotin carboxylase active site to that of the carboxyltransferase, which transfers the carboxyl group onto acetyl-CoA, forming malonyl-CoA. ACCase has four functional regions: BCCP, biotin carboxylase, carboxyltransferase and a fourth region, suggested by Wood (1977) to be regulatory. This is significant as ACCase has a high flux control coefficient for the fatty acid synthesis pathway (discussed below).

There are two main types of ACCase. *E. coli* and many other prokaryotes have an ACCase in which each of the enzymatic activities is present on a separate protein. This dissociable multienzyme complex is called the 'prokaryotic' form. It is present in only a few plant types, for example pea chloroplasts and some other dicotyledon plastids.

Grasses, yeast, fungi and animals have another ACCase form. Here all the functional domains are present on a single, high molecular mass polypeptide chain. This is termed the 'eukaryotic' form. As all catalytic domains are on one polypeptide, the BCCP region has to be flexible enough to move between the two active sites of biotin carboxylase and carboxyltransferase. Eukaryotic ACCases are very sensitive to graminicides, cyclohexanediones and aryloxyphenoxypropionates (Harwood, 1991a,b), unlike the prokaryotic form which is essentially resistant to attack by these herbicides.

There are multiple isoforms of ACCase and it is also present at several separate subcellular locations. This is because, as well as being required for *de novo* fatty acid synthesis in the plastid, malonyl-CoA is also required for fatty acid elongation and the formation of secondary metabolites, all of which occurs in the cytoplasm.

ACCase is believed to have a high flux control coefficient, on occasion as high as 0.5-0.6 for *de novo* fatty acid synthesis (the flux control coefficient is a key parameter in the Metabolic Control Theory. It is a measure of the sensitivity of the total flux through a pathway to the infinitesimal variation in enzyme activity. If the flux control coefficient for an enzyme is 1, it has complete control on the flux through the pathway; if it is 0 it has no control). Page, Okada and Harwood (1994) altered the flux through the lipid biosynthesis pathway for barley and maize using two specific inhibitors of ACCase (sethoxydim and fluazifop). The data gained indicated apparent flux coefficients for barley and maize of 0.58 and 0.52 respectively.

ACCase is regulated in a complex manner by a combination of pH and  $Mg^{2+}$ , ATP and ADP levels. Also by feedback inhibition, phosphorylation, regulation of substrate levels and control of gene transcription by transcription factors such as FadR. This regulation is reviewed by Ohlrogge and Jaworski (1997).

Plastidial acetyl-CoA, the substrate for ACCase, is believed to be supplied either by the action of plastidial pyruvate decarboxylase/dehydrogenase or the movement of cytosolic acetate into the plastid, where it is the substrate for acetyl-CoA synthase. In some plants tissues other photosynthetic products (for example malate or sucrose) may be an indirect source of acetate. This area has been under investigation for many years, radiolabelled [ $^{14}C$ ] acetate has been often been used as a precursor to enable tracking of the products of fatty acid synthesis (Roughan and Slack, 1982).

### **1.3.2 The reactions of fatty acid synthesis**

Fatty acids are synthesised in the plastid by the repeated incorporation of two carbon units to initiate and then extend an acyl chain to 16 or 18 carbons long. The products of fatty acid synthesis may be used in the plastid or exported into the cytoplasm, where further chain extension and modification may occur, shown schematically in figure 1.2. The chemical reactions of *de novo* fatty acid synthesis are conserved for virtually all organisms. Following the production of plastidial acetyl-CoA and malonyl-ACP, successive additions of 2 carbon units (supplied by malonyl-ACP) initially to acetyl-CoA and subsequently to the growing acyl-chain are made. Chain extension involves a cycle of four reactions, the first is a condensation reaction involving the decarboxylation of a

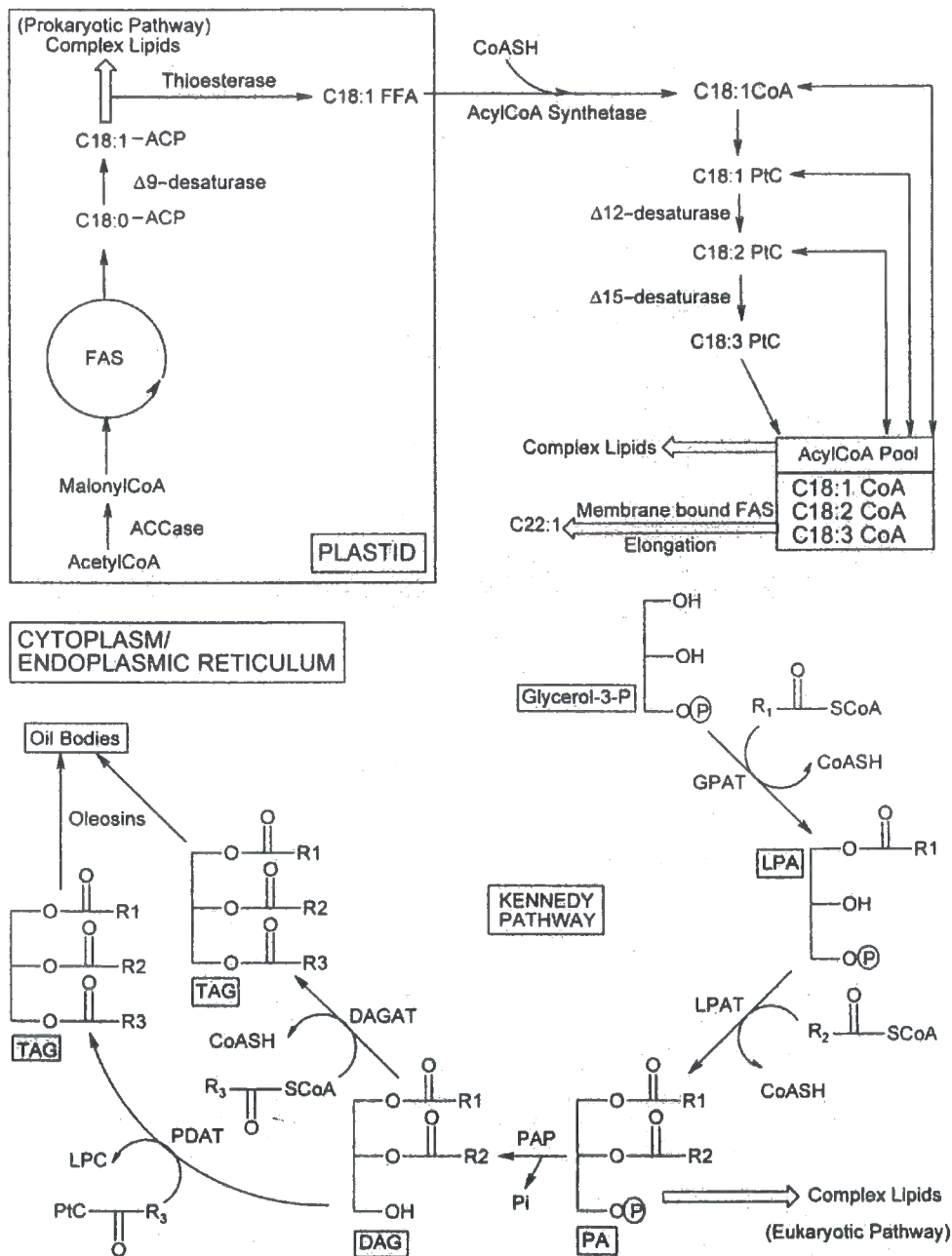


**Figure 1.2** Schematic diagram illustrating the compartmentalisation and overall organisation of lipid biosynthesis in higher plants. Figure is from Slabas *et al*, 2001.

malonyl-ACP with concomitant linkage to acetyl-CoA or a growing acyl-ACP chain, forming  $\beta$ -ketoacyl-ACP. The acyl chain (now two carbons longer) undergoes three more reactions to produce a fully reduced acyl-ACP: reduction to a hydroxylated acyl group, dehydration and then further reduction. These reactions are shown in figure 1.3.

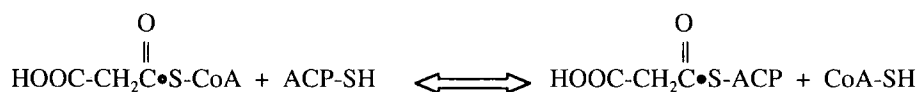
Ketoacyl synthase III (KASIII) uses acetyl-CoA as the primer for the initial condensation reaction (this enzyme is believed to have intrinsic acyltransferase properties - Acetyl-CoA:ACP transacylase exists in all plants but the physiological role of this enzyme is unclear as it appears to be functionally redundant Jaworski *et al*, 1993).

### **1.3.3 Acyl-carrier protein (ACP)**

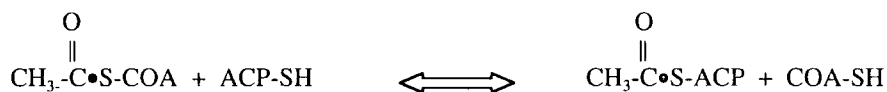
ACP is a protein containing a pantothenic group, central to fatty acid synthesis and the FAS complex (figure 1.4). It was first purified from *E. coli*, in which it is one of the most abundant proteins. It has since been purified and cloned from many plants. There is strong conservation of amino acid sequence between leaf and seed forms, but not necessarily at nucleotide level), for instance in *Arabidopsis thaliana* (Post-Beittenmiller *et al*, 1989). There is also a high level of heterogeneity between ACPs from different plants (Harwood, 1996).

ACP from prokaryotes is a low molecular weight (approximately 9 kDa), enzymatically stable, acidic protein. In eukaryotes the protein is believed to be much larger, central to FAS with a 'swinging' pantothenic arm to deliver the nascent acyl chain to the relevant catalytic FAS domains in turn.

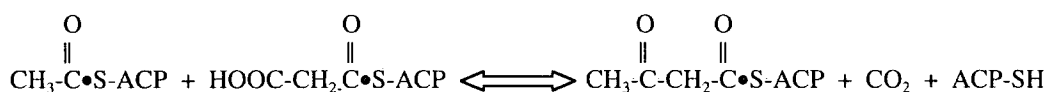
### MALONYL TRANSFERASE



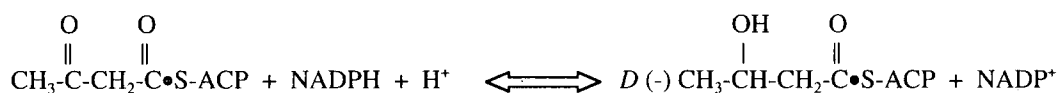
### ACETYL TRANSFERASE



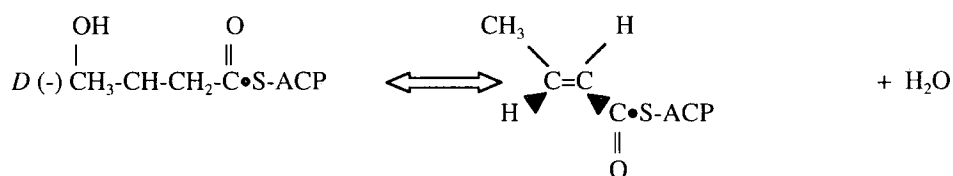
### β-KETOACYL-ACP SYNTHASE I AND II (KAS III UTILISES ACETYL CoA)



### β-KETOACYL-ACP REDUCTASE



### β-HYDROXYACYL-ACP DEHYDRASE



### ENOYL-ACP REDUCTASE

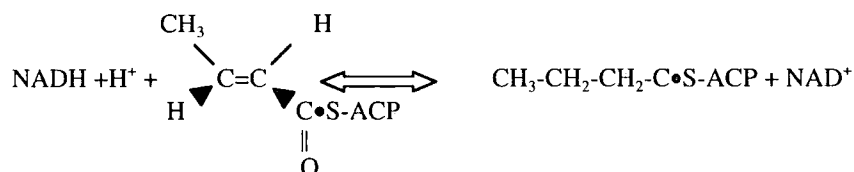


**Figure 1.3** The chemical steps involved in fatty acid synthesis. Adapted from Slabas and Fawcett, 1992.

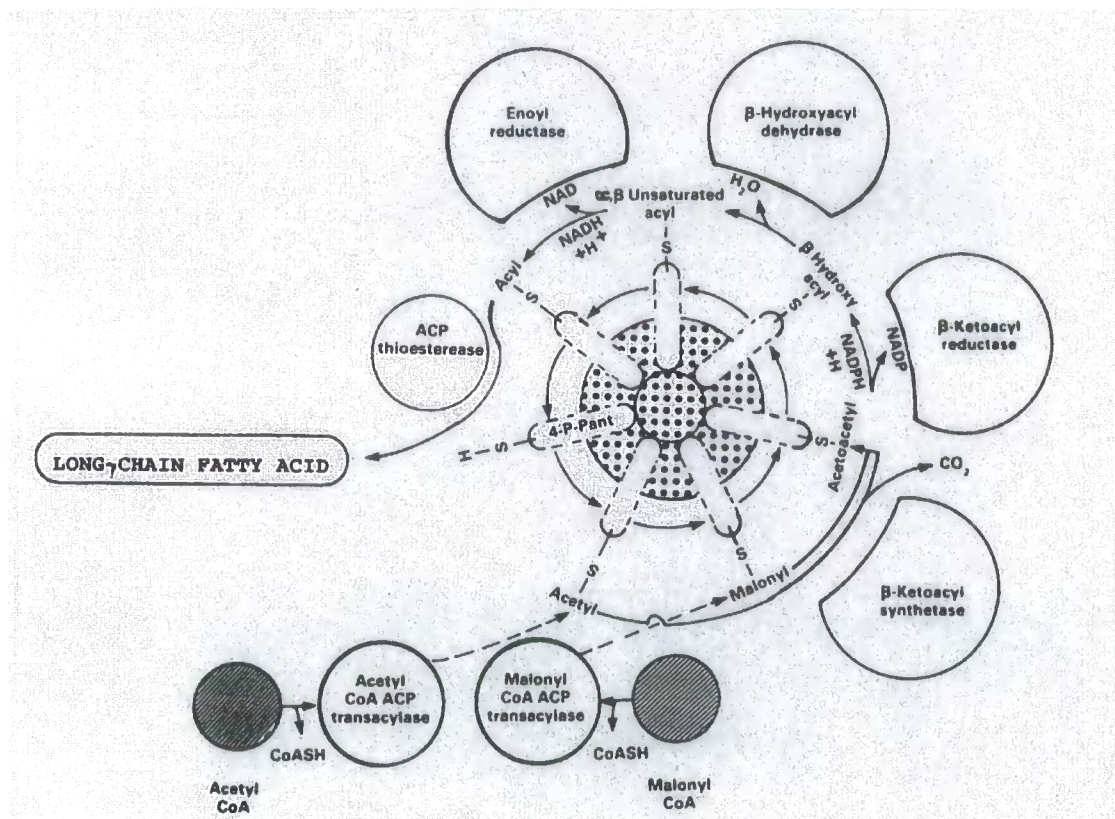


**Figure 1.4** ACP is a central component of *de novo* fatty acid synthesis. 4-P Pant represents reduced pantothenyl-ACP. Figure is from Slabas and Fawcett, 1992.

The presence of complex gene families has been demonstrated in several plant species, including Barley (Hansen, 1987), Spinach leaf (Scherer and Knauf, 1987), *Brassica napus* (Safford *et al*, 1988) and *Arabidopsis* (Post-Beittenmiller 1989, Lamppa and Jacks, 1991). This complex gene family may be the result of the complicated interbreeding involved in the production of modern crops, or it may be required for the production of several necessary plant isoforms and their regulation. There are frequently several species of ACP in plants, discernable either by immunological detection or by differences in pI, often with tissue specific-distribution. Initial predictions were that leaf would have one isoform and the seed would have two – one a core FAS component and the other involved in TAG storage. However, at least three ACP isoforms were discovered in rape embryo (Safford *et al*, 1988) and more recently in other species including *Thunbergia alata* and *Coriandum sativum* (Suh *et al*, 1999). ACP expression has been closely correlated to deposition of storage lipids and thus demonstrates tissue and temporal specific regulation (Turnham and Northcote, 1982 and 1983).

ACP is present in the plastid, esterified to the growing acyl chain during fatty acid synthesis. Guerra *et al* (1986) and Suh *et al* (1999) showed that the relative activities of the competing acyl-ACP thioesterase and acyltransferase were influenced by the ACP isoform of the substrate. Thus ACP type may have a role in the channelling of fatty acids between the prokaryotic and eukaryotic pathways. ACP is also present in plant mitochondria as demonstrated by immunolocalisation studies performed by Mikolajczyk and Brody (1990).



#### **1.3.4 Fatty acid synthase (FAS)**

Two types of Fatty Acid Synthase are well characterised, designated FAS I and FAS II. Animals and yeast have a multifunctional enzyme complex which contains large polypeptides that are capable of catalysing several fatty acid synthesis reactions. Each polypeptide has several separate catalytic domains. This type of fatty acid synthase is known as Type I FAS (Bloch and Vance, 1977; Battey and Ohlrogge, 1990).

Plants and the majority of bacteria contain a complex in which there are several smaller proteins that have individual enzyme activities which are easily dissociable from one another. This complex is highly organised and extensive metabolite channelling occurs (Roughan, 1997). This type of fatty acid synthase is known as Type II FAS (Volpe and Vagelos, 1973). Important regulatory questions have recently been raised regarding the arrangement of FAS II into multi-molecular complexes, or 'metabolons' (Roughan and Ohlrogge, 1996).

#### **1.3.5 The Kennedy pathway**

Plant triacylglycerols (TAGs) are produced by the classic Kennedy Pathway (Kennedy, 1961; Harwood and Page, 1994), which involves two acylations of glycerol-3-phosphate (G3P), a dephosphorylation to produce diacylglycerol and a further acylation. Acylation steps occur at the endoplasmic reticulum and the acyl-donor molecule is acyl-CoA. Glycerol-3-phosphate acyltransferase catalyses the transfer of a fatty acid from an acyl-donor to the *sn*-1 position of glycerol-3-phosphate to yield 1-acylglycerol-3-phosphate (or lysophosphatidic acid). Lysophosphatidic acid acyltransferase (LPAAT) then

catalyses the formation phosphatidic acid, which is dephosphorylated by phosphatidic acid phosphatase (PAP) to form diacylglycerol. Diacylglycerol acyltransferase (DAGAT) performs the final acylation step to form triacylglycerol.

These enzymes have been purified and partially characterised from several plant tissues (Harwood, 1998, Stobart *et al*, 1998). Substrate selectivity of the acyltransferase enzymes, together with the pool of acyl-CoA substrates available, influences the types of TAG synthesised. As TAGs are primarily a storage product and do not have a functional role to play in, for instance, membrane fluidity, a much wider range of acyl-groups can be incorporated into TAGs (however, TAG storage tissues are not necessarily metabolically inert -see below).

### **1.3.6 Oil body formation**

Virtually all plant species synthesise triacylglycerols in their developing seeds. TAGs are deposited and stored in discrete organelles called oil bodies until germination when they are catabolised for use as an energy and carbon source. As the harvest of seed oils from crop species is an important industry, there has been much interest in the mechanism of oil body formation.

Oil bodies contain a core of triacylglycerols enclosed within an outer monolayer of phospholipid. Associated with this outer monolayer is a class of proteins called oleosins which are believed to stabilise oil bodies to prevent coalescence during seed desiccation (Murphy *et al* 1993, reviewed by Frandsen *et al*, 2001). Enzymes responsible for the

synthesis of TAGs ('Kennedy Pathway' enzymes - see above) are located at the endoplasmic reticulum (ER), which is involved in oil body biogenesis (Lacey and Hills 1996; Napier *et al*, 1996).

In 1978 Wanner and Theimer proposed the mechanism of oil body formation. TAGs accumulate between the leaflets of the ER phospholipid bilayer. Wanner and Theimer suggested that this accumulation results in swelling of the ER to form TAG filled vesicles. When these vesicles reach a 'critical size' they bud off to form an oil body surrounded by a phospholipid monolayer. Thus, mature oil bodies form by budding from the ER (Huang, 1992, Napier *et al*, 1996). The timing of oleosin insertion into the oil body is more poorly understood and it is not known whether or not TAG deposition and oleosin production are spatially and temporarily separated. Seemingly different results have been obtained in different plants. In *Brassica napus* TAGs are synthesised before oleosins (Murphy and Cummins, 1989), whereas the two have been shown to appear at the same time in *Zea mays* and soybean (Herman, 1987, Tzen *et al*, 1993).

In 1997 Sarmiento *et al* proposed a new model for oil body formation in which the oilseeds in early stages of development produce oil bodies with minimal protein coats. These fuse with oleosin-rich oil bodies during mid to late stages in seed development. Oleosin has been demonstrated to be co-translationally inserted into the ER, mediated by a signal recognition particle (SRP) (Hills *et al*, 1993, Thoyts *et al*, 1995).

TAG may comprise 90-95% of the oil body organelle constituents. Several studies have indicated that TAG storage tissues are not metabolically inert - desaturases, transacylases and acyltransferases may play a further role in TAG remodelling (Sarmiento *et al*, 1998; Mancha and Stymne, 1997; Murphy, 1999)

### **1.3.7 Prokaryotic and Eukaryotic pathways**

There are two main products of the plastidial FAS system 16:0- and 18:1-ACP - key substrates for further metabolism. Two distinct pathways exist for the incorporation of these fatty acids into cellular components: the Prokaryotic and Eukaryotic pathways. A simplified schematic view detailing the pathways of fatty acid incorporation into various cellular components in the plant cell is shown in figure 1.5.

*The Prokaryotic Pathway.* This pathway is so called because the products remain within the plastid, an organelle that has been functionally compared to prokaryotic organisms. The stromal G3PAT is the first step in the prokaryotic pathway and is frequently highly specific for 18:1-ACP (Dormann *et al* 1994), most notably in spinach. The second acylation is catalysed by a membrane bound lysophosphatidic acid acyltransferase (LPAAT) which typically esterifies 16:0 to the *sn*-2 position to yield 1-18:1, 2-16:0-phosphatidic acid (Ohlrogge *et al*, 1993, Murphy, 1994).

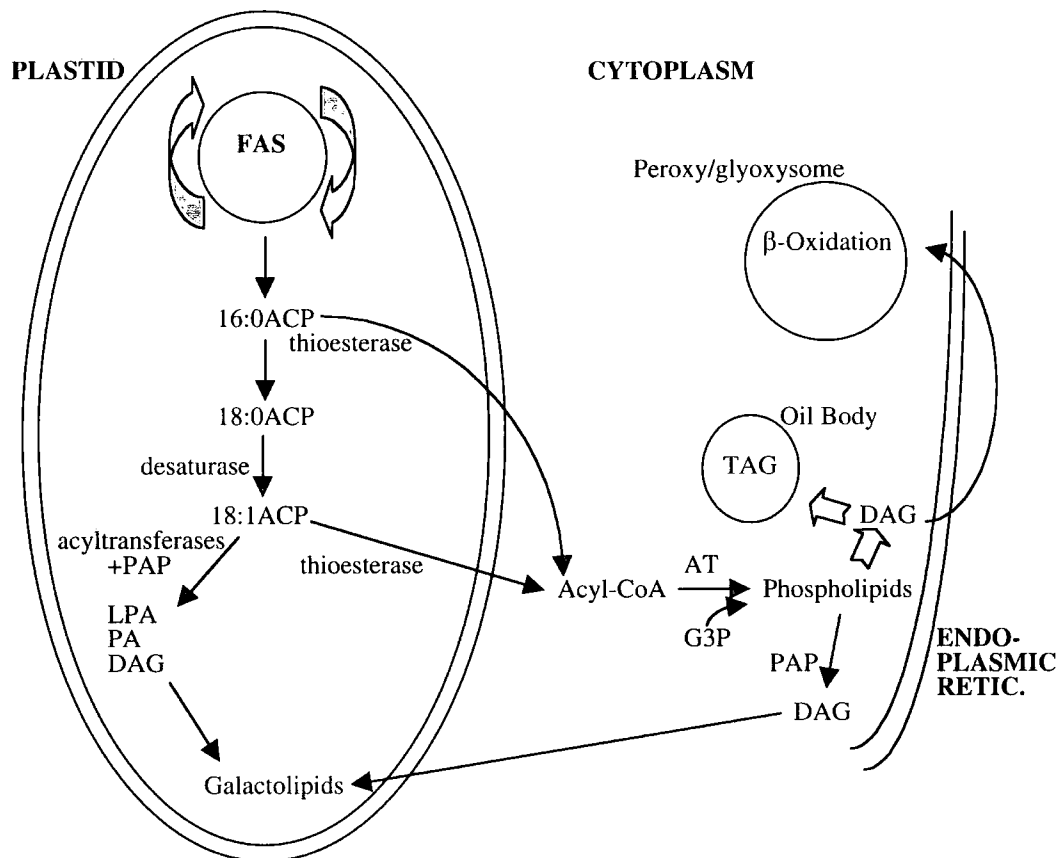


**Figure 1.5 Simplified schematic of the pathways of fatty acid incorporation into cellular components in the plant cell.**

Monogalactosidyl diacylglycerol (MGDG) is formed from diacylglycerol (DAG) by the action of a galactosyltransferase enzyme located in the inner envelope membrane, and is the most abundant chloroplast lipid. Dismutation of two MGDG molecules produces digalactosidyl diacylglycerol (DGDG), catalysed by MGDG: MGDG galactosyltransferase, thought to be present in the outer envelope membrane (Browse and Sommerville, 1991). A sulphoquinovosyltransferase is responsible for SQDG formation -less is known about this enzyme but it is thought to have access to the stromal side of the

inner chloroplast envelope and use the same pool of DAG as the enzymes mentioned above (Browse, 1993; Browse and Sommerville, 1991).

There are several desaturase enzymes specific to the chloroplast. For instance, 16:0 at the *sn*-2 position of PG is frequently converted to  $\Delta^3$ -*trans*-16:1 (Miquel and Browse, 1992; Browse and Sommerville, 1991). Other desaturases are present at varying levels of activity and with different specificities, see 1.4.2. The balance of substrate specificities of these desaturases is responsible for the ultimate lipid composition of chloroplastic membranes. MGDG, DGDG and SQDG are inserted into the thylakoid membrane and provide part of the specific hydrophobic micro-environment that favour reactions of photosystems I and II.

*The Eukaryotic Pathway.* An acyl-ACP thioesterase catalyses the first committed step in this pathway, hydrolysing the 16:0 and 18:1-ACPs to free fatty acids which are transported across the plastid envelope membranes and converted to acyl-CoA thioesters. Acyl-CoAs are used by membrane bound G3PAT and LPAAT acyltransferases at the endoplasmic reticulum to produce phosphatidic acid (PA). Unlike prokaryotic lipids, eukaryotic PA has 18:1 at the *sn*-2 position. 16:0, if present at all, is usually positioned at *sn* -1. Phosphatidic acid is converted to the following phospholipids: phosphatidylcholine (PC), phosphatidylethanolamine (PE), phosphatidylinositol (PI), phosphatidylserine (PS) and phosphatidylglycerol (PG), compounds which are characteristic of extrachloroplast membranes. Fuller details of the intermediates and the

approximate flux through these pathways in *Arabidopsis* leaves are shown in the schematic figure 1.6

'Complex' lipids (galactolipids) are not produced via this pathway as only they are required in the thylakoid membrane. However, DAG produced via the eukaryotic route may return to the chloroplast. Labelling experiments have made it clear there is significant lipid exchange between the chloroplast and other cellular locations (Browse and Sommerville 1991). Lipid Transfer Proteins (LTPs) are thought to play a great role in transfer of lipids between different cellular membranes, although this area of lipid research is currently poorly understood.

The cytoplasm is also the site for further desaturation, chain elongation and acyl-group modification. Very long chain fatty acids (VLCFAs) are often produced in greater quantities by plants that make structural lipids, for example waxes, by the action of 3-ketoacyl-ACP synthase dependant elongases (Millar and Kunst, 1997; Leonard et al, 1998). Acetylation, epoxydation, and hydroxylation may also take place. The acyl-CoA pool can be channelled into the formation of signalling and membrane glycerolipids and the production of storage triacylglycerols.





## 1.4 Chilling sensitivity in plants

The primary energy source for plants is sunlight. The performance of crop plants depends on their ability to capture energy by photosynthesis, which in turn depends on integrity of photosynthetic membranes. The ability of plants to tolerate chilling temperatures seems closely correlated with the degree of unsaturation of fatty acids in the phosphatidylglycerol of chloroplast membranes (Nishida and Murata, 1996). The majority of membrane lipids are comprised of 16:0, 18:0 or 18:1 fatty acids. Those of particularly chilling tolerant plants have elevated levels of polyunsaturated glycerolipids containing acyl groups from linoleic acid (18:2  $\Delta^9, 12$ ),  $\alpha$ -linoleic acid (18:3  $\Delta^9, 12, 15$ ) and  $\gamma$ -linoleic acid (18:3  $\Delta^6, 9, 12$ ), although  $\gamma$ -linoleic acid is rarely found in higher plants.

### 1.4.1 Membrane phosphatidylglycerol (PG) acyl-group composition - thioesterases and acyltransferases.

*De novo* biosynthesis fatty acid produces one compound, acyl-ACP, that is substrate for two different plastidial enzymes: glycerol-3-phosphate acyltransferase and acyl-ACP thioesterase. The relative activities of these two enzyme types determine the flux through the 'prokaryotic' and 'eukaryotic' pathways and the acyl composition of phosphatidylglycerol. Thioesterases, as G3PATs, are present as different forms that have different, distinct acyl-chain preference - one thioesterase type has a preference for unsaturated acyl-ACPs, another has a greater preference for 18:1-ACP (Dörmann *et al*, 1995; Jones *et al*, 1995). In addition, some plant plastids contain thioesterases with specificity for medium chain length (8-12 carbons) acyl-ACPs (Pollard *et al*, 1991;

Davies, 1993). The lipid profiles of TAGs in these plants contain elevated levels of medium chain length acyl groups

Glycerol-3-phosphate acyltransferase is present as a soluble enzyme in the plastid (Joyard and Douce, 1977) and competes with acyl-ACP thioesterase for acyl-ACP. Membrane bound lysophosphatidic acid acyltransferase (LPAAT) converts LPA into diacylglycerol. Membrane-bound acyltransferases at the endoplasmic reticulum can synthesise DAG in a similar fashion, using acyl-CoA as the acyl-donor. Some of this DAG pool re-enters the plastid and may be incorporated into membrane lipids (figure 1.4). Acyltransferases at each location have varying substrate selectivities and specificities. As a general rule, DAG synthesised in the chloroplasts has C18 and C16 groups at position *sn*-1 and C16 at position *sn*-2. DAG synthesised in the cytoplasm usually contains C18 and C16 groups at position *sn*-1 and C18 at position *sn*-2. The mixing of DAG from these two sources determines the pool available for membrane lipid (including 'complex', galactosidyl-containing lipids) synthesis.

#### **1.4.2 Desaturases**

Acyl-CoA and glycerolipid desaturases introduce double bonds at specific points of acyl chains in the endoplasmic reticulum (in the chloroplast stroma this is performed by glycerolipid and acyl-ACP desaturases). In the chloroplast, *de novo* fatty acid biosynthesis provides substrate for steroyl-ACP desaturase, the best characterised desaturase enzyme. Steroyl-ACP desaturase inserts a *cis* double bond at the  $\Delta^9$ -position of 18:0-ACP, converting the majority of the plastidial pool of steroyl-ACP to oleoyl-

ACP. The enzyme is soluble and has a relatively high activity (compared to KAS II) so that stearate rarely accumulates in plants. Steroyl-ACP desaturase was first purified from safflower (McKeon and Stumpf, 1982) and the crystal structure of the castor bean form has now been solved (Lindqvist *et al*, 1996). This has led to a rationalised approach to engineering of chain-length specificity and the orientation of the hydrogen abstraction (Cahoon *et al*, 1997, 1998).

Fatty acid desaturation occurs at a variety of sub-cellular locations and unsaturated fatty acids are important for many cellular functions, including synthesis of signalling molecules, cell expansion and increased membrane fluidity (reviewed by Somerville and Browse, 1996). Different activities and acyl-group and positional specificities of plant desaturases determine the ultimate acyl-profiles of both plastidial and cytosolic glycerolipids. The membrane lipid composition is known to have a significant effect on plant chilling tolerance (Nishida and Murata, 1996). Plants may alter their membrane acyl-group desaturation as a response to low temperatures. Temperature sensitive induction of desaturase genes has been studied for some years and is well characterised in bacteria (*des* gene family) and increasingly so in plants. More recently, sequence analysis of a plastidial omega-3 desaturase gene from *Brassica juncea* has led to the identification of putative *cis* elements in the 5' untranslated region, responsible for stress (temperature)-inducible expression (Garg *et al*, 2001).

Many plant desaturases are membrane bound and have proven difficult to purify and characterise. However, the identification of the *fab* and *fad* gene families in *Arabidopsis*

(together with sequencing of the *Arabidopsis* genome) have enabled the creation of many mutant plants, deficient in a variety of desaturase activities (Wallis and Browse, 2002). This has permitted the investigation of many aspects of desaturase activity and membrane lipid function. The study of desaturase enzymes is attracting much interest and transgenic approaches are being undertaken to produce pharmaceutically beneficial compounds, for example, polyunsaturated fatty acids (Napier *et al*, 1999; Napier and Michaelson, 2001).

#### **1.4.3 Other factors effecting chilling sensitivity**

There are many documented plant responses to chilling (2-6°C) temperatures. This complex process involves changes in morphology, metabolism and gene expression (Xin and Browse, 1998). Such changes may include growth reduction, increases in abscisic acid concentration, the accumulation of osmolytes and antioxidants and changes in the increased expression of several genes (Thomashow, 1999; Xin and Browse, 2000). Most cold-upregulated genes are already expressed during normal growth and several exhibit functional redundancy (the phenotypes of knock-out plants are the same as wild-type when grown at cold temperatures). Functional redundancy of responses to chilling stress may be the result of convergent evolution or simply indicative of the importance of overcoming the physiological effects of this environmental stress.

Temperature sensing in plants has also been a matter of much recent interest. Plieth *et al* (1999) proposed that membrane fluidity changes at low temperatures affect a change in  $\text{Ca}^{2+}$  ion channels which in turn may cause  $\text{Ca}^{2+}$  influxes responsible for activation of a

'mitogen-activated-protein (MAP) kinase' signalling cascade (Kiegle *et al*, 2000; Monroy *et al*, 1998). Histidine kinases and abscissic acid are thought to form (part of) the signalling cascade between plant temperature sensors (reviewed by Browse *and* Xin, 2001). However, many of the plant responses to chilling (2-6°C) temperatures appear to 'prepare' the plant for freezing (<0°C) conditions. They frequently have, cryoprotectant, osmotic or anti-dehydration roles.

## **1.5 Glycerol-3-phosphate acyltransferases in plants**

Glycerolipid synthesis occurs at three distinct sub-cellular locations, the mitochondria, the endoplasmic reticulum and the plastids. Therefore a (different) glycerol-3-phosphate acyltransferase exists at each of these locations to catalyse the initial acyltransferase step. The relative activities of G3PAT in preparations of chloroplasts, microsomes and mitochondria is approximately 6:3:1.

### **1.5.1 Mitochondrial G3PAT**

G3PAT from plant mitochondria is relatively poorly characterised and has been purified from only a handful of plant sources. The enzyme has been reported as a soluble intermembrane protein in pea leaves (Frentzen, 1990) but as an outer membrane protein in potato tubers (Frentzen, *ibid.*) and an inner and outer membrane protein in castor bean endosperm (Vick and Beevers, 1977). Mitochondrial G3PAT is reported to display higher activities with acyl-CoA than acyl-ACP substrates and have a slight preference for unsaturated acyl-groups (Frentzen, 1993).

### 1.5.2 Microsomal G3PAT

The endoplasmic reticulum (ER) is the main site of the 'Eukaryotic' pathway.

Cytoplasmic G3PAT is membrane bound, localised to the ER (Frentzen *et al*, 1990) and uses acyl-CoA as substrate. Frentzen *et al* (1993) reports that microsomal G3PAT specifically uses acyl-CoA substrates and is inactive with acyl-ACP. A slight preference for 16:0- over 18:1-CoA was also reported.

### 1.5.3 Plastidial G3PAT

G3PAT has been purified from chloroplasts of various plant sources and is well characterised (Joyard and Douce, 1977; Bertrams and Heinz, 1981; Cronan and Roughan, 1987; Ishizaki *et al*, 1988; Fritz *et al*, 1995) - a table showing a selection of purified and cloned plastidial G3PATs is to be found in chapter 5, table 5.1. More recently, the 3D structure of squash G3PAT has been determined (Turnbull *et al*, 2001a,b). The protein is known to be nuclear encoded, transported to the plastid via a target peptide, which is cleaved to yield the mature, active protein. The processing site for cleavage of the target peptide has been predicted (Murata and Tasaka, 1997). In some plant species several G3PAT isoforms have been identified (Ishizaki *et al*, 1988; Nishida *et al*, 2000)

Acyl-ACP is the plastidial substrate for plastidial G3PAT. Reported substrate specificities and selectivities vary greatly between species, for example G3PAT from bean (*Phaseolus vulgaris*) has no substrate preference (Fritz *et al*, 1995) whereas G3PAT from pea (*Pisum sativum*) has a strong substrate preference for 18:1 acyl-groups. (Frentzen *et al*, 1994).

## 1.6 Aims and Objectives

Recent years have seen rapid advances in research on the principle reactions responsible for lipid synthesis and metabolism in plants. Commercial interest has been taken in the modification of plants to produce unusual and valuable fatty acids in oilseeds and to increase the resistance of crop plants to membrane damage suffered at low temperatures. Acyltransferases are known to have an important role to play in both of these processes. The biochemical study of recombinant chloroplast glycerol-3-phosphate acyltransferase has been the main goal of this thesis.

The first objective of this study was to develop a (pre-existing) assay for the glycerol-3-phosphate acyltransferase so that it could be performed *in vitro* under physiologically relevant conditions. The most 'relevant' conditions are dictated partly by the literature (for instance, using the reported pH(s) of the chloroplast stroma), but also by the performance of G3PAT proteins in the assay (the activity and substrate selectivity of G3PAT proteins can vary dramatically depending on the assay conditions used). G3PAT performance has been measured under a range of assay conditions. Single and dual substrate assays have been performed using a range of acyl-ACP and acyl-CoA substrates. The effect of variation of pH has been measured. Inclusion of BSA, cyclodextrin and other proteins at varying levels have also been investigated.

The second objective was to investigate amino acid residues in recombinant chloroplast glycerol-3-phosphate acyltransferase that are postulated to have a role in binding of either G3P or acyl-ACP substrates. In addition, with the 3D structure of squash G3PAT

available, investigation of residues recently identified as lining the acyl-binding pocket was also undertaken. Several residues have been substituted using site-directed mutagenesis and the resulting effect on catalytic activity and/or substrate selectivity has been determined for each mutant.

A mutant G3PAT with novel selectivity was identified by chance, separately from the site-directed mutagenesis studies. The final aim of this thesis was to characterise the novel mutant, in terms of activity, substrate selectivity and kinetic measurements and compare them to the 'wild-type' protein. Complimentary to this aim was the determination of the kinetic mechanism and order of substrate binding for squash glycerol-3-phosphate acyltransferase, to enable a model to be proposed for the mode of altered substrate selectivity.



## **Chapter 2**

# **Materials and Methods**

## 2.1 Materials.

Radiochemicals (radiolabelled fatty acids and glycerol-3-phosphate) were purchased from Amersham and used at a specific activity of 55 Ci/mol.

Fatty acids, azido-fatty acids and acyl-CoA substrates were purchased from Sigma.

ACP was provided as a freeze dried powder by John Gilroy, University of Durham.

Solvents were purchased from BDH, research grade.

Acrylamide solutions and SDS PAGE apparatus were purchased from Biorad.

Ecoscint A scintillation fluid was purchased from National Dianostics.

Ultrafree™ centrifugal filter units were purchased from Millipore.

Bactotryptone (pancreatic digest of casein) and yeast extract for LB broth were obtained from BBL and Oxoid respectively.

Milli-Q purified water (MQH<sub>2</sub>O) was prepared in the lab using a distillation unit connected to a Millipore Milli-Q Plus water purification system.

Chromatography matrices and columns were purchased from Pharmacia.

Acyl-ACP synthetase 'overexpression' strain (AASO) was a gift from the laboratory of John Shanklin, Department of Biology, Brookhaven National Laboratory, Upton, New York 11786. (Reference, T. K. Ray and J. E. Cronan, Jr. (1976) Activation of long chain fatty acids with acyl carrier protein: Demonstration of a new enzyme, acyl-acyl carrier protein synthetase in *Escherichia coli*. *Proc. Natl. Acad. Sci. USA* **73** pp. 4374–4378).

G3PAT cDNA clones were obtained as a gift from Norio Murata, National Institute for Basic Biology, Myodaiji, Okasaki 444, Japan.

Subcloned G3PAT clones were obtained from Johan Kroon, University of Durham.

Quickchange™ mutagenesis kit(s) were purchased from Stratagene.

All other substrates and reagents were purchased from Sigma, unless otherwise indicated in the text.

## **2.2 Production and purification of recombinant Acyl-ACP Synthetase (AAS).**

References: Rock and Cronan, 1979; Jackowski, Jackson and Rock, 1994; Shanklin, 2000.

### **2.2.1 Growth of the Acyl-ACP synthase 'overexpression' strain (AASO).**

Acyl-ACP synthase expressing strain was seeded onto an agar plate containing 50 µg/ml ampicillin and 50 µg/ml kanamycin and grown at 30°C for 36 hours. Colonies were used to inoculate eight 3 ml cultures which were grown at 30°C until the optical density at 600 nm ( $OD_{600}$ ) reached 0.6 units. Each 3 ml culture was used to inoculate a 500 ml culture of Luria-Bertani (LB) broth containing 50 µg/ml ampicillin and 50 µg/ml kanamycin.

LB broth contained (per litre):	Bactotryptone	10g
	Yeast extract	5g
	NaCl	10g

Cultures were grown at 30°C, with shaking at 120 rpm, until  $OD_{600}$  reached 0.6 units (approximately 3 hours). Cultures were then grown at 42°C for one hour to induce expression of AAS (plasmid is temperature sensitive), followed by 4 hours at 37°C, during which  $OD_{600}$  reached approximately 1 unit. Cultures were transferred to 4°C and harvested using a Beckman J2-HC (rotor JA 10.500) at 7,000 rpm for 15 minutes. Cell pellets were resuspended in 10 ml of ice cold 50 mM Tris-HCl pH 8.0 and transferred to 15 ml falcon tubes. The cell suspensions were spun for 15 minutes at 4,000 rpm in a Jouan MR1822 centrifuge to harvest the cells. The supernatant was removed and pellets snap frozen in liquid nitrogen and stored at -80°C until required.

### **2.2.2 Preparation of membranes containing AAS activity.**

(Reference: Rock and Cronan, 1979)

All procedures carried out at 4°C or (where possible) on ice. All buffers were ice-cold. Pellets from 500 ml cultures were thawed on ice and resuspended in 10 ml 50 mM Tris-HCl pH 8.0. Cells were lysed by 3 passes through a French pressure cell at setting 25,000psi and centrifuged in a Jouan MR1822 at 10,000 rpm for 15 minutes to pellet cell debris. The supernatant was removed and MgCl<sub>2</sub> was added to a final concentration of 10 mM. The sample was transferred to fresh (ultracentrifuge) tubes and spun at 100,000g for 90 minutes in a Beckman L-70 (rotor 70Ti). Pelleted membranes appeared as a clear pellet – these were resuspended in 50 ml of 50 mM Tris-HCl pH 8.0 containing 1 M NaCl (to remove extrinsically associated membrane proteins) and 20 mM MgCl<sub>2</sub>. The sample was spun at 100,000g for 90 minutes. The supernatant was removed, pelleted membranes (from 4 litres of AASO culture) were resuspended in a total of 30 ml 50 mM Tris-HCl pH 8.0 containing 2% Triton X-100 and 20 mM MgCl<sub>2</sub> to achieve a protein concentration of 2-5 mg/ml. The sample was stirred on ice for 30 minutes to dissolve the AAS. The sample was spun at 100,000g for 90 minutes to pellet undissolved material. The supernatant assayed for AAS activity (see 2.3). The pellet was resuspended in 50 mM Tris-HCl pH 8.0 containing 2% Triton X-100 and 20 mM MgCl<sub>2</sub> and assayed likewise. Typically >90% of AAS activity was detected in the supernatant at this point. The sample was loaded onto a Blue-Sepharose column for purification.

### **2.2.3 Purification of Acyl-ACP synthetase using Blue-Sepharose chromatography**

(Reference: Rock and Cronan, 1979)

A 40 ml blue-sepharose fast flow (Pharmacia) column was prepared and allowed to settle. The column was washed with 200 ml 50 mM Tris-HCl pH 8.0 containing 2% Triton X-

100 and 1 M NaCl. The column was washed with >200 ml MQH<sub>2</sub>O followed by 200 ml 50 mM Tris-HCl pH 8.0 containing 4 M guanidine hydrochloride. The column was washed with >200 ml MQH<sub>2</sub>O and re-equilibrated by washing with 200 ml 50 mM Tris-HCl pH 8.0 containing 2% Triton X-100.

The sample was loaded onto the column and washed on with 50 mM Tris-HCl pH 8.0 containing 2% Triton X-100. 2 x 50 ml passes were collected. The column was washed with 600 ml 50 mM Tris-HCl pH 8.0 containing 2% Triton X-100 and 1 M NaCl to remove proteins other than AAS (in particular thioesterases) – 1 x 600 ml pass was collected. No significant levels of AAS were detected in any of the passes. AAS was eluted with 50 mM Tris-HCl pH 8.0 containing 2% Triton X-100 and 0.5 M KSCN. 2 ml fractions were collected and assayed (see 2.3). AAS activity was greatest in fractions containing a slight yellow/green colouration (Rock and Cronan reported AAS co-purification with a red cytochrome but it appeared yellow/green). Active fractions were pooled and ATP was added to a final concentration of 5 mM (for increased enzyme stability). Pooled fractions were dialysed against 3 x 2l of 50 mM Tris-HCl pH 8.0 containing 2% Triton X-100 to remove KSCN. Samples were aliquotted, snap frozen in liquid nitrogen and stored at -80°C.

### 2.3.1 Low volume assay (for Blue-sepharose column fractions)

100 mM Tris-HCl pH 8.0  
400 mM LiCl  
10 mM MgCl<sub>2</sub>  
2 mM DTT  
10 mM ATP  
2% Triton X-100  
1 mg/ml holo-ACP  
30 μM 1-<sup>14</sup>C 16:0 fatty acid (1:20 dilution of a 600 μM stock at 55 Ci/mole in 5% Triton X-100)

Stop solution: 5 mM KPO<sub>4</sub> pH 7.2  
0.2 mg/ml BSA  
10 mM MgCl<sub>2</sub>  
50% v/v Isopropanol (IPA)  
1.25% v/v Glacial acetic acid

Extraction solution: Petroleum ether (40-60°C fraction); saturated with 50% v/v IPA containing 1 mg/ml palmitic acid.

49

counted using a Packard 1600 TR liquid scintillation analyser. Counts per minute (dpm) measured nmoles of radiolabelled fatty acid incorporated into 16:0-ACP (with uncombined fatty acid removed) in the 10 minute incubation period. This was used to calculate enzyme activity, taking into account the following:

The specific activity of the fatty acid substrate = 55Ci/mole

1  $\mu$ Ci =  $2.22 \times 10^6$  dpm

One unit of acyl-ACP synthase activity is defined as the amount of protein required to produce 1 nmole C<sub>16:0</sub>-ACP per minute.

### **2.3.2 Large volume assay (for acyl-ACP synthesis mixture)**

A 40  $\mu$ l aliquot of the acyl-ACP synthesis reaction mixture (section 2.4) was removed into a 15 ml glass falcon tube containing 2 ml of reaction 'Stop' solution (see above). The mixture was vortexed and 2 ml of 'Extraction' solution were added. The mixture was vortexed and centrifuged in a Sigma 204 benchtop (rotor 133/94) at 3,000 rpm for one minute. The petroleum ether (upper layer, containing extracted free fatty acids) was carefully removed using a fine-tipped pipette. 2 ml extraction solution were added and removed as described above twice more – three extractions were sufficient to remove all uncombined fatty acids. 1 ml of the lower layer (containing acyl-ACP – equivalent to 20  $\mu$ l of acyl-ACP synthesis reaction mixture) was removed, mixed with 4 ml Ecoscint A scintillation-fluid and counted using a Packard 1600 TR liquid scintillation analyser. A 20  $\mu$ l aliquot of the original reaction mixture was also counted. An estimation of the incorporation of radiolabelled fatty acid into acyl-ACP was then made by comparison of the two counts.

For example: Count of acyl-ACP with uncombined fatty acid removed = 200,000 dpm  
 Count of reaction mixture (acyl-ACP and uncombined fatty acid) =  
 300,000 dpm

Therefore % fatty acids in acyl-ACP synthesis reaction mixture  
 incorporated into acyl-ACP =  $(200,000/300,000) \times 100\% = 66.6\%$

## 2.4 Synthesis and isolation of radiolabelled acyl-ACP substrates.

### 2.4.1 Acyl-ACP synthesis

The acyl-ACP synthesis reaction mixture was prepared by addition of the following reagents:

<u>Reagent</u>	<u>ml added to 16:0 tube</u>	<u>ml added to 18:1 tube</u>	<u>Final Concentration</u>
1 M Tris-HCl	1.1	1.1	100 mM
2 M LiCl	2.2	2.2	400 mM
1 M MgCl <sub>2</sub>	0.11	0.11	10 mM
50 mM DTT	0.44	0.44	2 mM
100 mM ATP (in Tris-HCl pH 8)	0.55	0.55	5 mM
20% Triton X-100	0.33	0.33	1%
1 mg/ml ACP (20 mM HEPES pH 6.8)	5.0	5.0	33 µM
<sup>14</sup> C 16:0 (600 µM; 55 Ci/mol; 5% Triton X-100	0.46	-	25 µM
<sup>3</sup> H 18:1 (600 µM; 55 Ci/mol; 5% Triton X-100	-	0.46	25 µM
Acyl-ACP Synthetase	0.8	0.8	33 U/ml
	11.0 ml	11.0 ml	Total volume

**Table 2.1 Acyl-ACP synthesis reaction conditions**

The reaction was incubated in a 30°C water bath for 12 hours, after which an aliquot was removed for assay (section 2.3) to ensure the reaction had produced a sufficient (>50%) yield of acyl-ACP.



#### **2.4.2 Isolation of acyl-ACP substrates using ion-exchange and hydrophobic interaction chromatography.**

A 10 ml Q-sepharose FF column was prepared, storage 20% ethanol was removed by washing with 20 ml of MQH<sub>2</sub>O. Bound material was removed by washing with 30 ml 20 mM Tris-HCl pH 7.0 containing 1 M NaCl. The column was washed with 40 ml MQH<sub>2</sub>O and equilibrated with 30 ml 20 mM Tris-HCl pH 7.0. The sample was diluted x4 with 20 mM Tris-HCl pH 7.0 to bring the LiCl concentration to  $\leq 100$  mM and loaded onto the column which was then washed with 40 ml 20 mM Tris-HCl pH 7.0. This was collected as Pass 1 (uncombined fatty acids do not bind to the Q-sepharose column). The sample was eluted with 20 mM Tris-HCl pH 7.0 containing 1 M NaCl. Fractions were collected using a Gilson fraction collector, fraction size was 80-100 drops (approximately 2 ml). An aliquot of 5  $\mu$ l of each fraction and 100  $\mu$ l of Pass 1 were counted using a Packard 1600 TR liquid scintillation analyser. Radioactive fractions were pooled, mixed and counted again to determine % <sup>14</sup>C-acyl-ACP formation.

A 10 ml octyl-sepharose FF column was prepared, storage 20% ethanol was removed by washing with 20 ml of MQH<sub>2</sub>O. Bound material was removed by washing with 40 ml 20 mM Tris-HCl pH 7.0 containing 80% v/v IPA. IPA was carefully removed by washing the column with >300 ml MQH<sub>2</sub>O. The column was equilibrated by washing with 20 ml 20 mM Tris-HCl pH 7.0. Pooled fractions from the Q-sepharose column were loaded onto the octyl-sepharose column and the column washed with 20 ml 20 mM Tris-HCl pH 7.0. This was collected as Pass 1 (ACP does not bind to the octyl-sepharose column). The column was re-equilibrated with 20 ml 20 mM N-ethyl morpholine acetate (NEMAc (volatile)) buffer pH 7.0. This was collected as Pass 2. The sample was eluted with 20 ml 20 mM NEMAc containing 40% v/v IPA. Fractions were collected in a Gilson fraction

collector, fraction size was 80-100 drops. 5 µl of each fraction and 100 µl of Pass 1 were mixed with 4 ml Ecoscint A scintillation-fluid and counted using a Packard 1600 TR liquid scintillation analyser. Acyl-ACP was found to elute in the first few fractions containing IPA – IPA drop-size is smaller and so these fractions are identifiable by their lower volume (fraction size is approximately 1ml). Radioactive fractions were pooled, mixed and counted again to determine % acyl-ACP recovery. Sample volume was reduced in a Jouan RC10.22 vacuum centrifuge until the acyl-ACP concentration reached approximately 80-100 µM. As IPA and NEMAc are volatile, Tris-HCl was added to give a final concentration of 50 mM in the concentrated sample. Acyl-ACP samples were snap frozen in liquid nitrogen and stored at –20°C prior to use.

## **2.5 Production and purification of recombinant G3PAT proteins.**

### **2.5.1 Production of squash G3PAT**

Squash G3PAT protein was expressed in *E. coli* BL21 (DE3) containing the pET 24a vector system, under the influence of the T7 promoter/DNA polymerase system (clone was obtained as a gift from Norio Murata, National Institute for Basic Biology, Myodaiji, Okasaki 444, Japan). Transformed cells were grown in 0.5 litre cultures (of L-B broth) at 37°C and induced to produce G3PAT by the addition of IPTG to a final concentration of 0.4 mM. Cells were grown for a further 3 hours after the addition of IPTG before harvesting using a Beckman J2-HC (rotor JA 10.500) at 7,000 rpm for 15 minutes. G3PAT production was confirmed using SDS PAGE, figure 2.1.

### **2.5.2 Preparation of crude, cell-free protein extracts (CFEs) of squash G3PAT**

Cell pellets were resuspended in 10 ml of ice cold 20 mM Tris-HCl pH 7.4 and transferred

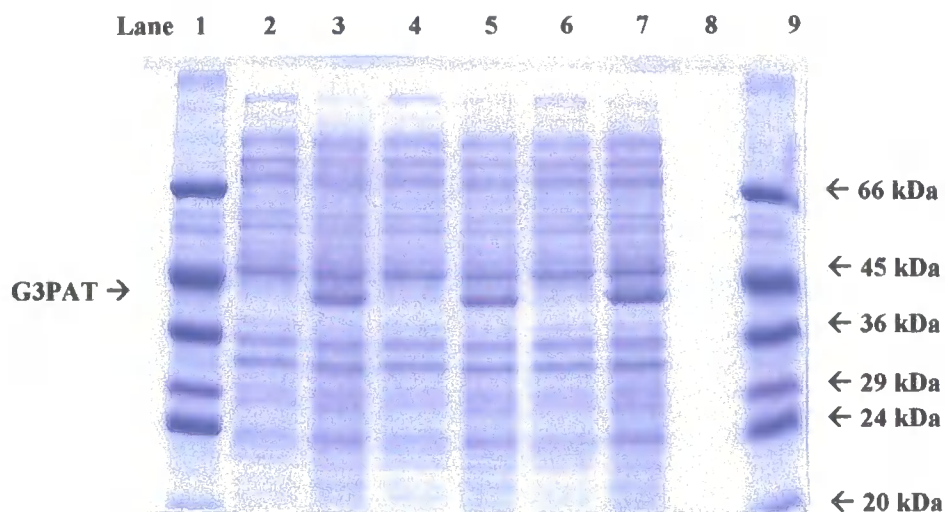


**Figure 2.1 SDS PAGE gel of *E. coli* cell lysates demonstrating production of the squash G3PAT protein.** Lanes 1 and 9 SDS7 molecular weight markers (from top) BSA, 66 kDa, Ovalbumin, 45 kDa, G-3-PDHe, 36 kDa, Bovine carbonic anhydrase, 29 kDa, Bovine trypsinogen, 24 kDa, Soybean trypsin inhibitor, 20 kDa, ( $\alpha$ -lactalbumin, 14.2 kDa - not on gel). Lanes 2, 4 and 6 Total protein from 50  $\mu$ l *E. coli* cells at OD<sub>600</sub> of 0.6 units (extracted by boiling for 5 minutes in SDS PAGE loading buffer) prior to addition of IPTG. Lanes 3, 5 and 7 Total protein from 50  $\mu$ l *E. coli* cells at OD<sub>600</sub> of approx 0.8 units, three hours after the addition of IPTG to a final concentration of 0.4 mM. (Lane 8 blank).

to 15 ml falcon tubes. The cell suspensions were centrifuged for 15 minutes at 4,000 rpm in a Jouan MR1822 centrifuge to harvest the cells. Cells were lysed in 20 mM Tris-HCl pH 7.4 using 3 freeze/thaw cycles in dry ice/ethanol and ice/water baths (Johnson and Height, 1994) and samples were centrifuged at 100,000 g for 1 hour at 4°C using a Beckman L-70 (rotor 70Ti) ultracentrifuge. The supernatant (a crude, cell-free soluble protein extract, CFE) was removed and tested for G3PAT activity (section 2.9). Confirmation of G3PAT presence in the extract was obtained by SDS PAGE analysis, figure 2.2. The amount of protein present in the G3PAT band was calculated via densitometric comparison with bands of known amounts of BSA, section 2.8.

### **2.5.3 Preparation of purified G3PAT**

G3PAT protein was purified from the supernatant via anion-exchange chromatography. A 40 ml Q-sepharose FF column was prepared, storage 20% ethanol was removed by washing with 100 ml of MQH<sub>2</sub>O. Bound material was removed by washing with 100 ml 20 mM Tris-HCl pH 7.0 containing 1 M NaCl. The column was washed with 200 ml MQH<sub>2</sub>O and equilibrated with 100 ml 20 mM Tris-HCl pH 7.0. CFE of squash G3PAT (approximately 5 mgs total protein) was loaded onto the column and washed on with 100 ml 20 mM Tris-HCl pH 7.0, collected as Pass 1. G3PAT was eluted with a gradient of lysis buffer containing 0 - 2M NaCl over 500 ml. Enriched fractions were pooled and NaCl was removed by dialysis against 20 mM Tris-HCl pH 7.0. Where necessary, sample was concentrated using Ultrafree™ centrifugal filter units with a 5 kDa molecular weight cut-off. Enriched fractions containing G3PAT activity were analysed by a combination of SDS PAGE and densitometric scanning to assess purity and quantify the levels of G3PAT protein in each fraction. The final, highly purified preparation contained a single band of 42 kDa demonstrated on SDS PAGE, figure 2.3.

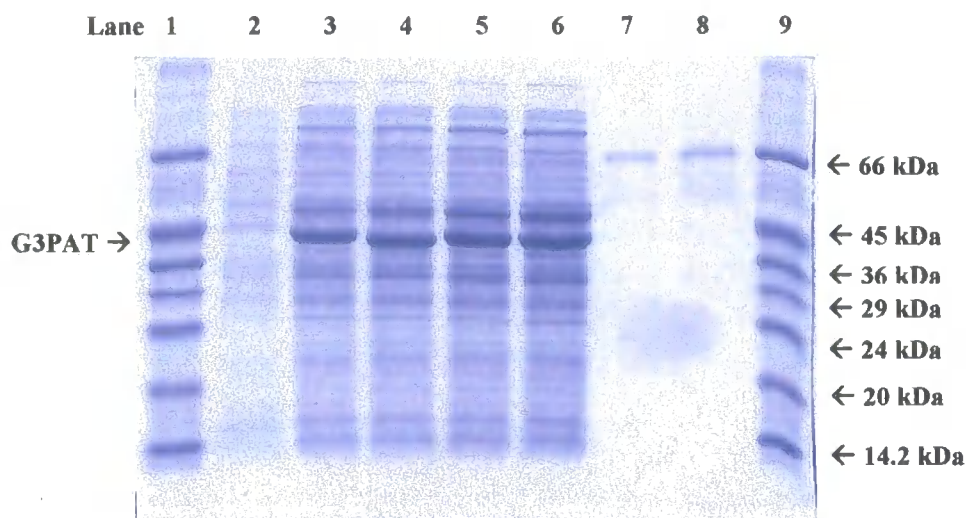


**Figure 2.2 SDS PAGE gel of *E. coli* cell-free extracts (CFEs) to demonstrate the presence of the squash G3PAT protein. Lanes 1 and 9** SDS7 molecular weight markers (from top) BSA, 66 kDa, Ovalbumin, 45 kDa, G-3-PDHe, 36 kDa, Bovine carbonic anhydrase, 29 kDa, Bovine trypsinogen, 24 kDa, Soybean trypsin inhibitor, 20 kDa,  $\alpha$ -lactalbumin, 14.2 kDa - not on gel. **Lane 2** Total protein from 50  $\mu$ l *E. coli* cells at OD<sub>600</sub> of 0.6 units (extracted by boiling for 5 minutes in SDS PAGE loading buffer) prior to addition of IPTG. **Lanes 3, 4, 5 and 6** 5, 5, 7 and 7  $\mu$ l respectively of squash G3PAT CFE. **Lanes 7 and 8** 100 ng and 200 ng respectively of BSA (the 66 kDa BSA band in lane 9 contained 1  $\mu$ g BSA). (Lane 8 blank).

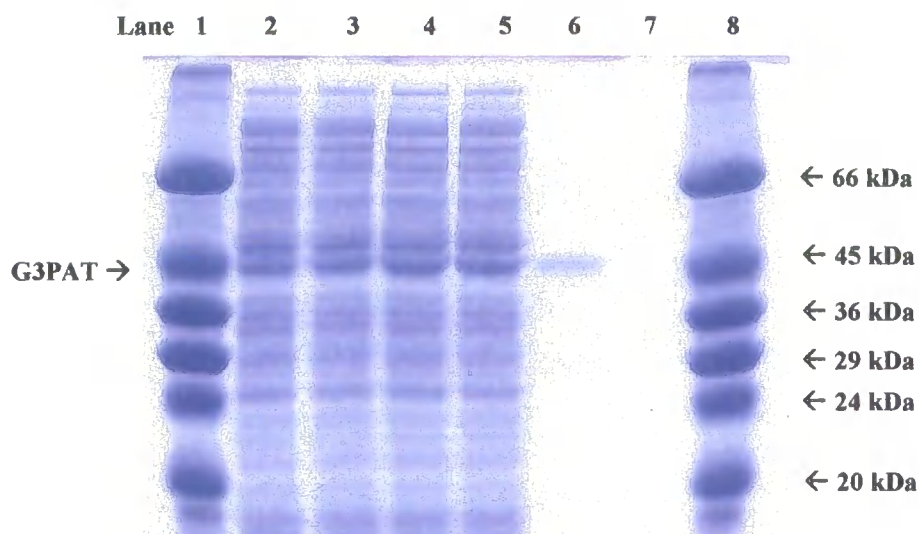


**Figure 2.3 SDS PAGE gel of squash G3PAT CFEs and purified protein.** Lanes 1 and 8 SDS7 molecular weight markers (from top) BSA, 66 kDa, Ovalbumin, 45 kDa, G-3-PDHe, 36 kDa, Bovine carbonic anhydrase, 29 kDa, Bovine trypsinogen, 24 kDa, Soybean trypsin inhibitor, 20 kDa, ( $\alpha$ -lactalbumin, 14.2 kDa - not on gel). Lanes 2, 3, 4 and 5 7  $\mu$ l of squash G3PAT CFE Lane 6 Approximately 100 ng of purified squash G3PAT – seen as a single band at 42 kDa. (Lane 7 blank).

## **2.6 SDS PAGE**

(Reference: Sambrook, Fritsch and Maniatis, 1989)

Apparatus used was the Mini Protean II system. Assembly of gel apparatus, gel preparation and electrophoresis were performed as described by Maniatis *et al*, (1989) and in the Biorad literature accompanying the Mini Protean II system.

### **2.6.1 12% SDS PAGE electrophoresis**

Samples were prepared by diluting into 1x SDS loading buffer and boiling for 5 minutes immediately prior to loading.

1x SDS loading buffer:

50 mM Tris-HCl (pH 6.8)

100 mM dithiothreitol

2% SDS

0.1% bromophenol blue

10% glycerol

Samples were electrophoresed at 100 volts (stacking gel) and at 200 volts (resolving gel).

All G3PAT proteins were resolved on 12% SDS PAGE gels. Gels were stained using Coomassie Brilliant Blue (Sigma) and destained in 10% glacial acetic acid; 1% glycerol.

### **2.6.2 18% Urea gel electrophoresis**

(reference: Post-Beittenmiller, Jaworski and Ohlrogge, 1990)

All ACP and acyl-ACP samples were electrophoresed on native (non-denaturing) polyacrylamide gels.

Resolving gel solution:

6.0 ml 30% Acrylamide:Bis-acrylamide (37.5:1) solution

2.5 ml 1.5 M Tris-HCl pH 9

0.625 ml 8 M urea

0.875 ml MQH<sub>2</sub>O

100 µl 10% w/v Ammonium persulphate

10 µl TEMED

Stacking gel solution:

1.5 ml 30% Acrylamide:Bis-acrylamide (37.5:1) solution  
2.5 ml 0.5 M Tris-HCl pH 6.8  
0.625 ml urea  
5.265 ml MQH<sub>2</sub>O  
100 µl 10% w/v Ammonium persulphate  
10 µl TEMED

Running (tank) buffer:

30.2g Tris (base)  
144g Glycine  
to 1 litre with MQH<sub>2</sub>O

Samples were prepared by diluting into 1x sample loading buffer.

1x sample loading buffer:

50 mM Tris-HCl (pH 6.8)  
0.1% bromophenol blue  
10% glycerol

Samples were electrophoresed at 100 volts. Gels were stained using Coomassie Brilliant Blue (Sigma) and destained in 10% glacial acetic acid; 1% glycerol.

## **2.7 Quantification of G3PAT in crude cell-free extracts (CFEs) and purified protein extracts via densitometric scanning**

Scanned polyacrylamide gels were analysed using the Biorad Multi-Analyst® PC Image Analysis software. Pixel density and band area were acquired using the GS-690 densitometer system. G3PAT bands were compared with known standards (on the same gel) of BSA and/or ovalbumin to estimate the quantity of G3PAT protein on the gel(s).



## **2.8 Standard lysophosphatidic acid (LPA) extraction and quantification**

Chloroform:methanol (1:1) was added to 1.5 ml eppendorf tubes in aliquots of 710  $\mu$ l.

The G3PAT assay reaction mixture was prepared (sections 2.9-2.11). After initiation of the G3PAT reaction, 80  $\mu$ l aliquots of the reaction mixture were removed into the eppendorf tubes containing chloroform:methanol, at timed intervals, to stop the reaction. To each tube 280  $\mu$ l of 1 M KCl/0.2 M H<sub>2</sub>PO<sub>4</sub> was added, vortexed and centrifuged at 13,000 g for 10 minutes. The mixture was partitioned under g-force into an upper aqueous layer (containing the product ACP) and a lower organic layer (containing the product, LPA, which was radiolabelled). 250  $\mu$ l of the lower layer was removed using a Hamilton syringe, the needle wiped and the sample transferred into a scintillation vial. The samples were dried in a Jouan RC10.22 vacuum centrifuge and resuspended in 280  $\mu$ l ethanol. 280  $\mu$ l Ecoscint A was added, tubes vortexed and counted using a Packard 1600 TR liquid scintillation analyser (single isotope (either <sup>14</sup>C or <sup>3</sup>H) counting for single substrate assays, dual isotope counting for assays using <sup>14</sup>C and <sup>3</sup>H-labelled substrates).

## **2.9 Assay for G3PAT activity**

### **2.9.1 Reaction mixtures**

The following reaction mixture was prepared to measure G3PAT activity using acyl-ACP substrate:

250 mM HEPES buffer pH 8.0  
300  $\mu$ M G3P  
5 mg/ml BSA  
2  $\mu$ M [ $1\text{-}^{14}\text{C}$ ] 16:0-ACP or [ $9,10\text{-}^3\text{H}$ ] 18:1-ACP (acyl group radiolabelled at a specific activity of 55 Ci/mole or 120,000 dpm/nmole)

The following reaction mixture was prepared to measure G3PAT activity using acyl-CoA substrate:

250 mM HEPES buffer pH 8.0  
5 mg/ml BSA  
400  $\mu$ M 16:0-CoA or 18:1-CoA  
30  $\mu$ M [ $\text{U-}^{14}\text{C}$ ] G3P (radiolabelled at a specific activity of 4.5  $\mu$ Ci/ $\mu$ mole - or 10,000 dpm/nmole).

### **2.9.2 Substrate quality**

The reaction mixture was divided into 340  $\mu$ l aliquots. 80  $\mu$ l of the reaction mixture was removed and processed as described in section 2.8 to quantify any free fatty acids (when using radiolabelled acyl-ACP) in the reaction mixture at the start of the reaction – this figure is counted as time = zero ( $T_0$ ) or ‘background’. Free fatty acids would be present if the acyl-ACP substrate had undergone any hydrolysis during storage – usually < 1%. If greater than 2% of the radioactivity was contributed by free fatty acids the sample was discarded and a fresh aliquot used. The  $T_0$  value when using radiolabelled G3P measured the amount of G3P present in the organic phase – usually very low (<0.1%).

### 2.9.3 Reaction initiation

The aliquots (now 260  $\mu$ l) of reaction mixture were mixed with 210  $\mu$ g of G3PAT protein to initiate the reaction and 80  $\mu$ l aliquots were removed at suitable time intervals (usually 1, 2 and 3 minutes but longer if the enzyme was active at a low level) and transferred to an eppendorf tube containing 710  $\mu$ l chloroform:methanol (1:1). LPA was isolated using phase partition, as described in section 2.8, and counted in the liquid scintillation counter (LSC) using a single isotope counting protocol.

Enzyme activity was plotted as pmol LPA formed per minute. This assay was most often used to identify active fractions during purification of G3PAT proteins.

### 2.10 Assay for G3PAT selectivity

(1 unit of G3PAT enzyme activity (U) = amount of enzyme required to transfer 1 pmol of fatty acid to G3P per minute).

The following reaction mixture was prepared to measure G3PAT selectivity using acyl-ACP substrates:

- 250 mM HEPES buffer pH 8.0
- 300  $\mu$ M G3P
- 5 mg/ml BSA
- 1  $\mu$ M [1- $^{14}$ C] 16:0-ACP (55 Ci/mole)
- 1  $\mu$ M [9,10- $^3$ H] 18:1-ACP (55 Ci/mole)

[The following reaction mixture may be prepared to measure G3PAT selectivity using acyl-CoA substrates but has not been performed by the author:]

- 250 mM HEPES buffer pH 8.0
- 5 mg/ml BSA
- 300  $\mu$ M G3P
- 10  $\mu$ M [1- $^{14}$ C] 16:0-CoA (55 Ci/mole)
- 10  $\mu$ M [9,10- $^3$ H] 18:1-CoA (55 Ci/mole)

The reaction mixture was divided into 340  $\mu$ l aliquots. An aliquot of 80  $\mu$ l of the reaction mixture was removed from each reaction tube and used to calculate  $T_0$  values as described in section 2.9. G3PAT protein was added to the remaining reaction mixture (210  $\mu$ g to start the reaction) and 80  $\mu$ l aliquots were removed at suitable time intervals (usually 1, 2 and 3 minutes). Removed aliquots were transferred to eppendorf tubes containing 710  $\mu$ l chloroform:methanol (1:1) and LPA was isolated as described in section 2.8. Samples were counted in a liquid scintillation counter using a dual isotope counting protocol to quantify levels of [ $1\text{-}^{14}\text{C}$ ] 16:0-LPA and [ $9,10\text{-}^3\text{H}$ ] 18:1-LPA present.

Picomoles of both 16:0 and 18:1-LPA present in each of the 'timepoints' tested were calculated and the data were plotted as pmoles of 16:0 and 18:1-LPA formed over time. This is how the majority of substrate selectivity assay data is presented in this thesis. The assay can also be used to assess activity of G3PAT proteins using a standardised amount of protein under standard conditions by addition of the rates of 16:0 and 18:1-LPA formation under the conditions given above.

### **2.11 G3PAT assay using short chain substrates**

C<sub>4</sub>:0-CoA and C<sub>6</sub>:0-CoA substrates were purchased from Sigma. Assays were carried out in 250 mM HEPES NaOH pH 8.0 containing 5.0 mg/ml BSA with 33  $\mu$ M [1-<sup>14</sup>C] G3P (55 Ci/mol) and 0.1 mM acyl-CoA, in a total volume of 20  $\mu$ l. Assays were initiated by the addition of 16.25 ng of G3PAT and terminated after 5 minutes by the addition of 40  $\mu$ l of chloroform/ methanol (1:1). The samples (total volume 60  $\mu$ l) were mixed and loaded onto a TLC plate and run for three hours in Butanol:Acetic Acid:Water 5:2:3 to separate LPA from unreacted [1-<sup>14</sup>C] G3P. The TLC plate was exposed to photographic film before the LPA spot was scraped into 1 ml methanol, vortexed and added to 4 ml Ecoscint A. Samples were counted in a Packard liquid scintillation counter to determine the rate of incorporation of acyl-CoA into LPA.

### **2.12 Assay to determine binding of acyl-ACP and G3P substrates to G3PAT**

Radiolabelled [9,10-<sup>3</sup>H] 18:1-ACP, [1-<sup>14</sup>C] 16:0-ACP or [1-<sup>14</sup>C] G3P (100 pmoles of each at 55 Ci/mol) were incubated with 50 pmoles of G3PAT in the absence of the other substrate(s) for 5 minutes in 250 mM HEPES buffer pH 8.0. The samples (total volume 200  $\mu$ l) were centrifuged through a 30,000 Da molecular weight cut off membrane (Millipore Ultrafree® MC filter unit) and the radioactivity above and below the membrane determined. Radiolabelled substrate bound to G3PAT was retained by the membrane in the upper compartment, unbound substrate passed through the membrane into the lower compartment. In earlier experiments we determined that neither substrate was retained by this 30,000 Da cut off membrane or bound to boiled (denatured) G3PAT (ratio was less than 0.08 moles of substrate bound per mole of enzyme). Sample volume in both compartments was readjusted to 200  $\mu$ l and the sample removed and added to 4 ml

Ecoscint A prior to counting in a Packard liquid scintillation counter. Assays were performed in triplicate.

### **2.13 Microdialysis of BSA/acyl-ACP mixtures**

Radiolabelled [9,10-<sup>3</sup>H] 18:1-ACP and [1-<sup>14</sup>C] 16:0-ACP (both at 1.1  $\mu$ M) were mixed with BSA at either 1.25 or 5.0 mg/ml BSA in 250 mM HEPES-NaOH buffer pH 8.0 in a total volume of 100  $\mu$ l. The mixtures were incubated for 10 minutes at room temperature prior to dialysis for four hours against 2 ml 250 mM HEPES-NaOH buffer pH 8.0 through a 30,000 Da molecular weight cut-off membrane. Aliquots of the dialysis buffer were counted at intervals of 0.5, 1, 2, 3 and 4 hours to track dialysis of the acyl-ACPs through the membrane. When no BSA was used, >95% of both acyl-ACPs had dialysed through the membrane into the external buffer after 4 hours of dialysis.

## 2.14 Measurement of standard error values

Definitions:

SS = the sum of the squares of deviations of experimental values

n = the number of times the experiment was performed

$\sigma^2$  = experimental variance

S.E.M. = 1 standard error measurement

Standard error measurements given in this thesis have been calculated using the following formulae:

$$\sigma^2 = SS/(n-2)$$

and

$$S.E.M. = \sqrt{\sigma^2} = \sqrt{SS/(n-2)}$$

As defined in Fundamentals of Enzyme Kinetics by Athel Cornish Bowden:

“If the number of observations  $n$  in each experiment is infinite, then the true value of the parameter will lie within one estimated standard deviation of the calculated parameter in about 68% of this universe of conceivable experiments.... one may take two and three times the standard error as confidence limits for 95% and 99% respectively.”

It should also be noted that S.E.M. can only be calculated where the experiment has been repeated three or more times.

# **Chapter 3**

## **Development of an assay for G3PAT activity.**

**Investigation of factors that influence assay  
performance and determination of the range of  
permissible enzyme substrates.**



### 3.1 Introduction

Glycerol-3-phosphate acyltransferase (G3PAT) catalyses the transfer of a fatty acid group from an acyl donor to glycerol-3-phosphate at position *sn*-1. This reaction yields 1-acylglycerol-3-phosphate (or lysophosphatidic acid; LPA). In the 1960's Barron and Stumpf were the first to identify the activity of this class of enzyme in purified microsomal fractions from avocado (*Persea americana*) and G3PAT activity was subsequently identified in the chloroplasts, cytoplasm and mitochondria of several plant species (examples are given in Tables 5.1 and 5.2, chapter 5).

G3PAT in plant chloroplasts is a soluble protein localised to the stroma (Roughan and Slack, 1982) whereas cytoplasmic and mitochondrial G3PAT forms are membrane bound (Frentzen *et al*, 1983). These two forms are different proteins with distinct structures and substrate specificities. Plastidial G3PAT has a proven role (Murata *et al*, 1992) in the determination of membrane phospholipid composition which influences the sensitivity of plants to low, non-freezing or 'chilling' temperatures (2-6°C). Due to the impact that chilling sensitivity/resistance may have on levels of cold damage to crop plants and agricultural productivity, much interest has been taken in the study of G3PAT enzymes from a variety of plant sources, both chilling sensitive and tolerant. To assist purification of G3PAT it has been essential to develop assays for G3PAT activity. In order to determine whether the enzyme from a particular species has a substrate preference, assays that can differentiate between selective and non-selective forms are necessary.

In 1976, Bertrams and Heinz began to develop an assay for the acyl-CoA:*sn*-glycerol-3-phosphate acyltransferase reaction, using  $^{14}\text{C}$  radiolabelled glycerol-3-phosphate to measure acylation rates. This was one of the first attempt to develop a sensitive, low volume assay for G3PAT activity. Soluble and membrane bound fractions from spinach chloroplasts were used in a HEPES buffer system. Palmitoyl-CoA was the acyl donor and radiolabelled G3P ensured that acylation rates could be accurately followed. Full details of the reaction conditions are shown in Table 3.1. Assays were optimised with the objective of achieving maximum acylation rates. During assay optimisation, several interesting details were noted. These included:

1. Acylation rates were pH dependant with an optimum of approximately pH 7-8.
  2. When low G3PAT protein levels were used acylation rates were only linear if Bovine Serum Albumin (BSA) was included in the assay. The optimum rate occurred with BSA at 15 mg/ml.
  3. Maximum acylation rates were achieved when 16:0-CoA was present at 1.5mM
- The group postulated that the acyl-CoA:*sn*-glycerol-3-phosphate acyltransferase from spinach used the acyl-CoA substrate dispersed in a micellar form.

Component	Concentration in assay
HEPES-NaOH buffer pH 7.5	40 mM
G3P	200-250 $\mu\text{M}$
BSA	15mg/ml
Palmitoyl-CoA	750 $\mu\text{M}$
G3PAT protein solution	0.25 - 0.375 $\mu\text{g/ul}$

**Table 3.1 Summary of the reaction conditions used in acyl-CoA:*sn*-glycerol-3-phosphate acyltransferase assays by Bertrams and Heinz, 1976.**

Previously, Lamb and Fallon (1972) had investigated the activity of acyl-CoA:*sn*-glycerol-3-phosphate acyltransferase from rat liver microsomes. Using palmitoyl-CoA as the acyl donor and BSA levels of between 0 and 3.75 mg/ml, acylation rates were measured. Several important observations were made:

1. High levels of 16:0-CoA (above 30  $\mu$ M) cause inhibition of the G3PAT reaction.
2. BSA was shown to reduce inhibition of the G3PAT reaction caused by high 16:0-CoA concentrations, with 3.75 mg/ml giving the maximum acylation rate.

The group offered several theories to explain the effects noticed when BSA was included in the assays. One was that acyl-CoA deacylase activity is lowered by BSA. Deacylases, esterases that specifically hydrolyse fatty acyl-ester bonds, would reduce the pool of substrate available to the G3PAT enzyme. Another was that BSA may bind fatty acids released during the G3PAT reaction which would otherwise cause product inhibition, or that 'albumin activation' could occur. The enzyme is in a dilute solution with few other proteins in the reaction mixture and BSA may increase acylation rates via indirect stabilisation of the G3PAT protein. However, the best supported explanation was that BSA binds the acyl-CoA substrate and lowers the free acyl-CoA concentration to below the critical micelle concentration (CMC), reducing the inhibitory effects previously observed. This idea supports the suggestion of Bertrams and Heinz (1976) that acyl-CoA substrate is delivered to G3PAT in a micellar form.

Bertrams and Heinz continued to investigate acyl-CoA:*sn*-glycerol-3-phosphate acyltransferase activity in plant protein extracts. In 1981, important observations were

made using extracts from pea and spinach chloroplasts (Bertram and Heinz, 1981, for experimental conditions see table 3.2):

1. The pea plant has two G3PAT isofoms.
2. Thioesters (16:0-CoA substrate) were inhibitory above a concentration of 20  $\mu\text{M}$ .

This inhibition was counteracted by BSA, optimally at 6 mg/ml. Both pea isoforms exhibited maximum acylation rates when BSA was present at 6-10 mg/ml.

3. A buffer concentration of 250-300 mM produced maximum acylation rates.
4. The  $K_m$  for G3P was estimated to be approximately 0.7 mM.

The group explained the effect of BSA (point 1.) as BSA binding to acyl-CoA and reducing the concentration of free thioester in solution, agreeing with previous suggestions of how BSA reduced the inhibition of G3PAT. This work was also helpful as it provided useful guidelines for future researchers assaying G3PAT activity, specifically outlining the optimum concentrations of BSA, buffer and G3P.

Component	Concentration in assay
MOPS-NaOH buffer pH 7.4	250 mM
BSA	6 mg/ml
16:0-CoA	400 $\mu\text{M}$
G3P (0.3 Ci/mol)	2 mM
Pea and Spinach enriched protein extract	3.125 – 37.5 $\mu\text{g/ml}$
<b>Total</b>	

**Table 3.2 Summary of the reaction conditions used in acyl-CoA:sn-glycerol-3-phosphate acyltransferase assays by Bertrams and Heinz 1981.**

The natural substrate of plastidial G3PAT is acyl-ACP, not acyl-CoA (Frentzen *et al*, 1983). Traditionally, due to the commercial availability of a wide variety of acyl-CoAs,

experiments on both acyl-CoA:*sn*-glycerol-3-phosphate acyltransferase and acyl-ACP:*sn*-glycerol-3-phosphate acyltransferase have been performed using acyl-CoA substrates. However, the performance of this second group of enzymes, some of which are already known to exhibit selectivity for particular substrates over others, may be greatly different with acyl-CoAs than with the natural substrate, acyl-ACPs. For this reason it was recognised that assays using acyl-ACPs were likely to give results most similar to those *in vivo*. Following the reported purification and cloning of the *E.coli* gene for acyl-ACP synthetase (Rock and Cronan, 1979), it became possible to enzymatically synthesise acyl-ACP substrates for use in assays for G3PAT activity and substrate selectivity.

Frentzen *et al* (1983) continued to investigate G3PAT activity in extracts from pea and spinach chloroplasts. This group was the first to use acyl-ACP substrates in such assays and took the additional step of using substrate 'mixtures' comprising of palmitoyl-ACP and oleoyl-ACP thioesters to study the substrate selectivity of the G3PAT proteins. This approach has subsequently been employed by several groups investigating whether G3PAT proteins have preferences for particular substrates over others. For a summary of the experimental conditions used by Frentzen *et al* (*ibid*), see table 3.3. The work was also important as it indicated that the selectivity of acylation at the *sn*-1 position was dependant not only on the concentrations of acyl-ACP thioesters but also on the concentration of glycerol-3-phosphate. In addition it was demonstrated that, given the competitive conditions of oleoyl-ACP against oleoyl-CoA substrates, *sn*-glycerol-3-

phosphate acyltransferase would preferentially incorporate 18:1 fatty acid from the oleoyl-ACP: G3PAT prefers acyl-ACP substrates.

Component	Final concentration
MOPS-NaOH buffer pH 7.4	250 mM
BSA	0.125-0.5 mg/ml
18:1-ACP and 16:0-ACP (in different ratios)	4.5 $\mu$ M in total
G3P	1 mM
Pea and spinach purified acyltransferase fractions	3.75-7.5 $\mu$ g/ml

**Table 3.3 Summary of the reaction conditions used in G3PAT assays by Frentzen *et al* in 1983.**

Frentzen *et al* purified acyl-ACP:*sn*-glycerol-3-phosphate acyltransferase from the chloroplasts of squash and investigated its properties (Frentzen *et al*, 1987). Assay conditions used are detailed in Table 3.4. Again, several interesting observations were made using 18:1-ACP/16:0-ACP competitive conditions:

1. Alteration of the pH from pH 7.4 to pH 8.0 does not affect total acylation rates but can alter substrate selectivity. At the lower pH there is increased discrimination against 16:0.
2. This discrimination against 16:0 was also observed when the concentration of G3P was reduced from 30 to 0.3 mM.
3. Variation in the concentration of the thioester mixes (but not the ratio of 18:1 to 16:0) did not alter the resulting fatty acid selectivity.

It should be noted that three isomeric forms of stromal G3PAT were identified from squash (Frentzen *et al*, *ibid.*), designated AT1, AT2 and AT3. AT2 and 3 are very similar in properties having different pH optima,  $V_{max}$  and substrate preference to AT1.

AT1 is thought to have a preference for 18:1-ACP over 16:0-ACP, whereas AT2 and AT3 are non-selective.

Component	Final concentration
HEPES-NaOH buffer pH 7.4	250 mM
BSA	1.25 mg/ml
18:1-ACP, 18:0-ACP and 16:0-ACP	3-8 $\mu$ M
G3P	0.3-30 mM
Purified acyltransferase fractions of AT1, AT2 and AT3	25, 9000 and 6875 ng/ml respectively

**Table 3.4 Summary of the reaction conditions used in G3PAT assays by Frentzen *et al*, 1987.**

The group also emphasised the point that stromal ACP-thioester concentrations had been found to be approximately 4  $\mu$ M in illuminated chloroplasts, whereas in dark conditions the concentration of ACP-thioesters immediately dropped to zero (Soll and Roughan, 1982; Roughan, 1986). As the pH of an illuminated chloroplast stroma is 8.0, but under dark conditions it is pH 7.4 (Lea and Leegood, 1993), this indicates that the *in vivo* plastidial acyltransferases are only provided with substrates when the pH of the stroma is 8.0. This has considerable implications for assays of these enzymes and indicates that G3PAT normally functions *in vivo* at pH 8.0 with total acyl-ACPs at 4 $\mu$ M - these may be the most physiologically relevant conditions at which to carry out assays of G3PAT activity and selectivity.

Sauer and Heise (1983) used the uptake of exogenous radiolabelled G3P by isolated spinach chloroplasts to calculate the stromal concentration of G3P. They reported a stromal G3P concentration of between 0.1-0.2 mM. These calculations, however, were dependant on an estimation of stromal volume, not an experimentally validated figure.

Taking into account the work and findings of the various groups performing assays on G3PAT enzymes, it is apparent that an assay for G3PAT which is attempting to reflect the physiological conditions would take into account the following.

1. G3PAT enzymes appear to perform best at high concentrations (250 - 300 mM) of buffers such as MOPS-NaOH and HEPES-NaOH.
2. pH 8.0 is the most physiologically relevant pH (Soll and Roughan, 1982; Frentzen *et al*, 1987; Lee and Leagood, 1993)
3. Acyl-ACPs are the natural substrate.
4. BSA appears a necessary component of a linear assay for G3PAT activity.
5. Plastidial concentrations of acyl-ACPs are thought to lie in the range 4-6  $\mu\text{M}$ , with the sum of 16:0-ACP and 18:1-ACP concentrations approximately 2.6  $\mu\text{M}$  (Soll and Roughan, 1982).
6. Plastidial concentrations of G3P are thought to lie in the range 100-600  $\mu\text{M}$  (Sauer and Heise, 1984; Cronan and Roughan 1987).

Details of standard G3PAT assay conditions for assays using acyl-CoA and acyl-ACP substrates described in this thesis (single and dual substrate) are outlined in table 3.5.

#### Effects of Cyclodextrins and BSA on fatty acid binding and assays using acyl-thioesters

Cyclodextrins or cyclic glucosides can form stable monomolecular complexes with acyl-CoAs and their derivatives (Machida *et al*, 1973). This effect can stimulate reactions involving acyl-CoA substrates and, to a varying degree, modulate the chain-length pattern of the acylated product(s). This may occur if, for instance, there is differential



stability/binding capacity between two different acyl-CoA substrates, or if one acyl chain is derivatised in such a way as to interfere with insertion into the cyclodextrin molecule. Computer generated space-filled modelling shows that the external surface of a cyclodextrin is largely hydrophilic (i.e. C-OH groups etc.) whereas the internal surface is more hydrophobic (i.e. C-H groups etc.). Internal hydrophobic patches may be supplemented by chemical methylation to extend the apolar regions (Machida *et al*, 1973).

In simulation experiments on fatty acid synthesis (using yeast FAS from *M.phlei*)  $\alpha$ ,  $\beta$  and  $\gamma$ -cyclodextrins were all investigated and demonstrated to enhance the fatty acid synthetase reaction carried out by this enzyme complex. The enhancing effect observed on reaction rate was  $\alpha$ - >  $\beta$ - >  $\gamma$ -cyclodextrin. Where acyl-CoA is a substrate, cyclodextrins have been shown to have similar positive effects as BSA and mycobacterial polysaccharides (for example MMP or MGLP). Theories to explain the effects of cyclodextrins on the reactions involving acyl-CoA substrates either propose that cyclodextrins aid substrate presentation or remove negative feedback by binding fatty acids/reaction products.

BSA, as previously mentioned, is thought to act by either lowering the concentration of free acyl-CoA to below the critical micelle concentration (CMC), or by presentation of the acyl-CoA or acyl-ACP substrate to the G3PAT enzyme. It is known that the external surface of BSA has three hydrophobic domains, thought to be non-specific and it is postulated that acyl binding to these regions induces a conformational change, exposing

internalised acyl binding pockets which have differential affinities for particular acyl groups (Lamb and Fallon, 1972). In this way it is possible for BSA to bind different acyl-CoA or acyl-ACP substrates with differential affinities.

In this chapter the effects of a range of BSA concentrations have in assays on selective and non-selective G3PAT proteins have been investigated. Experiments have been performed to determine whether BSA can be replaced in the G3PAT assay with a) agents that are known to bind fatty acid containing compounds, for example cyclodextrins and b) other non-plastidial proteins. The synthesis of acyl-ACP substrates is discussed and experiments using acyl-CoA and acyl-ACP substrates with selective and non-selective G3PATs are detailed. There is interest in determining the basis of substrate selectivity in the G3PAT enzyme. The range of acyl-donating substrates that squash G3PAT utilises has been investigated. Crystals of squash G3PAT have been obtained (Turnbull *et al*, 2002a,b) and this work will be a useful preliminary study for attempts to soak short-chain acyl substrates into pre-existing crystals of squash G3PAT. Enzyme:substrate co-crystals may provide more structural information about the substrate binding domain(s). In addition, G3PAT is reported to use photo-reactive azido derivatives of acyl-CoA and acyl-ACP substrates in the G3PAT reaction. Such analogues have previously been used to probe the active sites of various enzymes (Hach *et al*, 1990; Rajasekharan *et al*, 1993 and Shockey *et al*, 1995), with UV illumination causing covalent modification of the active site with these probes. This work may be a useful introductory study to determine if the G3PAT active site can be probed directly using these compounds.

### 3.2 Standard assays for G3PAT activity and selectivity

The assays used in these studies follow the acylation rate of G3P by one or more acyl donor. Either the acyl group in acyl-ACP or -CoA or the G3P molecule carried a radiolabel of a known specific activity, so that the reaction product LPA could be accurately quantified following isolation using separation of aqueous and organic phases under centrifugation (section 2.7). The purpose of assays on G3PAT proteins fell into one of the following categories:

#### A. Single substrate or G3PAT activity assays

These assays were used to measure the rate of acylation of G3P to establish the amount of G3PAT activity present, either to detect active fractions during purification procedures or to quantify the rate at which a known amount of enzyme will use a particular acyl-CoA or acyl-ACP substrate. These assays used a single acyl donor as substrate and had substrate levels of several times the estimated  $K_m$  to enable detection of all the G3PAT activity present. Either the acyl group or G3P were radiolabelled. When radiolabelled G3P was used background radioactive counts present in the organic phase were much lower as the substrate is not prone to cleavage, unlike the CoA or ACP thioesters. In acyl-ACP and -CoA substrates the polarised bond ( $\sim$ ) between the acyl chain and the pantothenic group ( $\text{CH}_3\text{-CH}_2\text{n-CH}_2\text{-C(=O)-}\sim\text{S-Pantothenic-ACP}$ ) is prone to base-catalysed hydrolysis, releasing free fatty acids and pantothenic-ACP. This can be caused by either high pHs or specific thioesterases (present in the cell to specifically hydrolyse certain acyl-ACPs for subsequent export out of the plastid to serve as substrate for the synthesis of storage or

membrane lipids). Only acyl-ACP substrates with free fatty acid levels below 2% were used in G3PAT assays.

### B Dual substrate or G3PAT selectivity assays

These assays were used to measure the rate of G3PAT activity with two different substrates under competitive conditions. The acyl groups of the two substrates were differentially radiolabelled to enable the rate of enzyme activity with each substrate to be individually measured. For example [9,10-<sup>3</sup>H] labelled 18:1 and [1-<sup>14</sup>C] labelled 16:0-ACPs or -CoAs were most typically used. Acyl-ACPs were used in the majority of assays as they are the natural acyl-substrate. Substrate levels were chosen so as to be close to the estimated  $K_m$ . The majority of assays described in the results chapters are dual substrate assays.

The results for both assay types are presented as graphs of 18:1- or 16:0-LPA formed (or both) plotted against time. The plots show linear, positive rates of LPA formation over a period of time, usually less than five minutes to ensure that the initial, linear velocity was measured. Full details of the experimental conditions used for each type of assay are given in table 3.4. Performance of G3PAT from a) a chilling-sensitive (non-selective) species and b) an oleophilic (18:1-ACP selective) in a G3PAT dual substrate assay are shown in figure 3.1.

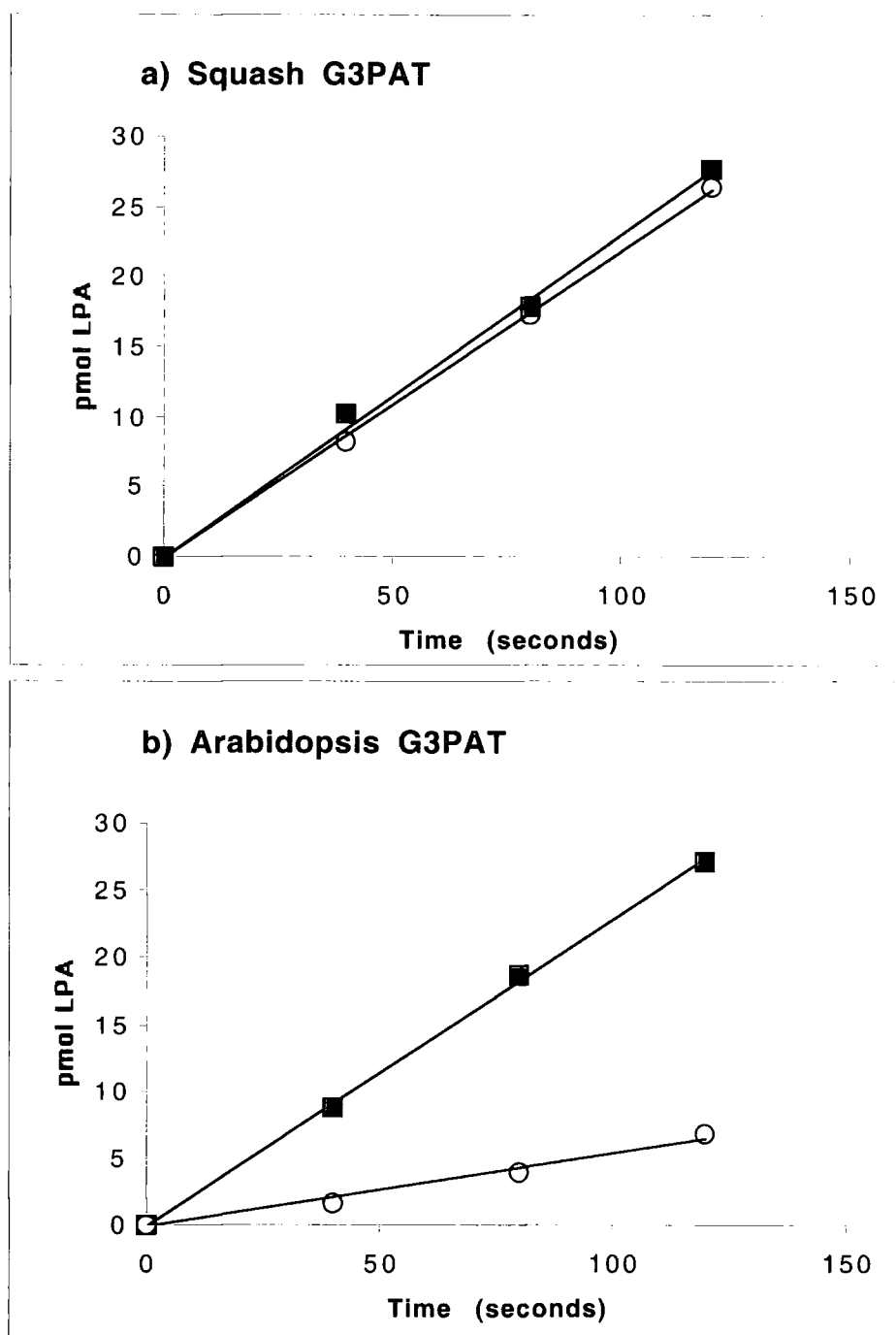


**Figure 3.1 Typical results format of G3PAT selectivity assays.**

The assays are performed under competitive conditions with 18:1-ACP and 16:0-ACP substrates each present at 1.1  $\mu$ M and results are displayed as rate of product (LPA) formation against time. ■ = 18:1 LPA. ○ = 16:1 LPA. Squash G3PAT (a), a non-selective enzyme uses both substrates at a similar rate. Arabidopsis G3PAT (b), an oleophilic enzyme, uses 18:1-ACP approximately 4-5 times faster than 16:0-ACP under standard conditions.

<b>G3PAT single substrate (activity) assay</b>	<b>G3PAT dual substrate (selectivity) assay</b>
<u>a) Using radiolabelled acyl-ACP and G3P</u>  250 mM HEPES-NaOH buffer pH 8.0 300 $\mu$ M G3P 2.2 $\mu$ M 18:1-ACP or 16:0-ACP 5 mg/ml BSA	<u>c) Using radiolabelled acyl-ACPs and G3P</u>  250 mM HEPES-NaOH buffer pH 8.0 300 $\mu$ M G3P 1.1 $\mu$ M ( $^3\text{H}$ )18:1-ACP 1.1 $\mu$ M ( $^{14}\text{C}$ )16:0-ACP 5 mg/ml BSA
<u>b) Using acyl-CoA and radiolabelled G3P</u>  250 mM HEPES-NaOH buffer pH 8.0 30 $\mu$ M G3P (variable) 400 $\mu$ M 16:0-CoA or 18:1-CoA 5 mg/ml BSA	<u>d) Using radiolabelled acyl-CoAs and G3P</u>  250 mM HEPES-NaOH buffer pH 8.0 300 $\mu$ M G3P 10 $\mu$ M ( $^3\text{H}$ )18:1-CoA 10 $\mu$ M ( $^{14}\text{C}$ )16:0-CoA 5 mg/ml BSA

**Table 3.5 Standard conditions for G3PAT assay types.**

### **3.3 Effect of a range of BSA concentrations on the dual substrate G3PAT assay**

In order to establish the effects of a range of BSA concentrations on the standard G3PAT selectivity assay, the assay was performed under standard conditions using 1.1  $\mu$ M 18:1-ACP and 16:0-ACP, but with varying levels of BSA from 0 - 5.0 mg/ml. Levels used were 0.0, 0.125, 0.50, 1.25, 2.5 and 5.0 mg/ml BSA. Assays were performed on purified G3PAT from squash, a non-selective enzyme form, using 210 ng of protein to initiate each assay. Assays were performed over two minutes and the results from these assays are presented in figure 3.2.

It is apparent that when no BSA is present, the data points do not correlate well and acylation rates for each substrate are below optimal. When BSA is added, even at levels

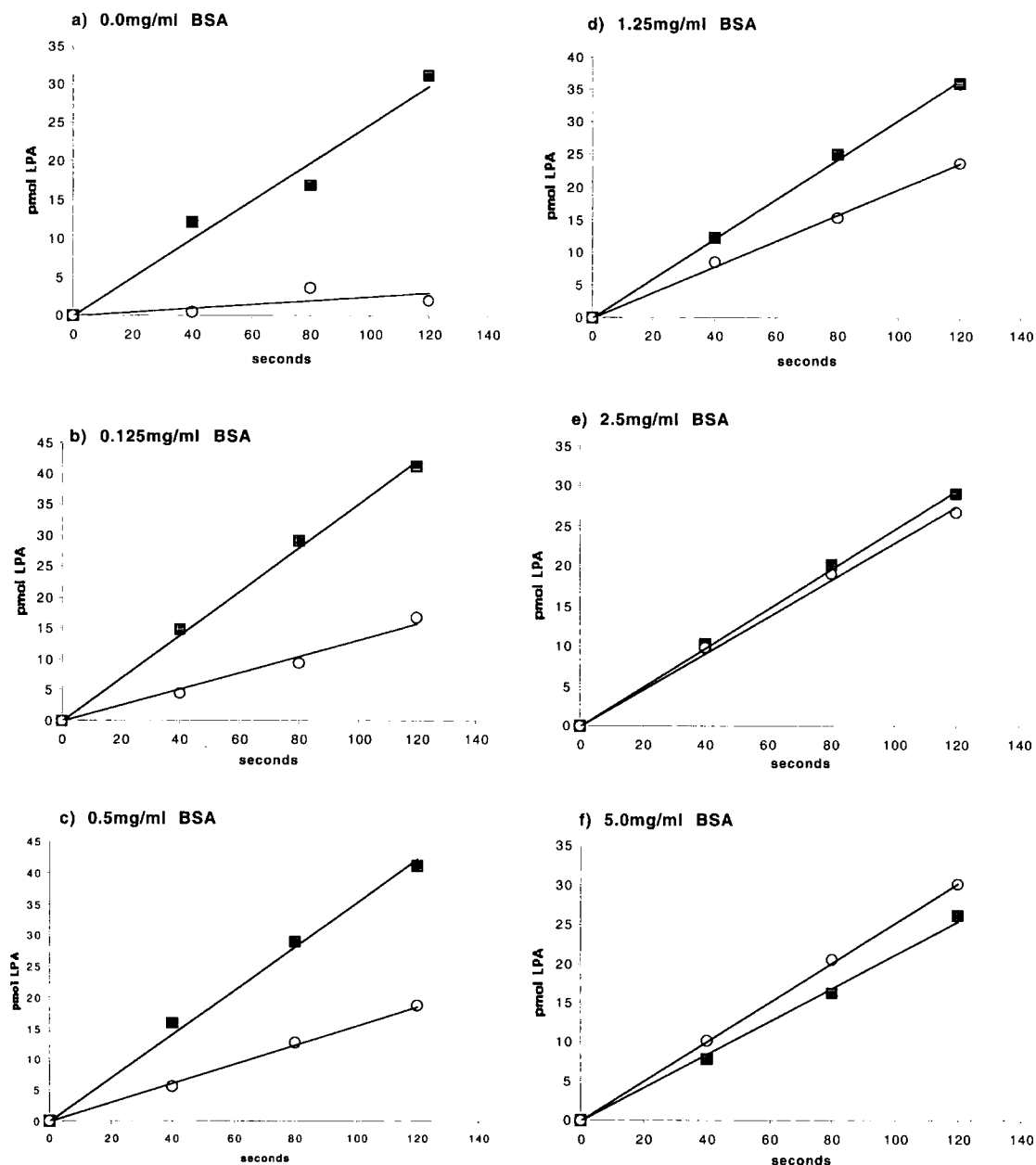


**Figure 3.2 Selectivity assays with squash G3PAT over a range of BSA concentrations.**

Assays were performed under standard G3PAT selectivity assay conditions with BSA concentrations of a) 0.0 mg/ml; b) 0.125 mg/ml; c) 0.5 mg/ml; d) 1.25 mg/ml, e) 2.5 mg/ml and f) 5.0 mg/ml. ■ = 18:1 LPA. ○ = 16:0 LPA

as low as 0.125 mg/ml, the assay becomes linear over the two minute period and the data points correlate more closely. At 0.125 mg/ml BSA the selectivity ratio (enzymatic rate with 18:1-ACP/ rate with 16:0-ACP) is approximately 2.7. As the BSA level increases towards 2.5 and 5.0 mg/ml, the enzyme behaves increasingly like a non-selective form as expected, having a selectivity ratio of approximately 0.9/1.0 i.e. the G3PAT is using both 18:1-ACP and 16:0-ACP at similar rates. As BSA levels increase from 0.125 to 5.0 mg/ml, the rate with 18:1-ACP reduces slightly, dropping from roughly 21 to 13 pmoles formed per minute. However, rates with 16:0-ACP are stimulated and rise from approximately 8 pmoles formed per minute to 15. If BSA is involved in presentation of the acyl-ACP substrate to the G3PAT enzyme then it appears that it has a different effect with 18:1- and 16:0-ACPs. This raises the interesting possibility that BSA binds these two substrates with different affinities.

### **3.4 Assessment of differential BSA-binding of 18:1-ACP and 16:0-ACP substrates under competitive conditions**

In order to determine whether BSA bound 18:1-ACP and 16:0-ACP with differential affinities, the substrates were dialysed away from BSA using microdialysis (method in section 2.13). Briefly, 1.1  $\mu\text{M}$  [9,10- $^3\text{H}$ ] labelled 18:1-ACP and [1- $^{14}\text{C}$ ] labelled 16:0-ACP were mixed with BSA at 1.25 mg/ml and 5.0 mg/ml in 250 mM HEPES-NaOH buffer pH 8.0. Following incubation at room temperature for 10 minutes, this mixture was dialysed against of 250 mM HEPES-NaOH buffer pH 8.0 for 4 hours through a 30 kDa dialysis membrane. The amount of each substrate dialysed away from the BSA was recorded at 0.5, 1, 2, 3 and 4 hours and results are shown in figure 3.3.



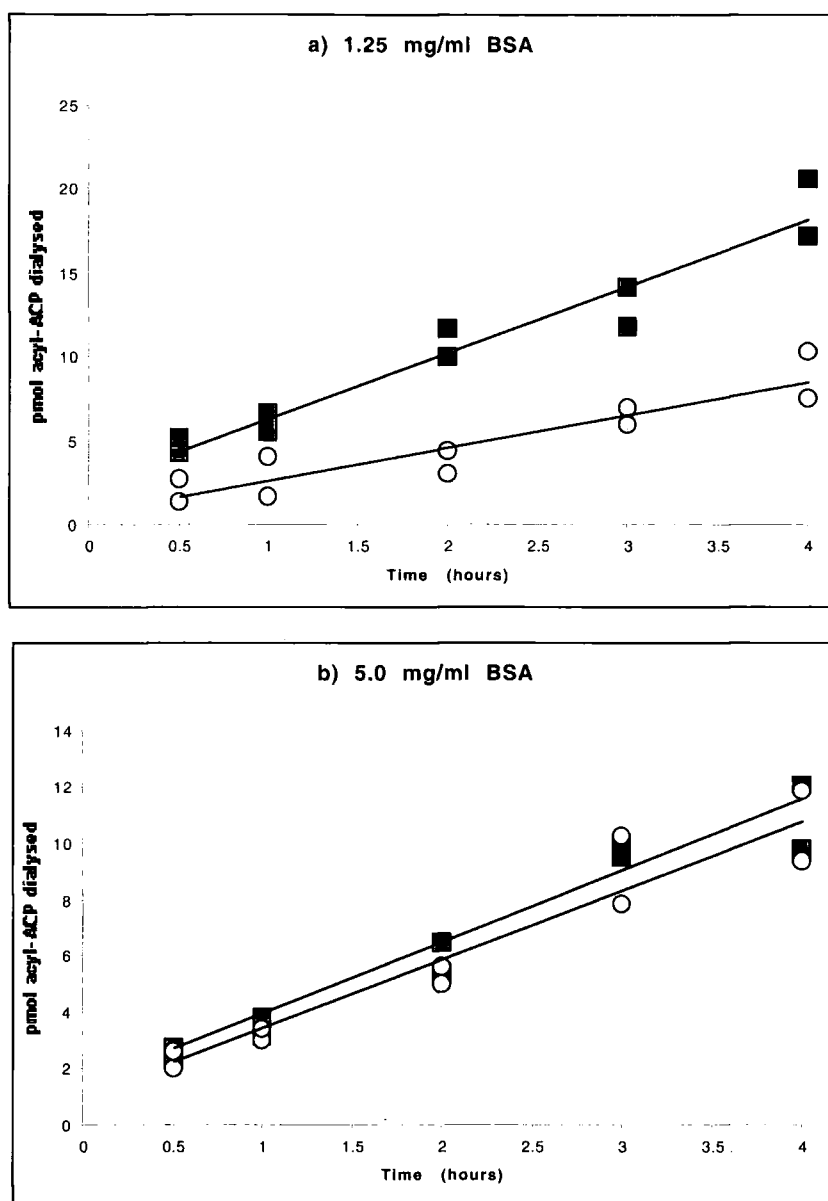


**Figure 3.3 Microdialysis to determine binding of 18:1 and 16:0-ACPs to BSA under competitive conditions.**

Assays were performed under standard microdialysis assay conditions using a) 1.25 mg/ml BSA and b) 5.0 mg/ml BSA. 1.1 $\mu$ M 18:1-ACP and 1.1 $\mu$ M 16:0-ACP were used in each case. ■ = 18:1 ACP dialysed. ○ = 16:0 ACP dialysed. At 1.25 mg/ml BSA 18:1-ACP is dialysed away from BSA more quickly than 16:0-ACP, indicating that it binds less strongly to BSA. At 5.0 mg/ml BSA both substrates dialyse away from BSA at a comparable rate.

These data suggest that BSA binds 18:1-ACP and 16:0-ACP with different affinities, but that this effect is dependant on the concentration of BSA and is greatly reduced at 5.0 mg/ml with respect to 1.25 mg/ml. The effect was observed to be even greater at 0.125 mg/ml BSA, but the data correlated very poorly and is not shown. It should also be noted that in each case >80% of each substrate remained bound to BSA, even after 4 hours of dialysis.

Additional evidence to suggest BSA has differential affinity for 18:1-ACP and 16:0-ACP has been provided using an ultrafiltration unit to separate unbound acyl-ACP substrates from BSA. In a modification of the G3PAT binding assay, section 2.11, 100 pmoles of 18:1- or 16:0-ACP were incubated with 500 pmoles of BSA for 5 minutes, prior to centrifugation through a 30 kDa molecular weight cut-off membrane. BSA was found to bind 16:0-ACP with greater affinity than 18:1-ACP – 1.6 times more 16:0-ACP is bound to the BSA and retained in the upper compartment under the ultrafiltration conditions. This data is displayed in table 3.6.

### **3.5 Investigation of the effects of 2,6-dimethyl $\beta$ -cyclodextrin, lysozyme and cytochrome C on the standard dual substrate G3PAT assay**

BSA has been shown to have an effect on the performance of the standard dual substrate G3PAT assay (section 3.2). This effect has been hypothesised to be due to a substrate

**Table 3.6 Differential binding of 18:1-ACP and 16:0-ACP substrates to BSA.**

100 pmoles of radiolabelled 18:1-ACP or 16:0-ACP were incubated with or without 500 pmoles of BSA in the absence of the second substrate for 5 minutes in 250 mM HEPES-NaOH buffer (total volume 100 µl). The mixture was centrifuged through a 30,000 Da molecular weight cut-off membrane. Substrate bound to BSA did not pass through the membrane and was retained in the upper compartment. Assays were performed in triplicate and results are presented as mean values  $\pm$  1 standard error measurement.

	+ BSA		- BSA	
	18:1-ACP	16:0-ACP	18:1-ACP	16:0-ACP
total pmoles of substrate in upper compartment	35.2 $\pm$ 2.65	56.4 $\pm$ 4.10	0.15 $\pm$ 0.06	0.10 $\pm$ 0.05
mmoles of substrate bound per mole of BSA	70.4 $\pm$ 5.30	112.8 $\pm$ 8.20	n/a	n/a

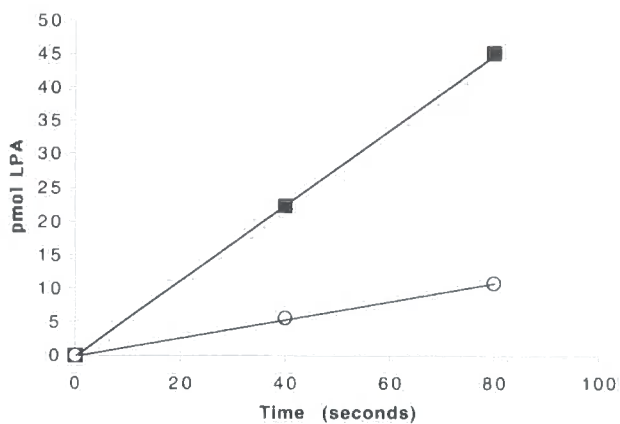
binding effect or differential presentation to the G3PAT enzyme. To establish whether this effect could be mimicked by other molecules, G3PAT substrate selectivity assays were performed with 2,6-dimethyl  $\beta$ -cyclodextrin, lysozyme and cytochrome C at levels of 0.5 mg/ml and 5.0 mg/ml. Cyclodextrins were investigated due to their proven role in fatty acid binding and presentation of acyl-containing substrates to their enzymes. Cytochrome C and lysozyme were investigated as both are structurally and functionally well characterised and neither are naturally present in the stroma or have known fatty acid binding capabilities (effectively included as 'negative controls'). If they alter substrate selectivity in the standard dual substrate G3PAT assay it is likely that this is via indirect stabilisation of the G3PAT protein or intermediates rather than direct binding of the G3PAT substrates, or by bulk solvent exclusion effects.

$\beta$ -cyclodextrins consist of a ring of 7 glucosides, making these molecules slightly larger than  $\alpha$ -cyclodextrins and more likely to accommodate an acyl chain and/or part of the acyl carrier protein. The apolar region(s) in the ring centre have been extended via the introduction of two methyl groups, increasing the chances of interactions between this region and the hydrophobic acyl chain.

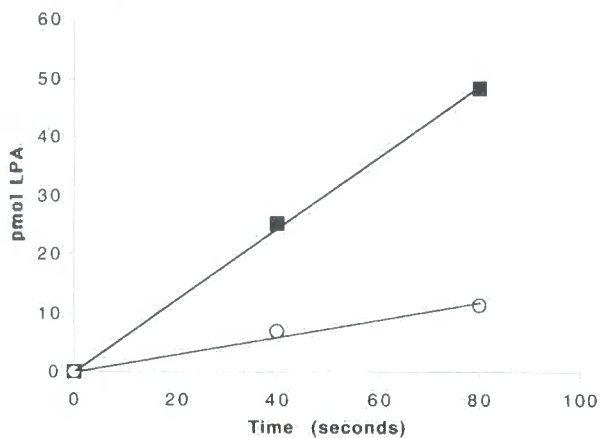
The effects of these compounds were investigated under standard G3PAT selectivity assay conditions. Cytochrome C, lysozyme, 2,6-dimethyl  $\beta$ -cyclodextrin were present at 0.5 or 5.0 mg/ml and the results are presented in figure 3.4. These data indicate that the proteins cytochrome C and lysozyme have little or no effect on acylation rates and the substrate selectivity of squash G3PAT, as there is little or no difference in the

**Figure 3.4 Effects of the proteins Lysozyme and Cytochrome C and the compound 2,6-dimethyl  $\beta$ -cyclodextrin on the substrate selectivity of squash G3PAT** Standard G3PAT selectivity assays using a) 0.5 mg/ml lysozyme, b) 5.0 mg/ml lysozyme, c) 0.5 mg/ml cytochrome C, d) 5.0 mg/ml cytochrome C, e) 0.5 mg/ml 2,6-dimethyl  $\beta$ -cyclodextrin and f) 0.5 mg/ml 2,6-dimethyl  $\beta$ -cyclodextrin. v = 18:1-LPA and O = 16:0-LPA.

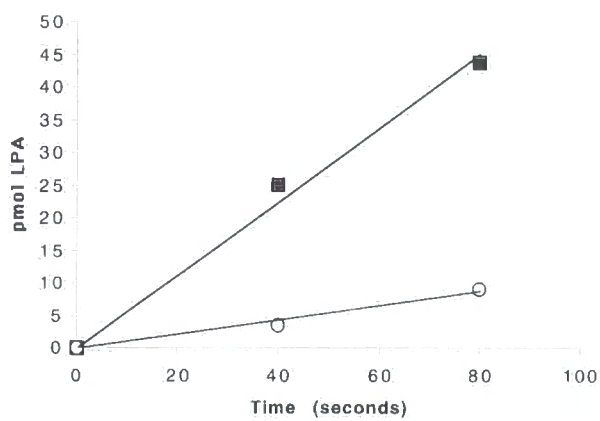
a) 0.5mg/ml Lysozyme



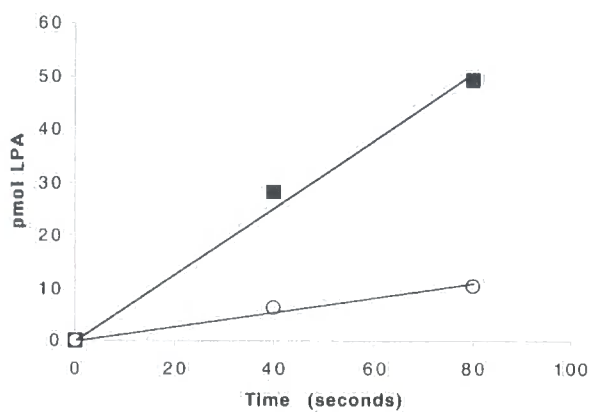
b) 5.0mg/ml Lysozyme



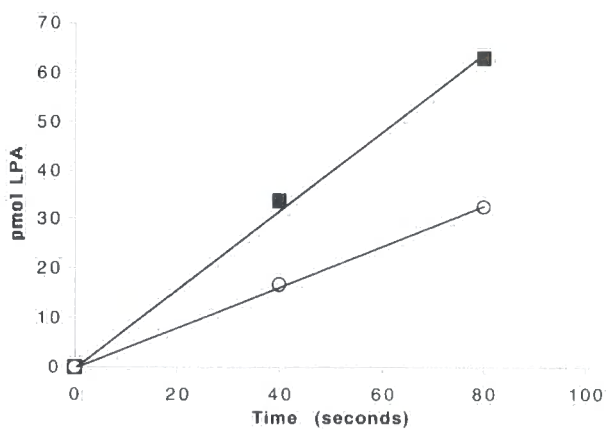
c) 0.5mg/ml Cytochrome C



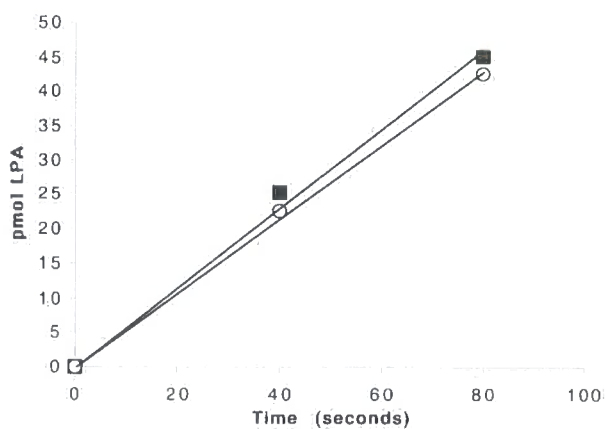
d) 5.0mg/ml Cytochrome C



e) 0.5mg/ml Cyclodextrin



f) 5.0mg/ml Cyclodextrin



performance of the standard G3PAT selectivity assay when the level of these proteins is raised from 0.5 to 5.0 mg/ml. However, a similar increase in the levels of 2,6-dimethyl  $\beta$ -cyclodextrin has a marked effect, altering both reaction velocities with 18:1-ACP and 16:0-ACP substrates and the substrate selectivity. The alteration of reaction velocities was similar to that observed when BSA levels were elevated from 0.5 to 5.0 mg/ml - 18:1-LPA production decreased slightly and 16:0-LPA production increased slightly resulting in an enzyme with a ratio of 18:1/16:0-LPA production of approximately 1:1. At both 0.5 mg/ml BSA and 0.5 mg/ml cyclodextrin the 'non-selective' G3PAT had an apparent preference for 18:1-ACP.

BSA and 2,6-dimethyl  $\beta$ -cyclodextrin may both affect a change in the performance of the squash G3PAT via a direct effect, probably presentation of the substrates to the binding/catalytic domain of the protein and both may have differential binding affinities for each of the 18:1-ACP and 16:0-ACP substrates.

Additional evidence to suggest 2,6-dimethyl  $\beta$ -cyclodextrin has differential affinity for 18:1-ACP and 16:0-ACP has been shown using an ultrafiltration unit to separate unbound acyl-ACP substrates from the cyclodextrin. In a modification of the G3PAT binding assay, section 2.11, 100 pmoles of 18:1- or 16:0-ACP were incubated with 500 pmoles of 2,6-dimethyl  $\beta$ -cyclodextrin for 5 minutes, prior to centrifugation through a 30 kDa molecular weight cut-off membrane. The cyclodextrin bound 16:0-ACP at greater levels than 18:1-ACP – 1.3 times more 16:0-ACP is bound to the cyclodextrin and retained in the upper compartment under ultrafiltration conditions, see table 3.7.

**Table 3.7 Differential binding of 18:1-ACP and 16:0-ACP substrates to 2,6-dimethyl-cyclodextrin.**

100 pmoles of radiolabelled 18:1-ACP or 16:0-ACP were incubated with or without 500 pmoles of 2,6-dimethyl-cyclodextrin (2,6MeCD) in the absence of the second substrate and centrifuged through a 30,000 Da molecular weight cut-off membrane. Substrate bound to BSA did not pass through the membrane and was retained in the upper compartment. Assays were performed in triplicate and results are presented as mean values  $\pm$  1 standard error measurement.

	<b>+ 2,6MeCD</b>		<b>- 2,6MeCD</b>	
	18:1-ACP	16:0-ACP	18:1-ACP	16:0-ACP
total pmoles of substrate in upper compartment	<b>0.38 <math>\pm</math> 0.32</b>	<b>0.50 <math>\pm</math> 0.40</b>	<b>0.19 <math>\pm</math> 0.16</b>	<b>0.20 <math>\pm</math> 0.19</b>
mmoles of substrate bound per mole of 2,6MeCD	<b>0.76 <math>\pm</math> 0.64</b>	<b>1.00 <math>\pm</math> 0.80</b>	n/a	n/a



### 3.6 Investigation of substrate selectivity under a range of conditions using G3PAT from squash and *Arabidopsis*

In joint work performed by the author, Johan Kroon (University of Durham) and Ted Schierer (University of Durham), G3PAT selectivity (dual substrate) assays were performed on crude cell-free extracts (CFEs) of squash and *Arabidopsis* recombinant G3PATs. The *Arabidopsis* CFE was prepared in a manner identical to the preparation of squash CFEs, section 2.3, and the protein produced was very similar in size to squash G3PAT, as it was cloned using the same predicted processing site (G3PAT processing sites are discussed by Murata and Tasaka, 1997). In this section only, CFEs of squash G3PAT protein NA4 and *Arabidopsis* G3PAT protein AR1 were used. An alignment of the N-termini of the constructs used is presented in figure 3.5.

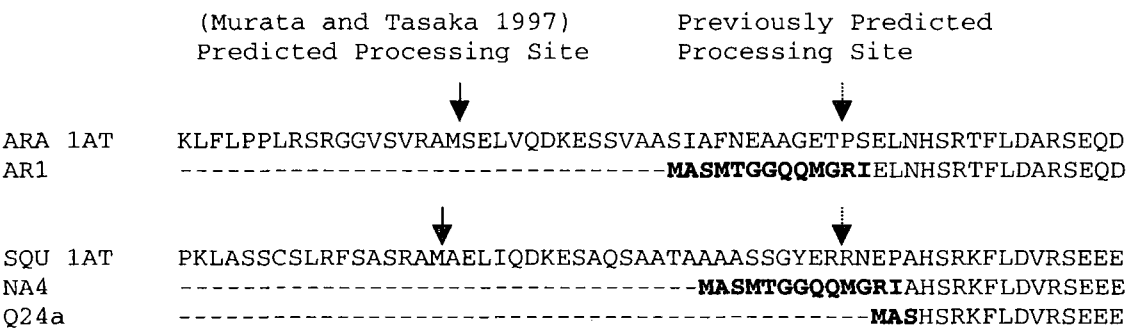


**Figure 3.5** Alignment of the N-termini of constructs ARA 1AT, AR1, SQU 1AT and NA4. Q24a has been included for comparison. ARA 1AT and SQU 1AT are the sequences for the full-length precursor from *Arabidopsis* and squash (AT2) respectively. AR1 and NA4 are the constructs originally used by our group for the plastidial proteins from *Arabidopsis* and squash, expressed at high levels in E.coli. **Bold** type indicates amino acids that have been coded for by vector DNA. Arrows indicate putative processing sites. The full squash and *Arabidopsis* protein sequences are detailed in figure 4.2.

Both NA4 and AR1 were assayed using dual substrate (18:1/16:0) assays with acyl-ACP and acyl-CoA substrates. Conditions investigated were 0.5 mg/ml and 5.0 mg/ml BSA and pH 7.4 and pH 8.0.

Assays were performed jointly and are only summarised herein to make the following points: (a table showing the full experimental data is appended - Appendix 2.)

1. Squash (AT2 isoform) is a G3PAT reported to have no substrate preference (Frentzen *et al*, 1987)
2. *Arabidopsis* is a G3PAT with reported selectivity for unsaturated (18:1) over saturated (16:0) acyl-groups (Wolter *et al*, 1992)
3. When using acyl-CoA substrates, very little difference in substrate selectivity was observed under any of the assay conditions
4. When using acyl-ACP substrates, *Arabidopsis* G3PAT exhibited greater substrate selectivity than squash G3PAT under all conditions tested
5. At 0.5 mg/ml BSA, acylation rates are higher than at 5.0 mg/ml, and squash G3PAT exhibits a preference for 18:1- over 16:0-ACP
6. At 5.0 mg/ml BSA both *Arabidopsis* and squash G3PAT exhibit substrate preference consistent with those expected, i.e. squash is non-selective and *Arabidopsis* has a preference for unsaturated (18:1) over saturated (16:0) acyl-ACPs.
7. At 5.0 mg/ml BSA, using acyl-ACP substrates there is little difference in performance of either enzyme between the pHs 7.4 and 8.0.

Taking these general conclusions into consideration, these data reinforce the contention that appropriate conditions for assay of soluble G3PAT lie in the vicinity of 5.0 mg/ml BSA using acyl-ACP substrates. Based on previous reports (Soll and Roughan, 1982;

Frentzen et al, 1987; Lea and Leagood, 1993) the most physiologically relevant pH at which to perform G3PAT assays is pH 8.0.

### **3.7 Investigation of the range of acceptable acyl-CoA and acyl-ACP substrates for the G3PAT reaction**

Squash G3PAT has been crystallised and shown to diffract X-rays to a high resolution (Turnbull *et al* 2002a). However, no enzyme-substrate co-crystals have yet been produced and the fine structural detail of the substrate binding sites remains poorly understood. If the lower limit for substrate chain length which still permits binding and catalysis (i.e. correct insertion of the substrate into the catalytic region) were to be confirmed, work could begin to soak these smaller, more soluble substrates into pre-existing crystals of squash G3PAT to obtain enzyme-substrate co-crystals.

An investigation of the range of substrates that squash G3PAT could use and the rates at which catalysis occurred was undertaken. Standard single substrate G3PAT assays were performed using the following substrates: 12:0-ACP, 16:0-ACP, 18:1-ACP, 4:0-CoA, 6:0-CoA, 12:0-CoA, 16:0-CoA and 18:1-CoA. It was not possible to synthesise shorter chain length acyl-ACP substrates due to the minimum chain length requirements of both the acyl-ACP synthetase enzyme and the purification procedures for acyl-ACP substrates, which involve hydrophobic interaction chromatography, not practical with shorter acyl chain lengths. However, acyl-CoA substrates are commercially available and chain lengths as short as 4 carbons were able to be used in the assays (acyl-CoAs were purchased from Sigma, acyl-ACPs were synthesised as described in section 2.3).

Radioactive G3P was used to measure acylation rates in each case. Isolation and detection of short chain ( $n < 12$  carbons) LPA was performed on TLC plates using a single timepoint, as described in section 2.11. Isolation and detection of longer chain LPA was performed as per usual, via separation of aqueous and organic phases under centrifugation.

It was demonstrated that squash G3PAT will use 4:0-CoA and 6:0-CoA (Sigma) to produce LPA, although at much lower rates than with the longer chain substrates – figure 3.6. Squash G3PAT will also use 12:0-CoA, 16:0-CoA, 18:1-CoA and 12:0-ACP, 16:0-ACP and 18:1-ACP – figure 3.7. A summary of the velocity of the G3PAT reaction with each of these substrates in pmol LPA formed per minute is given in table 3.8.

### **3.8 Squash G3PAT uses 12-Azido oleoyl-ACP and 12-Azido oleoyl-CoA as substrates**

Substrate analogues containing azido groups, or their derivatives, have been used to probe the active site of several enzymes (Hach *et al*, 1990; Rajasekharan *et al*, 1993 and Shockey *et al*, 1995). The reactive group covalently links to amino acid side chains in its immediate vicinity using UV energy, and can be used to obtain direct structural evidence regarding the active site of an enzyme, specifically relating to the amino acids in contact with the substrate(s).

As a preliminary study to the development of this approach for squash G3PAT, it was investigated whether 12-azido oleoyl-ACP and 12-azido oleoyl-CoA could be used as

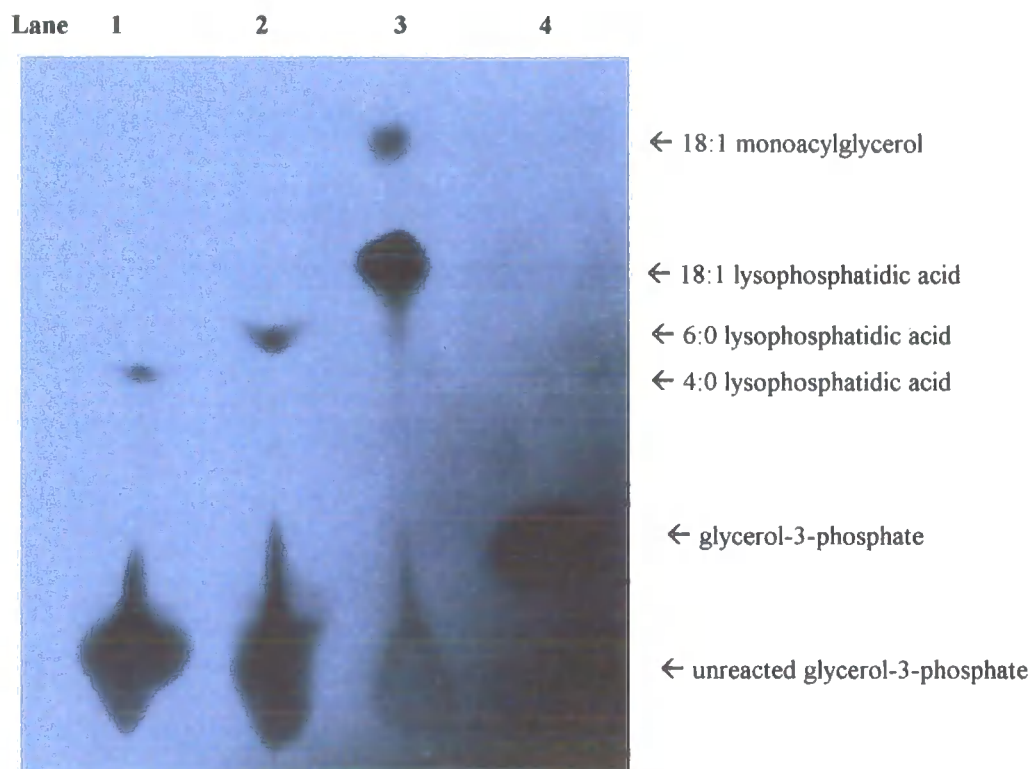


**Figure 3.6** Autoradiograph of TLC analysis of G3PAT assays using short chain acyl-CoA substrates. Single timepoints were taken after 5 minutes and separated in the solvent mixture butanol:acetic acid:water 6:3:1. **Lane 1** 4:0-CoA. **Lane 2** 6:0-CoA. **Lane 3** 18:1-CoA. **Lane 4** G3P.

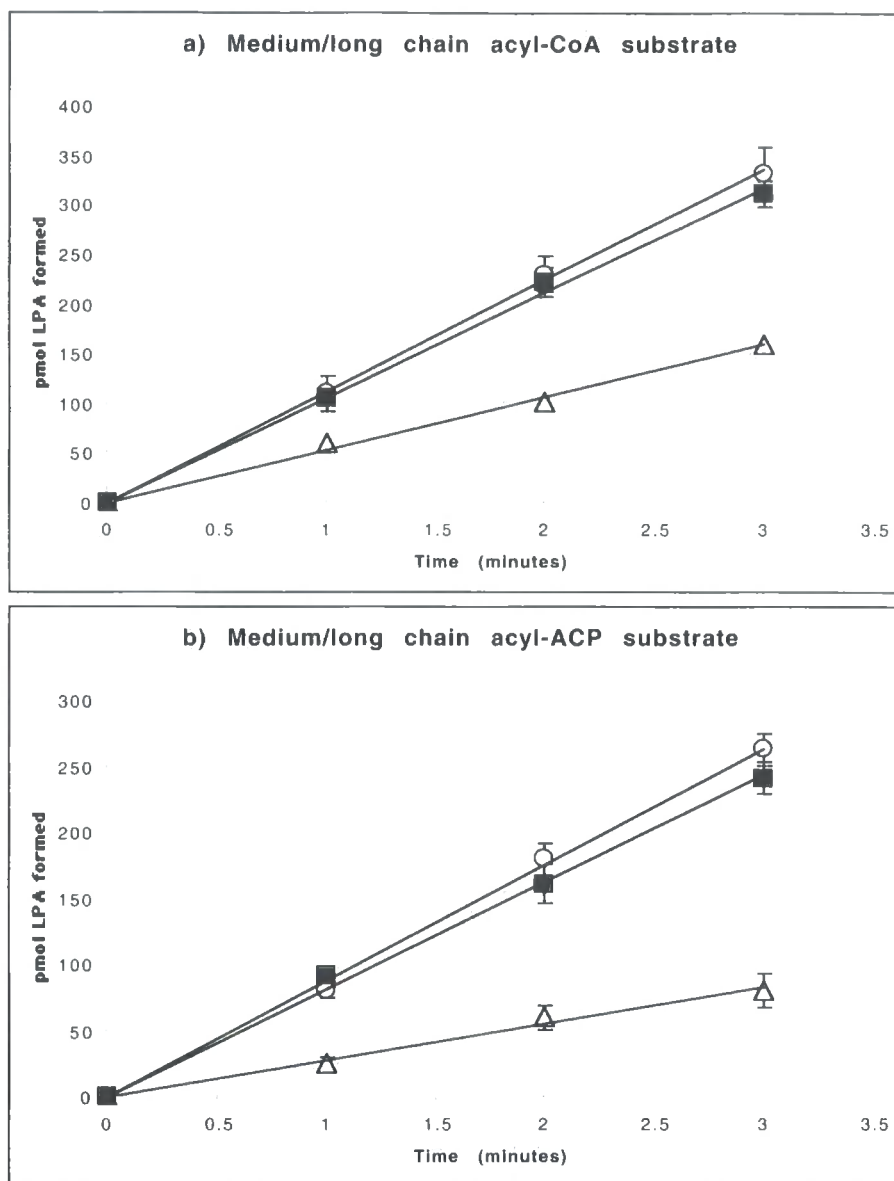


**Figure 3.7 Single substrate assays using acyl-ACP and acyl-CoA substrates.** Assays to show the catalytic velocity of squash G3PAT with a) 12:0-, 16:0- and 18:1-CoA and b) 12:0-, 16:0- and 18:1-ACP substrates. ■, 18:1 LPA; ○, 16:1 LPA; △, 12:0 LPA formed. Assays were performed in triplicate and results are presented as mean values  $\pm$  1 standard error measurement.

**Table 3.8 G3PAT reaction velocities with various acyl-CoA and -ACP substrates.**

Velocity is presented as pmol LPA formed per minute per mg G3PAT under the following conditions: Acyl-CoAs - 400  $\mu$ M acyl-CoA and 300  $\mu$ M G3P. Acyl-ACPs - 10  $\mu$ M acyl-ACP and 300  $\mu$ M G3P. Assays were performed in triplicate and results are presented as mean values  $\pm$ 1 standard error measurement. \*Assay performed on one occasion only.

	Velocity
<b>C<sub>4:0</sub>CoA</b>	5.1 $\pm$ 0.4
<b>C<sub>6:0</sub>CoA</b>	11 $\pm$ 1.1
<b>C<sub>12:0</sub>CoA</b>	55.3*
<b>C<sub>16:0</sub>CoA</b>	120 $\pm$ 4.3
<b>C<sub>18:1</sub>CoA</b>	111 $\pm$ 4.7
<b>C<sub>12:0</sub>ACP</b>	28 $\pm$ 3.2
<b>C<sub>16:0</sub>ACP</b>	83 $\pm$ 1.9
<b>C<sub>18:1</sub>ACP</b>	81 $\pm$ 2.8

substrates in such assays. Acyl-CoAs and -ACPs and azidoacyl-CoAs and -ACPs were incubated with squash G3PAT prior to initiation of the reaction with radiolabelled G3P. In addition, half of the assay mixtures were pre-illuminated with UV light (all illumination was at 254 nm unless otherwise stated) before G3P was added in order to ascertain whether the azido-acyl analogues could be used to irreversibly bind to the G3PAT active site, inactivating the enzyme, see figure 3.8.

The data illustrate that squash G3PAT will use both 12-Azido oleoyl-ACP and 12-Azido oleoyl-CoA as substrates. The rates observed for 12-Azido oleoyl-CoA and 12-Azido oleoyl-ACP were approximately 60% and 70% of the non-azido substrates respectively. UV pre-treatment of the mixture did not cause significant inactivation of the G3PAT as expected. This indicates that covalent attachment of 12-Azido oleoyl-CoA primarily in or around the active site may not have occurred. G3PAT samples from before and after the UV treatment were analysed via MALDI TOFF mass spectrometry. The results (figure 3.9) show that 1:1 binding of 12-Azido oleoyl-CoA does not occur. It is possible that some molecules attach at the active site, although only a very limited proportion. This proportion could perhaps be increased by optimisation of the incubation conditions and UV light intensity. However this work may still be a useful study to show G3PAT uses azidoacyl-derivatives as substrate. Protocols for the synthesis of these compounds and their use in assay have been established. Ongoing work is being carried out to see if 12-Azido oleoyl-CoA can be radiolabelled with  $^{32}\text{P}$  which would facilitate tracking of any peptides with one or more 12-Azido oleoyl-CoA molecules attached.



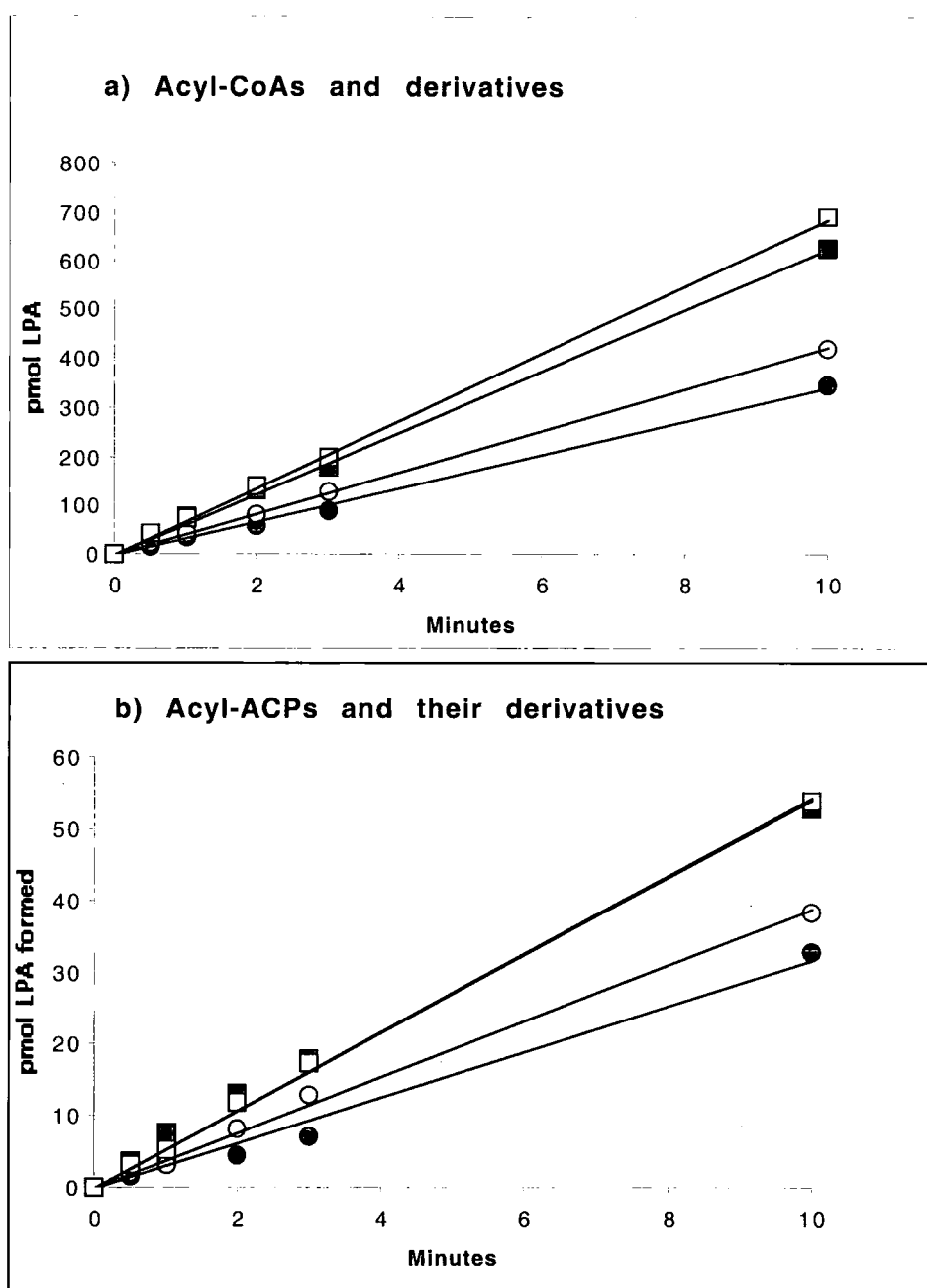
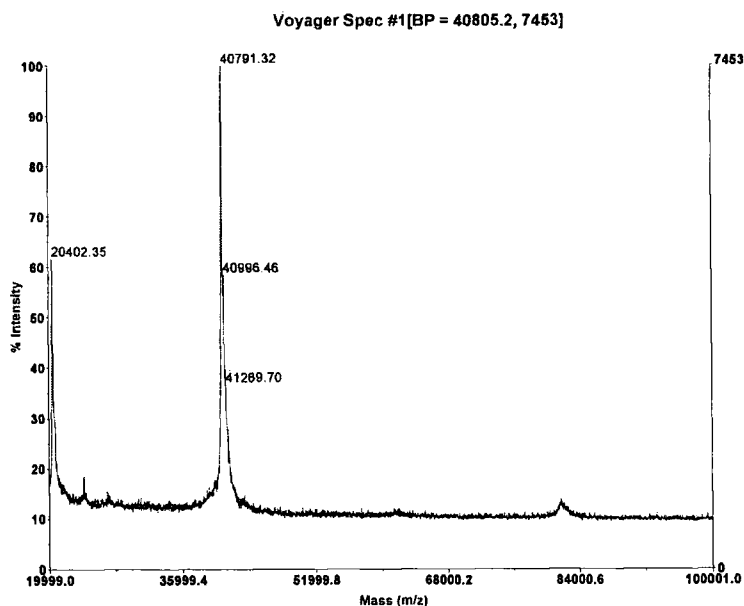


**Figure 3.8 Squash G3PAT uses azidoacyl-CoA and -ACP as substrates.**

Single substrate assays with or without UV flash using  $^{14}\text{C}$  G3P and a) oleoyl-CoA (18:1CoA) and 12-azido oleoyl-CoA (12Az18:1CoA) and b) oleoyl-ACP and 12-azido oleoyl-ACP as substrates. In both a) and b) products formed were □ = 18:1-LPA (no UV); ■ = 18:1-LPA (with UV flash); ○ = 12Az18:1-LPA (no UV) and ● = 12Az18:1-LPA (with UV flash).

a) MALDI TOF spectrum of purified squash G3PAT



b) MALDI TOF spectrum of purified squash G3PAT after pre-incubation with 12-Azidooleoyl-ACP under UV light

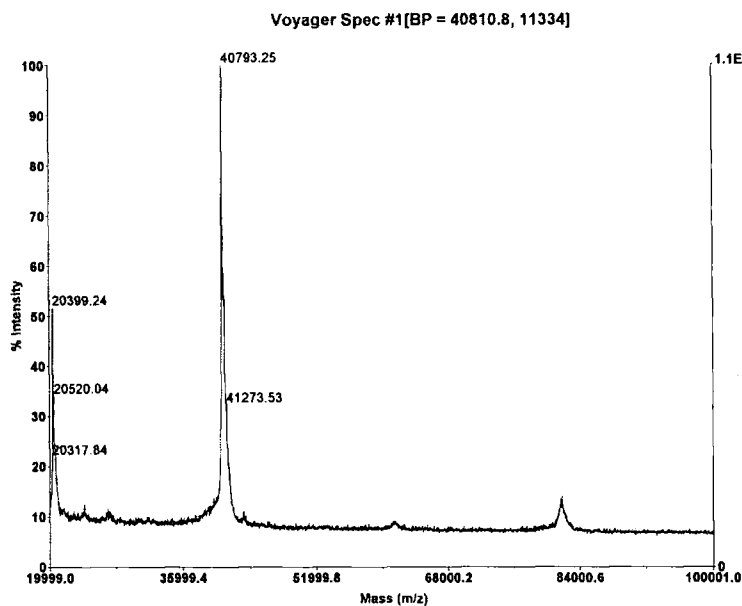


**Figure 3.9 MALDI TOF mass spectra of squash G3PAT before and after incubation with 12-Azidooleoyl-ACP.**

Spectra of purified squash G3PAT a) before and b) following a 10 minute incubation with 10  $\mu$ M 12-azidooleoyl-ACP under UV illumination. The mass of the G3PAT molecule is 40.8 kDa, mass of 12-azidooleoyl-ACP is 9174.5 Da and 12-azidooleic acid is 323.5 Da. The G3PAT peak is seen clearly but there is no peak at G3PAT plus 12-azidooleic acid or 12-azidooleoyl-ACP.



## **Chapter 4**

# **Substrate binding, activity and selectivity assays of G3PAT mutants.**

**Identification of residues important in substrate  
binding and catalysis.**

## 4.1 Introduction

### The advent of site-directed mutagenesis (SDM)

The development of techniques in the mid to late seventies for the rapid sequencing of large stretches of DNA (Sanger and Coulson, 1975; Maxam and Gilbert, 1977) was a milestone in the development of molecular approaches involving the study and manipulation of DNA. These advances facilitated the advent of methods which allowed predefined changes to be introduced into a known DNA sequence (Hutchison *et al* 1978), rather than previously used random mutagenesis using chemical or physical mutagens. Over recent years this method has increased in efficiency and flexibility into a sophisticated technique which is known as site-directed mutagenesis. Early work performed involved the synthesis of oligodeoxyribonucleotides which were complimentary to the stretch of single-stranded DNA to be mutated (Hutchison *et al* 1978). These oligonucleotides were used as specific mutagens, priming DNA synthesis and themselves becoming incorporated into the resulting heteroduplex molecule. This method, now known as primer extension site-directed mutagenesis, can also be adapted to produce multiple point mutations, insertions, deletions and transversions. A drawback to this method is that the double stranded heteroduplex molecules which are generated are contaminated with single stranded non-mutant template DNA and incomplete duplexes (partially double-stranded molecules). Methods exist for their removal (nuclease treatment, centrifugation, electrophoresis etc.), but are not always quick or convenient.

An alternative to primer extension site-directed mutagenesis is a technique known as cassette mutagenesis. A synthetic DNA fragment containing the complete desired mutant sequence is used to replace the corresponding sequence in the wild-type gene. Larger insertions/deletions can be more easily introduced with this technique, it is simple and the efficiency is close to 100%. However there will be a limited number of unique restriction sites flanking the region to be mutagenised which may limit the realistic number of different oligonucleotides that may be used.

PCR-based mutagenesis is another method of introducing mutations into DNA sequences. Single bases mismatched between the amplification primer and the template sequence become incorporated into future template sequences as a result of amplification. It is possible to introduce a mutation into a PCR-produced DNA fragment at any point along its length: two primary PCR reactions produce overlapping DNA fragments, both bearing the same mutation in the overlap region, this region allows the fragments to hybridise. One of the two hybrids extends via the action of DNA polymerase to produce a duplex fragment. The other hybrid is 5'-recessed, not a substrate for the polymerase and is effectively lost from the reaction mixture.

The type of mutagenesis used to produce mutant G3PAT proteins detailed in this chapter is a plasmid based mutagenesis technique - the Quickchange™ site directed mutagenesis kit from Stratagene.

## 4.2 Site-directed mutagenesis and the study of acyltransferases

Site directed mutagenesis is useful tool for the production of mutant proteins. Such proteins, if thoughtfully 'designed' and correctly studied may increase our understanding of the structural and functional relationships which govern their biological activity.

The information provided by amino-acid sequence alignments has allowed the identification of putative catalytic motifs based on absolute or partial conservation between species. Several groups have previously employed mutagenesis as a tool to create mutant acyltransferase proteins containing amino acid substitutions in critical regions or 'blocks' (Ferri and Toguri, 1997; Heath and Rock, 1998; Lewin *et al*, 1999). The mutant proteins were investigated for activity, substrate preference determinations were additionally performed in some instances. Studies have been carried out on acyltransferase proteins from a variety of species and subcellular compartments to assess the importance of different amino acid residues, either by chemical modification of such residues or their substitution for alternatives by site directed mutagenesis. Proteins from such diverse sources as bacteria (lipoate acyltransferase from *E. coli*; Russell and Guest 1991), mammals (carnitine acyltransferase from rat; Cronin 1997) and plants (plastidial lysophosphatidic acid acyltransferase from oilseed rape; Maisonneuve *et al*, 2000) have been investigated using site directed mutagenesis.

Useful work has been performed on G3PAT proteins by several groups attempting to identify amino acid motifs diagnostic for the *sn*-glycerol-3-phosphate acyltransferase reaction (Heath and Rock, 1998; Dircks *et al*, 1999 and Lewin *et al* 1999). Sequence

analysis has revealed that G3PAT proteins from many plant species share a highly conserved domain that contains 'invariant' histidine and aspartic acid residues in a specific configuration. This region has become known as the H(X)<sub>4</sub>D box, with a histidine and aspartic acid residue separated by four variable 'spacer' residues. One or more residues in this region are proposed to have catalytic importance. Heath and Rock investigated the role of the invariant histidine H306 (position in the published *E. coli* sequence, NCBI accession number 130326). The investigation was performed on two enzymes with acyltransferase activity: G3PAT from *E. coli* and the bifunctional 2-acylglycerophosphoethanolamine acyltransferase/ acyl-ACP synthetase. In both cases site-directed mutagenesis was used to convert the histidine in the H(X)<sub>4</sub>D box to an alanine residue. The resulting loss in activity was presented as evidence to support the theory that the histidine residue was directly involved in catalysis of the acyltransferase reaction. When the aspartate residue D311 in *E. coli* G3PAT was substituted for alanine the mutant enzyme had significantly reduced catalytic activity but was also reported not to assemble into the cytoplasmic *E. coli* membrane (as determined by membrane isolation, flag-epitope tagging of the carboxy-terminus and immuno-detection with monoclonal M2 antibody (Heath and Rock, 1998)). This indicates that D311 may have an important role in G3PAT activity as well as protein folding and membrane insertion.

Lewin *et al* (1999) identified four regions of strong homology when comparing amino acid sequences of G3PAT (*PlsB*), lysophosphatidic acid acyltransferase (LPAAT) and dihydroxy-acetone phosphate acyltransferase DHAPAT from *E. coli*. These regions were termed blocks I-IV and were each proposed to contain invariant residues essential for

catalysis of the acyltransferase reaction. The role of these residues was investigated by a combination of chemical modification and site-directed mutagenesis. It was determined that D311 was crucial to the G3PAT reaction, whereas H306 - whilst important - could be substituted for glycine and retain 22% of wild type activity. When histidine residues were chemically modified by DEPC, 50% of wild type activity was retained. The group postulated that this result indicates H306 may not be absolutely essential for the *PlsB* acyltransferase reaction.

Within the H(X)<sub>4</sub>D box other residues are often be highly conserved between species. In many bacteria the sequence is HXSXXD. In most chilling resistant plants the sequence is HQSEAD and in many chilling sensitive plants the sequence is HQTEAD (see figure 4.2). The importance of the residue shown in bold was also investigated by Lewin *et al* (1999). In *E.coli* the residue is S308 – the substitution S308A was described to have only modest effects on *PlsB* activity. The results of a similar substitution by our group of the same residue in plastidial G3PAT is reported in section 4.5.

Lewin *et al* (1999) also identified the residues F351, I352, R354, E385, G386 and P421 as residues which, if substituted, had a significant effect on the catalytic activity of *PlsB* (measured as a drop in V<sub>max</sub>). These residues were said to be located in or around the hydrophobic acyl-binding cleft, but no structural data for *PlsB* is available so this is difficult to determine. Minimal proof that the mutant proteins did not have a perturbed 3D structure (despite correct membrane insertion) was offered so the precise reason for the drop in activity of these proteins remains undetermined.



The work of these groups has been a useful step forward in understanding the chemistry of the membrane-bound G3PAT reaction. The work described in this chapter is intended to continue to elucidate the mechanisms for both substrate binding and catalysis in the plastidial (soluble) G3PAT enzyme from squash.

#### **4.3 Functional regions/motifs in plant plastidial G3PAT proteins.**

Plant G3PAT is nuclear encoded; a target peptide is responsible for the transport of this protein to the plastid (Murata and Tasaka, 1997). In the plastid the target peptide is cleaved away to produce the mature protein. The form of G3PAT used in these studies was a clone created in the vector system pET 24a, named Q24a. The protein is 28 residues shorter than the most recently predicted processing, beginning at the previously predicted processing site, see figure 4.1. The newly predicted processing site has been published by Murata and Tasaka in 1997. However, the truncated form coupled to the RUBISCO transit peptide has been demonstrated to be successfully transported to the plastid in tobacco plants, where the enzyme is biologically active and non-selective (Murata *et al* 1992).

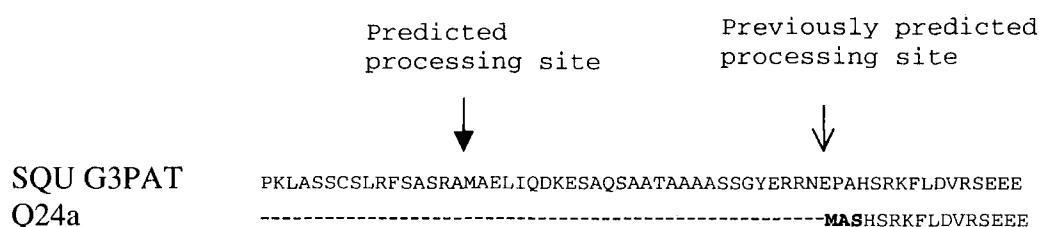


**Figure 4.1 N-terminal amino acid alignment of squash plastidial G3PATs.** SQU G3PAT is the full length precursor from squash (NCBI accession number AB049134.1) Residues shown in **bold** are coded for by the vector, pET24a.

Alignment studies performed on plastidial G3PAT proteins from a variety of plant sources permitted the identification of regions or single residues which were invariant or highly conserved between species. The alignment used is shown in figure 4.2. In addition to the information provided by sequence analysis, detailed structural information is available on squash G3PAT following the recent publication of its 3D structure (Turnbull *et al* 2001a,b). This combined information has been central to the design of a rationalised site-directed mutagenesis approach to study the catalytic mechanism of squash G3PAT reaction. It has also permitted the mutagenesis of residues thought to be located within or near to putative substrate binding regions.

Three negatively charged residues near the H(X)<sub>4</sub>D box, K193 R235 and R237 form a region strongly attractive to the positively charged phosphate moiety of glycerol-3-phosphate, the suggested binding site for G3P. The H(X)<sub>4</sub>D box was determined to be located at the mouth of a hydrophobic cleft lined with 14 residues which made Van der Waal contacts with a computer modelled palmitoyl-pantothen substrate. These residues

CLUSTAL W (1.7) multiple sequence alignment of Q24a and G3PAT from seven chilling sensitive (top) and four chilling resistant (bottom) plant species.

. = Conserved                   : = Highly conserved                   \* = Invariant

Q24a (SQUASH) -----  
SQUASH -----  
FIGLEAF -----  
CUCUMIS MFILSAVSSSSSSSSSSVPSSLPPFSLSPSISLSFSRVSLPPSSSSSSSSSLKFLPLSLHF  
ELAEIS-S -----MLVPSALPRVSR-----VSAARFSVSGVGSSPALSSRSCTSLDSSV  
CARTHAMUS -----MSIFFSPSSPTLFFS-----TTNANPRVSPSSSPSAFTPPLSSSRLRP  
ELAEIS-H -----MTDSFAHCASHIN---YRHKMKTMFIFSTPCCSPSTAFFSP---F  
PHASEOLUS -----MSMTGSSAYYVAHAIPFRLRLSNKTM LLLSTPPTTFFPTSTTPRVTL  
  
PISUM -----MTDSFAHCASHIN---YRHKMKTMFIFSTPCCSPSTAFFSP---F  
ARA -----MTLTFSSSAATVAVAAATVTSSARVPVYPLASSTLRGLVSFRLTAKKL  
SPINACIA -----MLVLSSSAPPVLEVCKDRVSSS-FSTSSSSSSSAFSAVVFRSFFTR  
VICIA -----MTDSFAHYASHIN---IRPKTKTMLIFSTPCCSPSTAFFSP---F

Q24a (SQUASH) -----  
SQUASH -----MAELIQDKESA---QSAATAAAASSGYE-----RR--N  
FIGLEAF -----MAELIQDKESA---QSAATAAAASSGHE-----RR--N  
CUCUMIS TPPKLSSPHSFLRFSASRAMAELIQDKESA---HTPSTTDVT-----R--N  
ELAEIS-S RSSLRRCPG-IYTSRTKAVVEAVESKASAREWRSVAVKRAVLASDTG-----AE--E  
CARTHAMUS ILRGFPCLAFSAPANAAGTAETVHGKNKWS--PSSSSSAATQPSAG-----S  
ELAEIS-H RASNSKPLR-----STLSLRSSISSS-SITSTSHCSLAFNIVKHKEKN-----VVSANMT  
PHASEOLUS LSSTSSSSS-----SSISLRSSSTAPSPSCSSVTPKDNCLASAKHSP-----PNMS  
  
PISUM RASNSKPLR-----STLSLRSSISSS-SITSTSHCSLAFNIVKHKEKN-----VVSANMT  
ARA FLPPLRSRGG----VSVRAMSELVQDKESS---VAASIAFNEAAG-E-----TP--S  
SPINACIA FNSSLICCCS----SKLKLMDALTALPSSSSSSTSASASYSAAAKSVEEENHEIPVKKEDDN  
VICIA RASNCKPLRS---STLCRLSLTSSATSITSTSNSSLAFNIVKPKEKN-----VVSANMT  
CONSENSUS

Q24a numbering   1           10           20           30           40           50           59  
Q24a (SQUASH) MASHSRKFLDVRSEEEELLSCIKKETEAGKLPPNVAAGMEELYQNYRNAVIESGNPKAD-E  
SQUASH EPAHSRKFLDVRSEEEELLSCIKKETEAGKLPPNVAAGMEELYQNYRNAVIESGNPKAD-E  
FIGLEAF EPAHSRKFLDVRSEEEELLSCIKKETEAGKLPPNVAAGMEELYQNHNAVIESRNPKAD-E  
CUCUMIS DPPHSRAFLDLRSEEEELLSCIRRETEAGKLPSNVAAGMEELYQNYKNAVFESGNPKAD-E  
ELAEIS-S EVGHSRSFLRARSEEEELLSYIRKEVETGRLSSDIANGLEELYNYRNAVLQSGDPRAN-K  
CARTHAMUS DHGHSRTFIDARSEQDLLSGIQRELEAGTLPKHIAQAMEELYQNYKNAVLQSAAPHA-E  
ELAEIS-H SSVSSRTFLNAQNEQDVLSGIKKEVEAGTLPASIAAGMEEVYLNKYSAVIKEWRSQSNRN  
PHASEOLUS ASVSSRTFLNAQSEQDVFAGIKKEVEAGSLPANVAAGMEEVYNNYKKAQVIQSGDPKAN-E  
  
PISUM SSVSSRTFLNAQNEQDVLSGIKKEVEAGTLPASIAAGMEEVYLNKYSAVIKSGDPKAN-E  
ARA ELNHSRTFLDARSEQDLLSGIKKEAEAGRLPANVAAGMEELYWNYKNAVLSSGASRAD-E  
SPINACIA QLLRSRTYRNVRSAEELISEIKRESEIGRLPKSVAYAMEGLFHYRNAVLSSGISHAD-E  
VICIA SSVSSRTFLNAQNEQDVLSGIKKEVEAGTLPASIAAGMQEVYLNKYSAVIKSGDPKAN-E  
CONSENSUS       \*\* :   .:   :::   \*:: \* \* \* . : \* .: : : :. \*\* :. . :. .

Q24a numbering	60	70	80	90	100	110	119
Q24a (SQUASH)	IVLSNMTVALDRILLDVEDPFVFSSHHKAIREPFDYYIFGQNYIRPLIDFGNSFVGNLSL						
SQUASH	IVLSNMTVALDRILLDVEDPFVFSSHHKAIREPFDYYIFGQNYIRPLIDFGNSFVGNLSL						
FIGLEAF	IVLSNMTVALDRILLDVEDPFVFSPHHKAIRE-FDYYMFGQKYIRPLIDFGNSFVGNPYL						
CUCUMIS	IVLSNMTVALDRILLDVEDPFMFSPHHKAIREPFDYYTFGQNYVRPLIDFENSFVGNLSL						
ELAEIS-S	IILSNMAVAFDRILLDVEDPFTFSPHHQAIREPFDYYMFGQNYIRPLIDFRRSYIGNISI						
CARTHAMUS	IVLSNMRVAFDRMFLDVKEPFEEFSPYHEAILEPFNYMFGQNYIRPLVNFRESYVGNVSV						
ELAEIS-H	CINKIRLPLIDRIFLDVKEPFVFEAHHKAKREPFDYYMFGQNYIRPLVDFETSIVGNMPL						
PHASEOLUS	IVLSNMIALLDRVFLDVTDPFVFOPHHKAKREPFDYYVFGQNYIRPLVDFKNAYVGNMPL						

PISUM	IVLSNMTALLDRIFLDVKEPFVFEAHHKAKREPFDDYMFQGNYIRPLVDFETSYVGNMPL
ARA	TVVSNMSVAFDRMLLGVEDPYTFNPYHKAVREPFDDYMFVHTYIRPLIDFKNSYVGNASI
SPINACIA	IVLSNMSVMLDFVLLDIEDPFVFPPFHKAIREPADYYSFGQDYIRPLVDFGNSYVGNIAI
VICIA	IVLSNMTALLDRIFLDVKEPFVFEAHHKAKRGPFDDYMFQGNYIRPLVDFETSYVGNMPL
CONSENSUS	. . . : * : * : : * : * : * : * : * : * : * : * : * : * : * : *

	HQX <sup>HEAD</sup>						
Q24a numbering	120	130	140	150	160	170	179
Q24a (SQUASH)	FKDIEEKLQQGHNVVLISNHQTEADPAII	SLLLEKTNPYIAENTIFVAGDRV	LADPLCKP				
SQUASH	FKDIEEKLQQGHNVVLISNHQTEADPAII	SLLLEKTNPYIAENTIFVAGDRV	LADPLCKP				
FIGLEAF	FKDIEEKLQQGHNVVLISNHQTEADPAII	SLLLEKTNPYIAENTIFVAGDRV	LADPLCKP				
CUCUMIS	FKDIEEKLHQGHNVVLISNHQTEADPAII	SLLLEKTNPYIAENMIYVAGDRV	IADPLCKP				
ELAEIS-S	FSDMEEKLQQGHNVLM	SNHQTEADPAII	ALLLERTNSHIAETMVFVAGDRV	LTDP			
CARTHAMUS	FGVMEEQLKQGDKVVLISNHQTEADPAV	I	ALMLLETTNPHISENIIYVAGDRV	ITDP			
ELAEIS-H	FIQMEEQLKQGHNII	LM	SNHQSEADPAII	ALLLEMRLPHIAENLIYVAGDRV	ITDP		
PHASEOLUS	FIEMEEKLKGHNII	LM	SNHQTEADPAII	SLLLETRL	PYIAENLTYVAGDRV	ITDP	

PISUM	FIQMEEQLKQGHNIILMSNHQSEADPAIIALLLEMRLPHIAENLIYVAGDRVITVPLCKP
ARA	FSELEDKIRQGHNIVLISNHQSEADPAVISLLLEAQSPFIVENIKCVAGDRVITDPLCKP
SPINACIA	FQEMEEKLKQGDNIILMSNHQSEADPAVIALLLKTNLSLIAENLIYIAGDRVITDPLCKP
VICIA	FIQMEEQLKQGHNIILMSNHQSEADPAIIALLLEMQLPHIAENLIYVAGDRVITDPLCKP
CONSENSUS	* : * : * : * : * : * : * : * : * : * : * : * : * : * : * : *

Q24a numbering	180	190	200	210	220	230	238
Q24a (SQUASH)	FSIGRNLICVYSKKHMF	DIPELTETKRKANTRSLK	EMALLLRGGSQ	LIWIAPSGGRDRP			
SQUASH	FSIGRNLICVYSKKHMF	DIPELTETKRKANTRSLK	EMALLLRGGSQ	LIWIAPSGGRDRP			
FIGLEAF	FSIGRNLI	SVYSKKHMLDIPELAET	KRNANTRTLK	EMALLLRGGSQ	LIWIAPSGGRDRP		
CUCUMIS	FSIGRNLICVYSKKHML	DIPELAETKRKANTRSLK	EMALLLRGGSQ	LIWIAPSGGRDRP			
ELAEIS-S	FSMGRNLLCVYSKKHM	DDVPELIEMKRRANTRSLK	EMALLLRGGSQ	IWIAPSGGRDRP			
CARTHAMUS	FSMGRNLLCVYSKKHM	NDVPELAEMKKRSNTRSLK	GRMALLLRGGSQ	IWIAPSGGRDRP			
ELAEIS-H	FSIGRNLICVYSKKHML	DNPELVDMKRKANTRSRK	EMAMLLRSGSQ	IWIWITPSGGRDRP			
PHASEOLUS	FSIGRNLICVYSKKHML	DDPALVEMKRTANIRALK	EMAMLLRNGSOLV	IWIAPSGGRDRP			

PISUM	FSIGRNLCVYSKKHMLDNP	ELVDMKRKANTRSRK-EMAMLLRSGSQIIWIAPSGGRDRP
ARA	FSMGRNLCVYSKKHMNDP	ELVDMKRKANTRSLK-EMATMLRSGGQLIWIAPSGGRDRP
SPINACIA	FSMGRNLLCVYSKKHMYDDP	ELVDVKKRANTRSLK-ELVLLL RGGSKIWIAPSGGRDRP
VICIA	FSIGRNLCVYSKKHMLDNP	ELIDMKRKANTRSLK-EMATLLRSGSQIIWIAPSGGRDRP
CONSENSUS	*****	*****

		L261					
Q24a numbering	239	250	260	270	280	290	297
Q24a (SQUASH)	DPSTGEWYPAPFDASSVDNMRRLIQHSDVPGHLFPLALLCHDIMPPPSQVEIEIGEKRVI						
SQUASH	DPSTGEWYPAPFDASSVDNMRRLIQHSDVPGHLFPLALLCHDIMPPPSQVEIEIGEKRVI						
FIGLEAF	DPLTGEWYPAPFDASSVDNMRRLLVQHSDVPGHLFPLALLCHDIMPPPSQVEIEIGEKRVI						
CUCUMIS	DPSTGEWYPAPFDASSVDNMRRLLQHSGAPGHLFPLALLCYDIMPPPSQVEIEIGEKRVI						
ELAEIS-S	DPSTGEWHPAPFDVSSVDNMRRLVEHSSVPGHIYPLSLLCYEVMPPPQVEKQIGERRTI						
CARTHAMUS	DPITNQWFPAPFDATSLDNMRRLLVDHAGLVGHIYPLAILCHDIMPPPLQVEKEIGEKSWI						
ELAEIS-H	VANSGEWAPAPFDSSSDNMRRLLVDHSSPPGHIYPLAILCHDIMPPPLKVEKEIGEKRRI						
PHASEOLUS	DAQTREWVPAPFDISSVDNMRRLVEHSGPPGHVYPLAILCHDIMPPPLKVEKEIGEKRRI						
PISUM	VANSGEWAPAPFDSSSDNMRRLLVDHSGPPGHIYPLAILCHDIMPPPLKVEKEIGEKRRI						
ARA	NPSTGEWFPAPFDASSVDNMRRLVEHSGAPGHIYPMSSLLCYDIMPPPPQVEKEIGEKRVL						
SPINACIA	DAVTGEWYPGTFDFAALDNMRRLVEHAGRPGHIYPLALLCYDIMPPPAQVEKEIGEKRVM						
VICIA	VANSGEWAPAPFDSSSDNMRRLLVDHSGPPGHIYPLAILCHDIMPPPLKVEKEIGEKRRI						
CONSENSUS	. : :* *..** :*:*****:*. : **::*:*:*:*:*:*:** :** :***: :						
Q24a numbering	298	310	320	330	340	350	357
Q24a (SQUASH)	AFNGAGLSVAPEISFEEIAATHKNPEEVREAYSKALFDSVAMQYNVLKTAISGKQGLGAS						
SQUASH	AFNGAGLSVAPEISFEEIAATHKNPEEVREAYSKALFDSVAMQYNVLKTAISGKQGLGAS						
FIGLEAF	AFNGAGLSVAPEISFDEVAATHKNPEEVREAYSKALFDSVAMQYTVLKTAISGKQGLGAS						
CUCUMIS	SFNGTGLSVGPEISFDEIAASRDNPDEVREAYSKALYDSVAKQYNVLKAAIDGKQELEAS						
ELAEIS-S	SFHGVLGSLVAPELNFNELTAGCETPEEAKAFAFSQALYNSVGEQYNVLKSAIHEHRGLNAS						
CARTHAMUS	SFHGTGISVAPEINFQEVNTASCGSPEEAKAAYSQALYDSVCEQYKVLHSAVHGGKGLEAS						
ELAEIS-H	SYHGTGISTAPEISFSNTTAACENPEKAKDAYTKALYDSVTEQYDVLKSAIHGKKGLQAS						
PHASEOLUS	CFHGAGISVAPAISSFSETTATCENPEKAK-VFSKALYNSVTEQYNVLKSAIQGKKGFEAS						
PISUM	SYHGTGISTAPEISFSNTTAACENPEKAKDAYTKALYDSVTEQYDVLKSAIHGKKGLQAS						
ARA	GFHGTGLSIAPEINFSDVTADCESPNEAKEAYSQALYKSVNEQYEILNSAIKHRRGVEAS						
SPINACIA	SFHGVGSVEPEINYNVDVSLGCKNDEEAKSVYGQALYNSVNEQYNVLKAAIHGKQGSAS						
VICIA	SYHGTGISTAPEISFSSTTAACENPETAKDAYTKALYDSVTEQYDVLKSAIHGKKGLQAS						
CONSENSUS	::*.*:* * :.... : . : . : :*:*.** ** :*:*: : **						
Q24a numbering	358	367	SPECIES (in full)				
Q24a (SQUASH)	TADVLSLQPW----		<i>Cucurbita moschata</i>				
SQUASH	TADVLSLQPW----		<i>Cucurbita moschata</i>				
FIGLEAF	IADVLSLQLW----		<i>Cucurbita ficifolia</i>				
CUCUMIS	VADVLSLQPWI---		<i>Cucumis sativus</i> L.				
ELAEIS-S	NSIISLSQPWQ---		<i>Eleis guineensis</i> (Kroon)				
CARTHAMUS	TPSVLSLQPLQFLD		<i>Carthamus tinctorius</i> L.				
ELAEIS-H	TPVVLSLQPWK---		<i>Eleis guineensis</i> (Harwood)				
PHASEOLUS	TPVVTLSQLPWK---		<i>Phaseolus vulgaris</i>				
PISUM	TPVVLSLQPWK---		<i>Pisum sativum</i>				
ARA	TSRVLSLQPWN---		<i>Arabidopsis thaliana</i>				
SPINACIA	TPTTSLSQLPWAS--		<i>Spinacia oleracea</i>				
VICIA	TPVVLSLQPWK---		<i>Vicia faba</i>				
CONSENSUS	. :***						

**Figure 4.2** Clustal W (1.7)<sup>TM</sup> multiple amino acid sequence alignment of Q24a and G3PAT from seven chilling sensitive (top) and four chilling resistant (bottom) plant species. Invariant residues are indicated with \*. The positions of the H4XD box and residue L261 are indicated above the sequence.

were H139, E142, V166, A167, G168, R170, V189, H194, L213, I229, R235, N257, M258 and L261. The 'jaws' of the cleft made near contact at the residues K193 and D251. These charged residues were proposed to facilitate salt bridge formation, excluding bulk solvent from the fatty acid binding fold. Palmitoyl-pantethene substrate cannot be modelled into the cleft entirely unambiguously so computer models should be supported with conventional biochemical studies. The predicted structure of the catalytic and acyl-binding pocket with modelled palmitoyl substrate is shown in schematic form in figure 4.3.

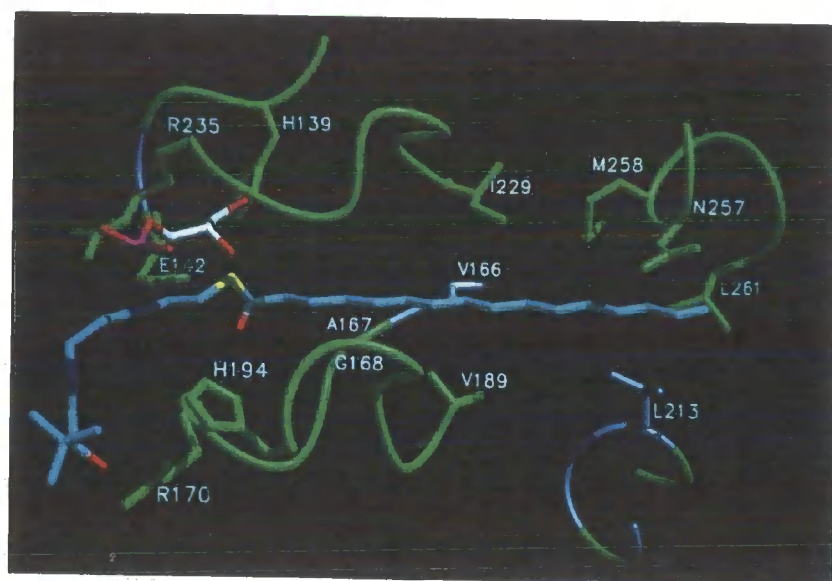
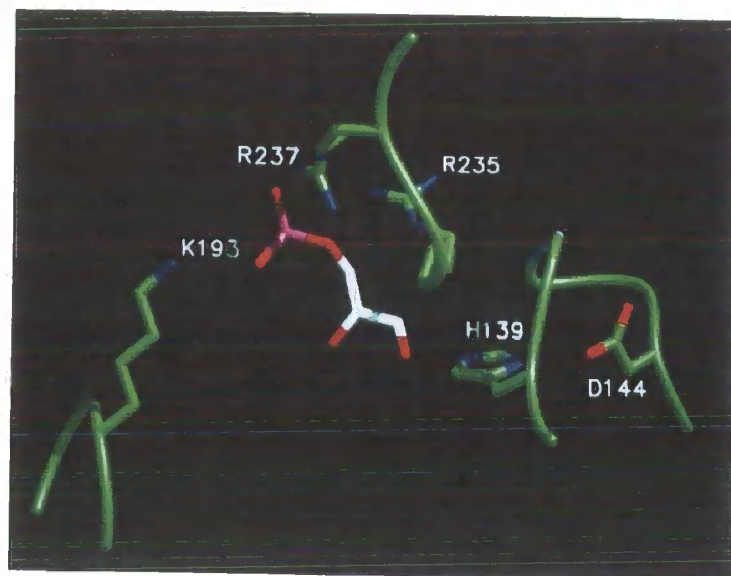
Structural information and conventional sequence alignments, has been used to design several G3PAT mutant proteins. Analysis of the catalytic and substrate binding properties of these proteins are detailed in sections 4.3 - 4.5.

**Please note:** All mutants detailed in this chapter were created by William J. Simon as part of a combined disciplinary approach to the study of G3PAT (see Appendix 1 - paper in press). However, all investigations of molecular and biochemical properties (assays of enzyme activity, substrate preference, substrate binding and  $K_m$  and  $V_{max}$  determinations) have been carried out solely by myself, and so are described herein. All mutant proteins were assayed using standard absolute amounts to permit the direct comparison of catalytic velocities and substrate selectivities.

**Figure 4.3 (Top) Structural diagram of the glycerol-3-phosphate (G3P) binding site with modelled G3P molecule.** The three residues thought to be critical for G3P binding are K193, R235 and R237. Positively charged regions are shaded blue. Negatively charged regions are shaded red.

**Figure 4.3 (Bottom) Structural diagram of the acyl- and glycerol-3-phosphate binding sites with modelled G3P and palmitoyl-pantothen substrate.** Residues that make Van der Waal contacts with the palmitoyl-pantothen substrate are H139, E142, V166, A167, G168, R170, V189, H194, L213, I229, R235 , N257, M258 and L261. Positively charged regions are shaded blue. Negatively charged regions are shaded red. The thioester bond is shaded yellow.

Diagrams were provided by A.P. Turnbull (Krebs Institute for Biomolecular Research, Department of Molecular Biology and Biotechnology, University of Sheffield).



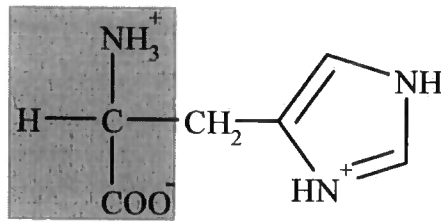


#### 4.4 Analysis of mutant G3PAT proteins – G3P binding pocket

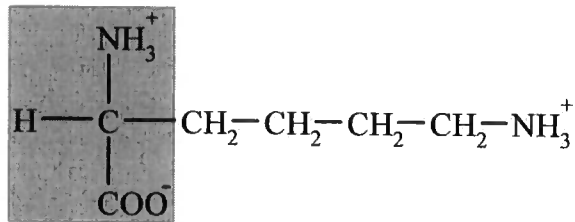
Structural information regarding squash G3PAT has indicated that the residues K193, H194, R235 and R237 are located close to one another, forming a pocket of local positive charge (Turnbull *et al*, 2001(a and b); Appendix 1 and figure 4.3). This pocket is the proposed binding region for glycerol-3-phosphate. Each of these residues were individually substituted for a serine residue. Serine is a relatively small, non-charged, hydroxyl containing amino acid, lysine, histidine and arginine are not (see figure 4.4). In each case the activity and selectivity (where possible) of the mutant enzymes were determined in dual-substrate assays. Mutant proteins K193S, R235S and R237S were wholly inactive, whereas H194S retained 79% of wild type (Q24a) activity and was essentially non-selective (a ratio of 18:1/16:0-ACP usage of 0.8 was measured). These data, shown in figure 4.5, are consistent with the proposed function of the residues K193, R235 and R237 as a docking site for G3P. H194 may play a supplementary role in G3P binding.

To determine whether the mutant proteins had a perturbed 3D structure, substrate binding experiments were performed to ensure that they could still bind the first-bound substrate, acyl-ACP (determination of substrate binding order is discussed in chapter 5). The binding capacity of the three inactive mutant G3PAT proteins was compared to the binding capacity of the original construct Q24a, the results are presented in Table 4.1.

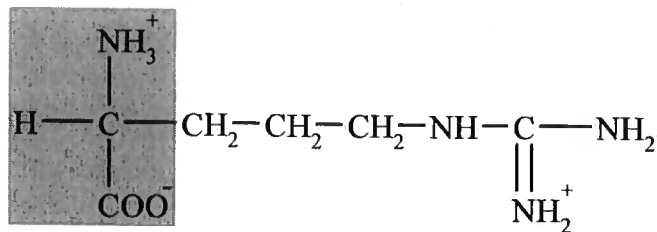
a) Histidine



b) Lysine



c) Arginine



d) Serine

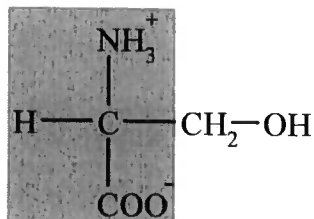


**Figure 4.4 Schematic diagram of amino acid residues a) histidine b) lysine c) arginine and d) serine.**

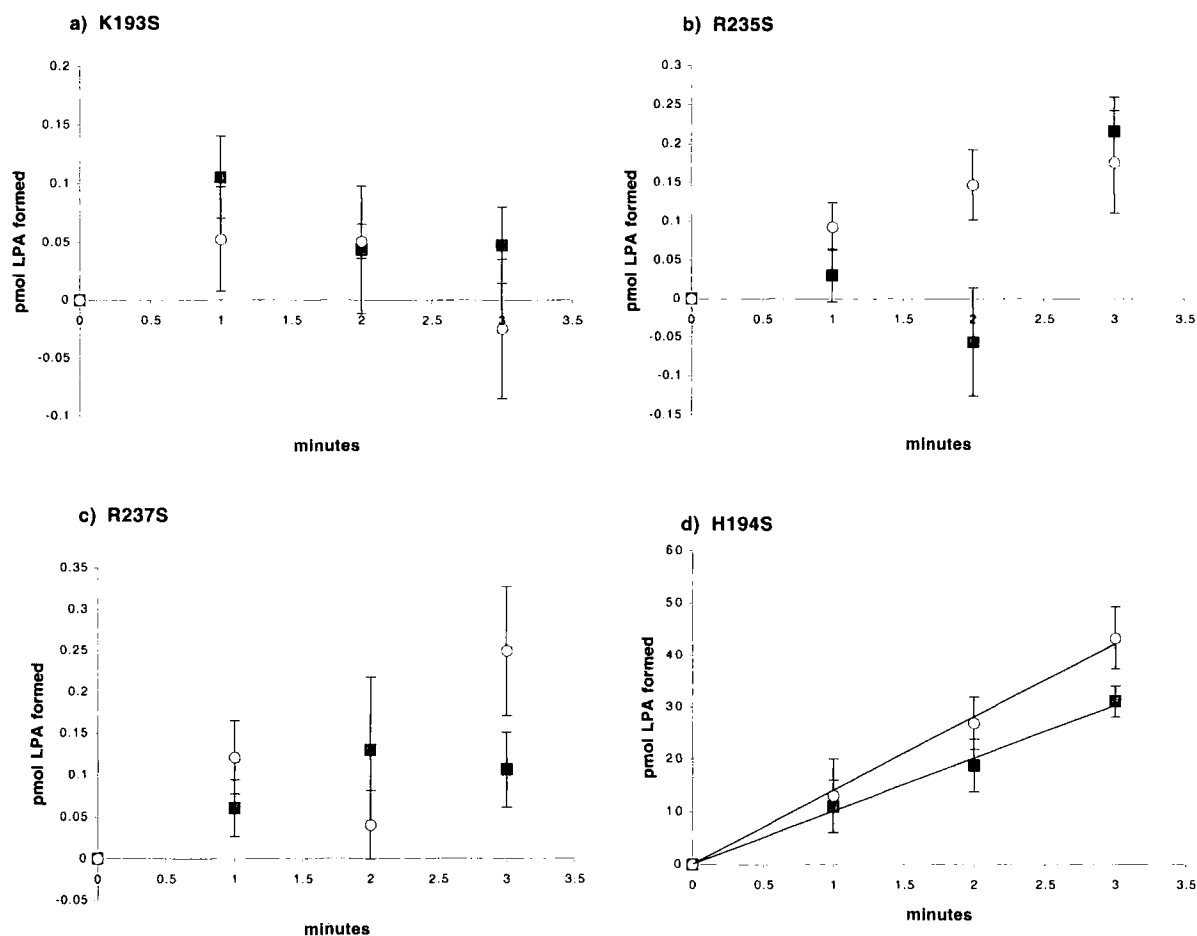


**Figure 4.5 Substrate selectivity assays on squash G3PAT mutant proteins K193S, R235S, R237S and H194S.**

The assays are performed under competitive conditions with 18:1-ACP and 16:0-ACP substrates present at 1.1  $\mu\text{M}$  and results are displayed as rate of product (LPA) formation against time. ■ = 18:1-LPA. ○ = 16:0-LPA. Mutant proteins K193S, R235S and R237S are inactive with both 18:1-ACP and 16:0-ACP substrates. H194S uses both substrates, with a 18:1/16:0 ratio of approximately 0.8. Experiments were performed in triplicate and results are presented as mean values  $\pm$  one standard error measurement.

G3PAT mutant protein	Molar ratio – moles of 18:1-ACP substrate bound per mole of G3PAT
Q24a	0.95 ± 0.01
K193S	0.91 ± 0.02
R235S	0.91 ± 0.05
R237S	0.90 ± 0.03

**Table 4.1** The mutant enzymes K193S, R235S and R237S retain their ability to bind acyl-ACP substrate. Results are given in moles of 18:1-ACP substrate bound per mole of G3PAT ± one standard error unit. 100 pmoles of radiolabelled 18:1-ACP was incubated with 50 pmoles of G3PAT protein in the absence of G3P and centrifuged through a 30,000Da molecular weight cut-off membrane. Substrate bound to G3PAT did not pass through the membrane and was retained in the upper compartment.

The mutant enzymes K193S, R235S and R237S can still bind acyl-ACP at levels very close to wild type, indicating that the 3D structure at the substrate binding region/active site is not grossly perturbed or blocked. This conclusion is supported by further structural data – crystals of the mutant enzymes K193S, R235S and R237S have been produced and their structures solved. The mutant proteins have structures highly homologous to each other and to Q24a (communication from A.P. Turnbull, Krebs Institute, University of Sheffield). As acyl-ACP binding is unaffected, it seems likely that the residues K193, R235 and R237 are crucial for G3P binding.

**4.5 Analysis of mutant G3PAT proteins – can a single residue substitution in the H(X)<sub>4</sub>D box result in alteration of substrate selectivity?**

The H(X)<sub>4</sub>D box is an amino acid sequence conserved in the G3PAT enzyme throughout many species (figure 2) and characteristic of the acyltransferase reaction (Heath and Rock, 1998). The motif has the consensus of HQSEAD in oleate selective (chilling tolerant) and HQTEAD in non-selective (chilling sensitive) species (Kroon, 2000). Q24a

(the wild type squash protein) has a threonine at position 141. The substitution T141S was performed and the resulting mutant G3PAT was assayed for activity and selectivity. Somewhat surprisingly, the mutation did not seem to affect catalytic activity to any significant degree. T141S was found to have an activity close to that of Q24a (106% of total moles of LPA formed per minute by Q24a) and an identical selectivity - a ratio of 18:1/16:0-ACP usage of 1.0 was measured.

The mutant E142A was created to investigate the role of the glutamic acid in the H(X)<sub>4</sub>D box. The mutant was found to be entirely inactive. The substitution of glutamic acid for a relatively small residue such as alanine is unlikely to result in a major conformational change around the region of the active site. It may be the case that without a negatively charged residue at this point, the electron density around different residues within the H(X)<sub>4</sub>D box is sufficiently perturbed so as to interfere with the relay of charge in this region and so disrupt catalysis. It is also possible that the increase in electron density associated with the negatively charged side chain of glutamic acid may permit the formation of hydrogen bonds that stabilise that the enzyme:substrate complex

Serendipity has also contributed to this study. The Q24a mutant L261F, fortuitously created by PCR error during a cloning step, has a near wild type activity but an altered substrate selectivity. The residue L261 is located at the distal end of the acyl-binding pocket, away from the catalytic H(X)<sub>4</sub>D domain. An analysis of the properties of L261F and fuller discussion of the effects of this mutation are presented in chapter 5.

#### 4.6 Analysis of mutant G3PAT proteins – acyl-ACP binding pocket

Several mutant G3PAT proteins were created to study the effect residues in the acyl-binding pocket and other areas of the protein. It was also noted that plastidial G3PAT contains four cysteine residues (numbering in Q24a is C20, C177, C188, C278) which are highly conserved when compared to several other plant species (figure 4.2). These residues were not located near to the acyl-binding pocket but were thought worthy of investigation on the basis of sequence alignment data alone. Each of these cysteine residues were individually converted to a serine; a residue of almost identical size, but in which the  $-\text{CH}_2-\text{SH}$  side group is a  $-\text{CH}_2-\text{OH}$ . The activity and selectivity of each of these enzymes were determined under standard dual substrate assay conditions (18:1-ACP/16:0-ACP), table 4.2. The cysteine residues were not proposed to have a structural role, for example in the formation of disulphide bridges, although this could have been investigated by the creation of double or treble cysteine mutants, or the inclusion of a reducing agent, such as DTT or  $\beta$ -mercaptoethanol in G3PAT assays.

Mutant - based on Q24a numbering	Activity as % of w.t. (Q24a) <sup>1</sup>	Selectivity as ratio of 18:1-LPA/16:0-LPA formation
Q24a	100 (arbitrary)	1.0
C20S	94 ± 6.1	1.1
C177S	96 ± 7.2	1.0
C188S	115 ± 8.9	0.8
C278S	106 ± 4.6	1.0

**Table 4.2 Mutants C20S, C177S, C188S and C278S have activity and substrate selectivity similar to wild type.** Assays were performed in triplicate and the results are presented as mean values ± 1 standard error measurement.

<sup>1</sup>Percentage activity is calculated by assigning the wild type enzyme an activity of 100% and comparing the total LPA formed per minute (18:1- and 16:0-LPA combined)

The residues V166, R170, H194, L213 and N257 were all predicted to line the acyl-binding pocket, being close enough to make Van der Waal contact with computer

modelled palmitoyl-pantothe substrate (communication from A.P.Turnbull, Krebs Institute, University of Sheffield). The following mutations were generated: V166A, R170S, H194S, L213S and N257S. The activity and selectivity of each of these mutant proteins was determined under standard dual substrate assay conditions (18:1-ACP/16:0-ACP) and the results are presented in table 4.3.

Mutant - based on Q24a numbering	Activity as % of w.t. (Q24a) <sup>1</sup>	Selectivity as ratio of 18:1-LPA/16:0-LPA formation
Q24a	100 (arbitrary)	1.0
V166A	97	1.5
R170S	5.6	not determined <sup>2</sup>
H194S	79	0.8
L213S	104	1.3
N257S	106	0.8

**Table 4.3** The activity and selectivity of acyl-binding pocket mutant G3PATs. Assays were performed in triplicate and the results are presented as average values.  
<sup>1</sup>Percentage activity is calculated by assigning the wild type enzyme an activity of 100% and comparing the total LPA formed per minute (18:1 and 16:0LPA combined)  
<sup>2</sup>The selectivity of this enzyme is more difficult to determine as the rates of enzyme activity are very low and closer to the margins of error.

The mutants V166A, H194S, L213S, N257S displayed activity and substrate selectivity close to wild type. The mutant R170S had a reduced catalytic activity and a substrate selectivity more difficult to measure (point 2, table 4.3) The primary data for R170S (plot of formation of pmoles 18:1- and 16:0-LPA against time) is presented in figure 4.6. It can be seen that, although the mutant enzyme may have a novel selectivity (16:0-LPA appears to be formed more quickly than 18:1-LPA) the very low enzymatic rates mean that the levels of error are large in comparison to selectivity measured. This means that it is difficult to determine the selectivity of this enzyme with confidence.

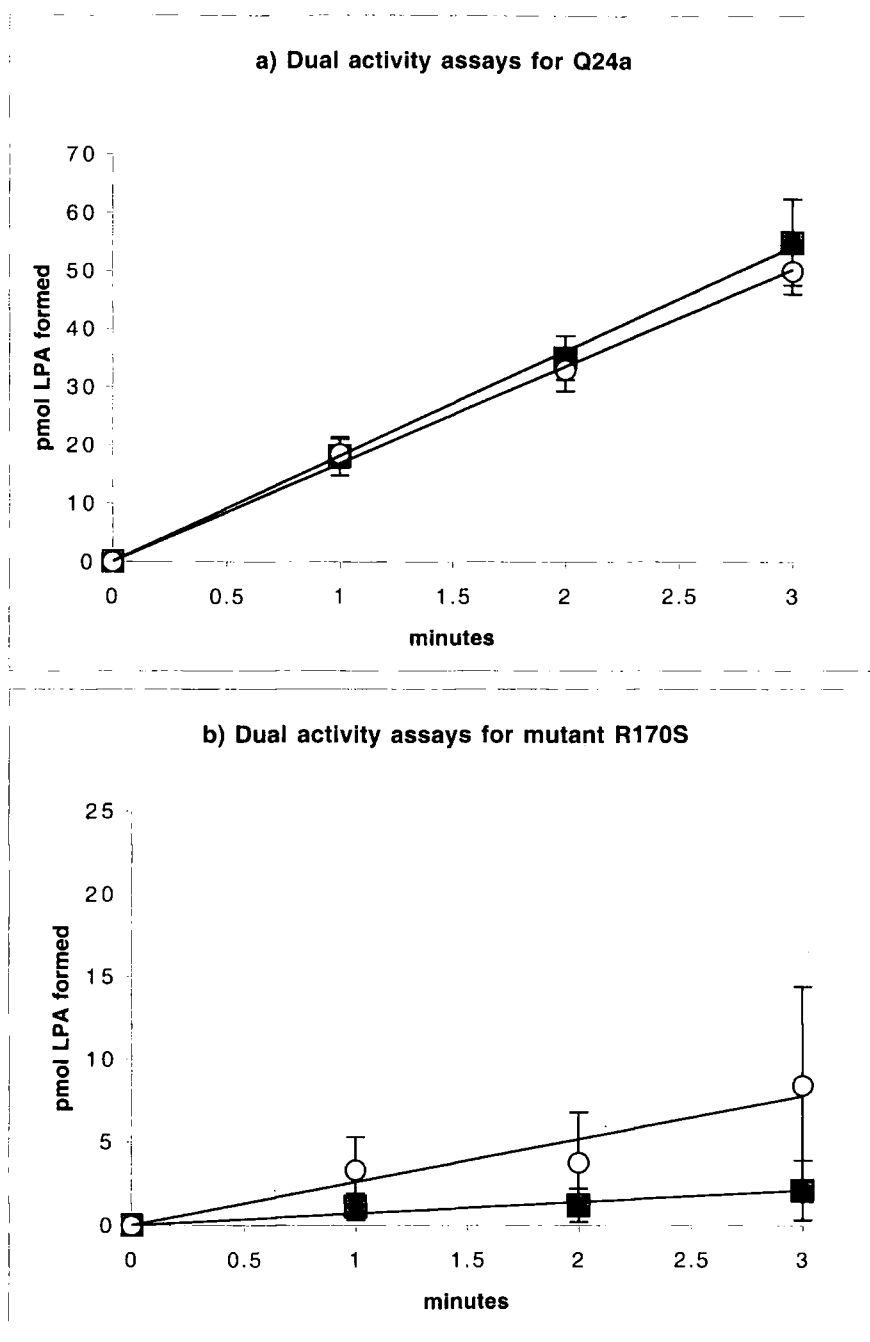


**Figure 4.6 Substrate selectivity assays on Q24a and mutant R170S**

The assays are performed under competitive conditions with 18:1-ACP and 16:0-ACP substrates each present at 1.1  $\mu\text{M}$  and results are displayed as rate of product (LPA) formation against time. ■ = 18:1 LPA. ○ = 16:1 LPA. Squash G3PAT (a), a non-selective enzyme uses both substrates at a similar rate. R170S (b) uses 16:0-ACP faster than 18:1-ACP rates are low. Error bars show  $\pm 1$  standard error measurement.



## 4.7 Discussion

Several residues have been identified as essential for G3PAT activity. R235 and R237 are predicted to form part of the G3P binding pocket, along with K193, a residue which has also previously been implicated in salt bridge formation to exclude bulk solvent from the acyl-binding pocket, thus increasing the hydrophobicity of this micro-environment (Turnbull *et al*, 2001b).

E142 is also essential for catalysis. It is uncertain why this is – the residue may be important for charge-relay (donation or acceptance of a de-localised electron) in the active site or for hydrogen bond formation with the substrate, see discussion in chapter 6.

The residue R170 is also important for enzyme activity, though not essential. When this residue is mutated to serine the enzyme is still active, but at very low levels. This is a result that was not predicted by either alignment or structural studies. Structural data places this residue within the acyl-binding pocket (figure 4.3). It may have a subsidiary role in substrate binding or substrate orientation. Arginine has a long, positively charged side chain ( $-(\text{CH}_2)_3\text{-NH-C}(\text{NH}_2^+)(\text{NH}_2)$ ) which may interact with  $\delta$ -negatively charged oxygen atoms between ACP and the hydrocarbon chain of acyl-ACP (ACP-S-CO-(CH<sub>2</sub>)<sub>n</sub>-CH<sub>3</sub>). Further investigation of this residue is recommended, either by chemical inactivation or the creation of mutants in which the residue is substituted for a variety of other residues. Low catalytic rates make determination of substrate selectivity difficult, but early indications suggest this mutant may have a substrate preference for 16:0-ACP

over 18:1-ACP. This is an unusual result as most enzymes investigated to date have had no reported selectivity, or have been selective for 18:1-ACP over 16:0-ACP.

Mutation of the residue H194 does not alter the rate of G3PAT catalysis to any great extent. The modest drop in activity (to approximately 80% of that of Q24a) may be due to loss of non-essential hydrogen bonds with the substrate, or a reduction in the charge-stabilisation of essential residues nearby (K193 is an adjacent residue).

The conserved cysteines C20, C177, C188 and C278 appear to be non-essential for G3PAT activity. Their role in squash plastidial G3PAT may be to ensure the protein remains correctly folded, either by the formation of di-sulphide bonds or by other favourable interactions. The majority of other mutations made to the acyl-binding region had little effect on G3PAT activity or selectivity. Of these the most surprising is T141S. It could logically be expected that this residue, different between selective and non-selective enzymes but conserved within each group, would play at least some role in the determination of substrate preference. However, there must be another reason for the pattern of conservation observed in sequence alignments as the mutated enzyme has virtually identical catalytic velocity and substrate selectivity to Q24a. Where alteration of the enzyme characteristics was anticipated, but not observed, this could be due to substitution for residue that was not different enough from the original. This is, after all, only the 'first round' of site-directed mutagenesis, the permutations for further mutagenic study are numerous. The amount of structural data available for this enzyme means that it is an ideal target for investigation. It is hoped that the structure of plastidial G3PAT

will be solved with acyl-substrate co-crystallised, bound in the active site. This will greatly increase knowledge of the structural and functional relationships at work in this region.

# **Chapter 5**

## **Kinetic analysis of wild type and mutant G3PAT proteins.**

**Determination of G3PAT catalytic mechanism and  
substrate binding constants for Q24a and Q24a L261F.**

## 5.1 Introduction

Plastidial G3PATs have been purified from various plant sources including squash (*Cucurbita moschata* - Ishizaki et al, 1988; Nishida et al, 2000) , pea (*Pisum sativum* - Weber et al, 1991), spinach (*Spinacia oleracea* - Ishizaki-Nishizawa et al, 1995) and *Arabidopsis thaliana* (Nishida et al, 1993). A list of the G3PATs cloned or purified from various sources and their substrate selectivity (if determined) is shown in table 5.1 for plastidial/soluble G3PAT and table 5.2 for membrane bound G3PAT. It is apparent from these studies that different plastidial G3PATs often display different selectivities for various acyl-ACP substrates. For example, G3PAT from Oil palm exhibits little selectivity between 16:0ACP and 18:1ACP groups (Kroon, 2000), whereas G3PAT from spinach has a strong preference for the longer, monounsaturated acyl group of 18:1ACP over 16:0ACP (Ishizaki-Nishizawa, *ibid.*).

Substantial effort has been made to determine the basis of substrate selectivity in this class of enzymes due to their proven role in the determination of membrane lipid composition (Murata et al, 1992). Initial surveys of acyl-group composition in complex lipids of chilling resistant and sensitive plants indicated a significant correlation between membrane lipid composition and chilling resistance (Murata et al, 1982; Murata, 1983). In 1992 Murata et al proved the link between the level of unsaturation of membrane lipids and chilling resistance - experimental verification was obtained when tobacco plants were transformed with cDNAs from a chilling sensitive

Species	S/R	Status	Acyl group pref.	Group responsible
<i>Arabidopsis thaliana</i> (Thale cress)	R	Amino acid sequence determined (from cDNA)	18:1	Nishida I, <i>et al</i> 1993
<i>Cucurbita moschata</i> (Squash)	S	Amino acid sequence determined for <b>AT1</b> isoform	18:1	Nishida I, <i>et al</i> 2000
<i>Pisum sativum</i> (Pea)	R	Amino acid sequence determined (from cDNA)	18:1	Weber S, <i>et al</i> 1991
<i>Spinacia oleracea</i> (Spinach)	R	Amino acid sequence determined (from cDNA)	18:1	Ishizaki-Nishizawa O <i>et al</i> , 1995
<i>Vicia fava</i> (Fava bean)	R	Amino acid sequence determined (from cDNA)	18:1	Liu JM <i>et al</i> , 1999

<i>Phaseolus vulgaris</i> (Bean)	S	Amino acid sequence determined (from cDNA)	No pref.	Fritz M <i>et al</i> , 1995
<i>Cucurbita moschata</i> (Squash)	S	Amino acid sequence determined for <b>AT2</b> and <b>AT3</b> isoforms	No pref.	Ishizaki O <i>et al</i> , 1988
<i>Cucumis sativus</i> (Cucumber)	S	Amino acid sequence determined (from cDNA)	No pref.	Johnson TC <i>et al</i> , 1992
<i>Elaeis guineensis</i> (Oil palm)	S	Amino acid sequence determined (from cDNA)	No pref.	Kroon JTM <i>et al</i>
<i>Oryza sativa</i> (Rice)	S	Amino acid sequence determined (from cDNA)	No pref.	Chen SN <i>et al</i> , 1999
<i>Cucurbita ficifolia</i> (Fingleaf gourd)	S	Amino acid sequence determined (from cDNA)	No pref.	

<i>Carthamus tinctoris</i> (Safflower)	S	Amino acid sequence determined (from cDNA)	N.D.	Bhella RS and MacKensie SL, 1994
<i>Peaonia californica</i> (Core eudicot)	?	Amino acid sequence determined (from cDNA)	N.D.	Tank DC and Sang T, 2001
<i>Citrus unshiu</i> (Satsuma orange)	?	Amino acid sequence determined (from cDNA)	N.D.	Kato M <i>et al</i> , 2001

**Table 5.1 Details of plastidial G3PATs cloned or purified from various species and their substrate selectivity (if determined).** N.D. = substrate preference not determined. S/R denotes whether the species is known to be chilling resistant (R) or sensitive (S).

Species	Status	Group responsible	Notes
<i>Elaeis guineensis</i> (Oil palm)	Amino acid sequence determined	Manaf A.M. and Harwood J.L., 2000	Preference for 16:0-CoA
<i>Persea americana</i> (Avocado)	150-fold purification from mesocarp microsomes	Eccleston V.S. and Harwood J.L., 1995	-
<i>Escherichia coli</i>	<i>plsB</i> gene cloned	Lightner V.A. et al, 1980	-
<i>Mortierella ramanniana</i> (Oleagenous fungus)	1308-fold purification (to homogeneity) from membrane fraction	Mishra S. and Kamisaka Y., 2001	Preference for 18:1-CoA over 16:0-CoA

<i>Xylella fastidiosa</i> (Bacterial plant pathogen)	DNA and amino acid sequence determined	Simpson A.J.G. et al, 2001	*
<i>Mycobacterium tuberculosis</i>	DNA and amino acid sequence determined	Cole S.T. et al, 2001	*
<i>Mycobacterium leprae</i> (Leprosy bacterium)	DNA and amino acid sequence determined	Cole S.T. et al, 2001	*
<i>Vibrio cholerae</i> (Cholera pathogen)	DNA and amino acid sequence determined	Heidelberg J.F. et al, 2001	*
<i>E.coli</i> 0157:H7 (Enterohaemorrhagic bact.)	DNA and amino acid sequence determined	Perna N.T. et al, 2001	*
<i>Pseudomonas aeruginosa</i> (Bacterial pathogen)	DNA and amino acid sequence determined	Stover C.K. et al, 2000	*
<i>Pasteurella multocida</i> (Bacterial pathogen)	DNA and amino acid sequence determined	May B.J. et al, 2001	*

<i>Caenorhabditis elegans</i> (Nematode)	Amino acid sequence determined	Blanchard M. and Bradshaw H., 1996	-
<i>Mus musculus</i> (Mouse)	Cloned from murine mitochondria	Yet S.F. et al, 1993	-
<i>Rattus norvegicus</i> (Rat)	Cloned from rat liver mitochondria	Bhat B.G. et al, 1999	-
<i>Homo sapiens</i> (Human)	DNA and amino acid sequence determined	N.C.B.I. Annotation Project 2002	**

**Table 5.2 Details of membrane bound G3PATs cloned or purified from various species.** \* denotes that a genome consortium published the pathogen genome and N.C.B.I. matched the probable G3PAT function by sequence similarity. \*\* denotes that the Human Genome Consortium published the genome and N.C.B.I. matched the probable G3PAT function by sequence similarity. For all entries except *Elaeis guineensis* (Oil palm) and *Mortierella ramanniana* (oleagenous fungus) the substrate preference has not been determined.

(*Cucurbita moschata*) and a chilling resistant (*Arabidopsis thaliana*) plant, expressed at a higher level than the endogenous G3PAT.

Acyl-group composition of phosphatidylglycerols from the leaves of the wild type and transgenic tobacco plants was determined. Analysis of the growth of these plants at chilling temperatures revealed that differences in the chilling sensitivity correlated closely with the extent of fatty acid unsaturation in phosphatidylglycerol. Furthermore, it was demonstrated for the first time that it is possible to alter the degree of phosphatidylglycerol fatty acid saturation by the insertion of a suitable acyltransferase. More recently the introduction of a cDNA for G3PAT from *Arabidopsis* into transgenic rice has been shown to increase levels of acyl-unsaturation in membrane phospholipids and increase the chilling tolerance of the photosynthetic apparatus [Yokoi *et al* 1998]. These studies offer sound experimental evidence that G3PAT enzymes affect chilling sensitivity of higher plants by determining the degree of acyl-unsaturation of membrane phospholipids.

Physical changes in membrane lipids have long been considered the primary event in chilling injury to plants and the case for membrane lipid composition determining the susceptibility of a plant to low, non-freezing temperatures is a strong one. However, it should be noted that other factors may be involved in temperature sensing and acclimatisation. Systems which detect temperature change and acclimatise higher plants to 'cold' or 'chilling' (low, non-freezing temperatures 2-6°C) have been identified and their components investigated (reviewed by Browse and Xin, 2001 and in Chapter



1). The expression of several genes which encode proteins with known enzymatic functions has been shown to be regulated by temperature change - alterations to cytoskeleton arrangement and calcium influxes are among the early changes that activate plant cold acclimation responses (Plieth *et al*, 1999). However, it is unclear whether these changes are to protect the plant against cold conditions or to prepare the plant for freezing conditions (0°C or below) prior to the onset of winter. Thus, even taking these findings into account, the majority of evidence implicates membrane fluidity as the factor with the most impact on chilling sensitivity and resistance.

This chapter (combined with chapter 4) investigates the basis for substrate selectivity in the G3PAT enzyme. Central to this approach is the establishment of an assay which can distinguish between selective and non-selective enzyme forms, using the natural substrate acyl-ACP and with conditions carefully chosen to mimic those *in vivo* (chapter 3). Once G3PAT enzymes are known to have different substrate selectivities, an attempt can be made to compare their structural and functional attributes.

Analysis of site-directed mutants (chapter 4) revealed that a single point mutation could alter squash G3PAT substrate selectivity without significantly affecting overall catalytic activity. This meant that both a selective and non-selective form of the squash enzyme were now available, both of which crystallised and diffracted an X-ray beam, enabling their 3D structure to be determined. This provided a suitable model for the investigation of substrate selectivity in this class of enzymes.

## 5.2 Cloning of selective and non-selective G3PAT enzymes and creation of the L261F mutant

Cloning steps detailed in this section were performed by Bill Simon and Johan Kroon, but biochemical and kinetic characterisation of the wild type and mutant enzymes were performed by the author.

A plastidial G3PAT cDNA clone from Squash (*Cucurbita moschata*) was a gift from Professor Norio Murata (National Institute for Basic Biology, Myodaiji, Okasaki 444, Japan). The coding sequence was cloned into the vector pET 17b for expression of the protein at high levels under selection of the antibiotic ampicillin (Kroon, 2000). In a further cloning step, the coding sequence for squash G3PAT was transferred to the vector pET 24a so that the protein could be expressed at high levels under selection of the antibiotic kanamycin (which has better thermal stability and lasts longer in bacterial culture). It was observed that the product of this final cloning step was no longer non-selective in assays performed by Hayman and Kroon, but exhibited a novel preference for 18:1-ACP over 16:0-ACP. Determination of the nucleotide sequence of the new construct revealed that three base changes had occurred during the PCR-based cloning steps, resulting in two amino acid substitutions in the C-terminal domain of the product. One (or both) of these mutations, L261F and P331S, was thus responsible for the dramatic change in substrate selectivity. Site directed mutagenesis was utilised to mutate each residue individually back to that occurring in the wild type cDNA, and then both at once to generate the mutants L261F, P331S and L261F/P331S. This generated a series of constructs, details of which are given in the sequence alignment

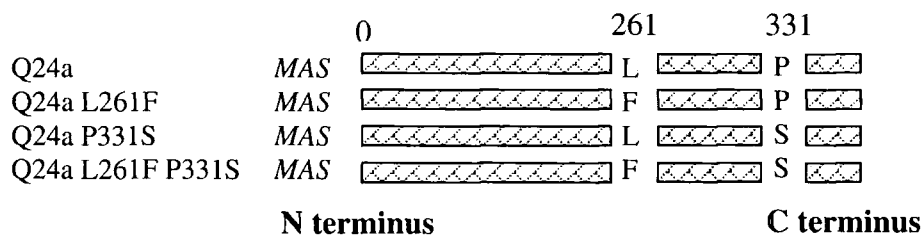


**Figure 5.1 Amino acid sequence alignment schematic of mutants Q24a, Q24a L261F, Q24a P331S and Q24a L261F P331S.** Characters in *italics* are coded for by the vector (pET24a) DNA. Numbering begins at the start of the coding sequence for squash G3PAT. For full sequence details of the Q24a construct see figure 4.2.

schematic in Fig 5.1. The 'wild type' construct (L261/P331) was termed Q24a. These constructs were transformed into *E. coli* BL21 (DE3) and expressed to a high level using the bacteriophage T7 promoter/T7 DNA polymerase system via IPTG induction. The following sections describe analyses carried out to characterise the wild type and mutant proteins.

### **5.3 Preparation and assay of wild type and mutant recombinant squash G3PATs produced in *E. coli*.**

G3PAT clones were kindly provided by Johan Kroon, University of Durham. The four cloned G3PATs detailed in section 5.2 were grown in 4 litre cultures and harvested as described in section 2.4. Briefly, cells were lysed in 20 mM Tris-HCl pH 7.4 using 3 freeze/thaw cycles in dry ice/ethanol and ice/water baths. The crude cell lysate was centrifuged at 150,000 g for 1hr at 4°C. The supernatant contained >95% of the G3PAT activity and was termed a crude Cell Free Extract (CFE) of G3PAT. The amount of G3PAT present in each CFE was determined by a combination of SDS PAGE and densitometric scanning (figure 2.1).

Using a standard amount of G3PAT per assay (210ng) to permit direct comparison of substrate selectivities and catalytic rates, each of the mutants Q24a, Q24a L261F, Q24a P331S and Q24a L261F P331S were assayed under standard selectivity assay conditions. This data is shown in figure 5.2.

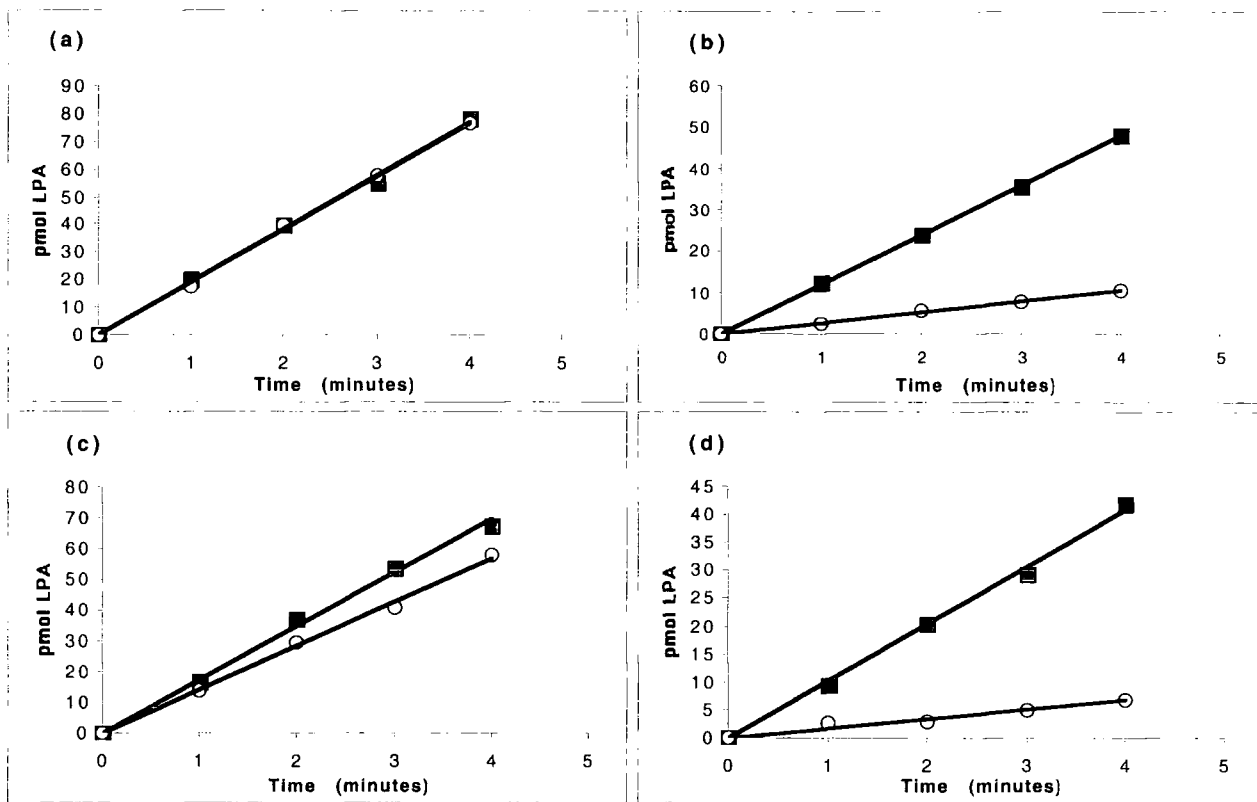


**Figure 5.2 Selectivity assays on Q24a, Q24a L261F, Q24a P331S and Q24a L261F P331S G3PAT proteins**

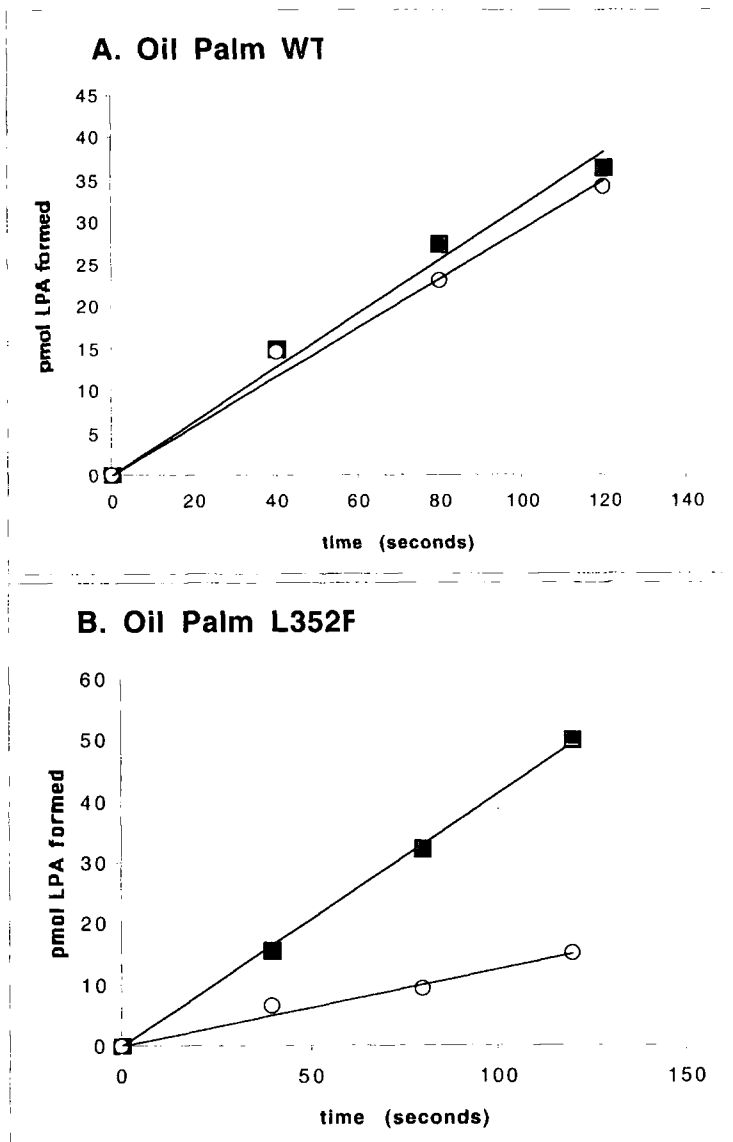
Standard selectivity assays were performed on a) Q24a, b) Q24a L261F, c), Q24a P331S and d) Q24a L261F P331S G3PAT proteins. ■ = 18:1-LPA. ○ = 16:0-LPA. The 18:1/16:0-LPA formation ratios are a) 1.0, b) 4.5, c) 1.2 and d) 6.0

Figure 5.2a demonstrates that the Q24a enzyme has little or no substrate selectivity. This wild type enzyme has an L residue at position 261 and a P residue at position 331. When an F is substituted at position 261, the enzyme exhibits a dramatically increased preference for 18:1ACP over 16:0ACP – a ratio of 4.5:1 (Fig 5.2b). When an S is substituted at position 331, the enzyme shows little alteration in substrate selectivity from wild type, using 18:1ACP to 16:0ACP in a ratio of 1.2:1 (Fig 5.2c). When both substitutions are made, the enzyme again exhibits a dramatically increased preference for 18:1ACP over 16:0ACP – a ratio of 6:1 (Fig 5.2d). It is evident from these data that the amino acid residue effecting the greatest alteration of substrate selectivity is at position 261. In order to substantiate this finding, the corresponding mutation was made in G3PAT from oil palm (*Elaeis guineensis*), another non-selective enzyme, to ascertain if the same mutation could create a similar effect in a G3PAT from an entirely different species, section 5.4.

#### **5.4 Creation of oil palm G3PAT mutant L352F and determination of its substrate selectivity**

Previous work on G3PAT enzymes resulted in the expression of a full-length oil palm G3PAT clone in *E. coli* using the vector system pET 24a. The product was shown to be active and have no substrate preference (Kroon, 2000). The sequence is included in the G3PAT alignment in Appendix 1. Using the Quickchange™ mutagenesis system the mutation L352F was made and expressed in *E. coli* using the vector system pET 24a (by Bill Simon).

Cell free protein extracts of the wild type and mutant oil palm G3PATs were prepared (section 2.5) and assayed for selectivity, see figure 5.3. These data illustrate that a single amino acid change can have a dramatic effect on the substrate selectivity of a G3PAT enzyme, in oil palm as well as squash. The wild type oil palm G3PAT uses 18:1ACP to 16:0ACP in a ratio of 1:1. The L352F mutant G3PAT uses 18:1ACP to 16:0ACP in a ratio of 3.3:1, i.e. the mutant enzyme now selects more than three times the amount of 18:1-ACP substrate over 16:0-ACP. These data support the hypothesis that the change in substrate selectivity is due to a direct effect at the substrate binding site rather than a gross conformational change in the protein structure or folding, as it is unlikely (but not impossible) that a conformational change would occur in exactly the same way in two enzymes from different plant species. In order to reduce this uncertainty and directly characterise the alteration of substrate selectivity, binding constants and maximum reaction velocities were determined for 16:0-ACP and 18:1-ACP in both the wild type and L261F mutant squash G3PAT proteins, section 5.5.



**Figure 5.3 Selectivity assay on oil palm wild type G3PAT and oil palm L352F G3PAT.** Assay was performed under standard G3PAT selectivity (dual substrate) assay conditions (see Chapter II).  $\square$  = 18:1-LPA.  $\circ$  = 16:0-LPA. (A) Oil palm wild type G3PAT has no substrate preference between 18:1-ACP and 16:0-ACP, utilising them in a ratio of 1.0:1. (B) Oil palm L352F G3PAT has a preference for 18:1- ACP over 16:0-ACP, in a ratio of 3.3:1.



## 5.5 Determination of kinetic constants for Q24a and Q24a L261F

A series of assays were performed on purified preparations of the G3PAT proteins Q24a and Q24a L261F to determine the maximum reaction velocities ( $V_{max}$ ) and binding constants ( $K_m$ ) for each of the substrates 18:1ACP, 16:0ACP and G3P. Following preliminary assays to estimate these constants, further assays were performed in order to accurately measure the values. Initial catalytic velocities were measured when one substrate was held at a constant, high level (10 or more times the estimated  $K_m$  value) and the second substrate was varied within the range  $0.2-5 \times K_m$ . The resultant velocities were analysed via Lineweaver-Burke plots to calculate the  $K_m$  and  $V_{max}$  values, as shown in figure 5.4. The results are summarised and given as mean values in table 5.3. The concentrations of the second substrate used were carefully chosen so that when the reciprocal values were plotted for Lineweaver-Burke analysis, the data points were equal distances apart and no 'bunching' of the data points occurred. For example, when G3P was held at a high concentration (20 mM) the concentrations of G3P were 1, 1.5, 2.5 and 10  $\mu$ M, giving near evenly spaced reciprocals of 1, 0.67, 0.4 and 0.1.

The results demonstrate a decreased binding ability of Q24a L261F for 16:0ACP, shown by an increase in the  $K_m$  value from 3.4 in the wild type to 9.2 in the mutant G3PAT. Q24a L261F also has a lower  $V_{max}$  when 16:0-ACP is used, approximately 47% of the  $V_{max}$  when 16:0ACP is used by the wild type enzyme. However, the mutant enzyme does not seem to demonstrate impaired binding or catalysis when using 18:1-ACP substrate, shown by a comparable binding constant ( $K_m$ ) and maximum

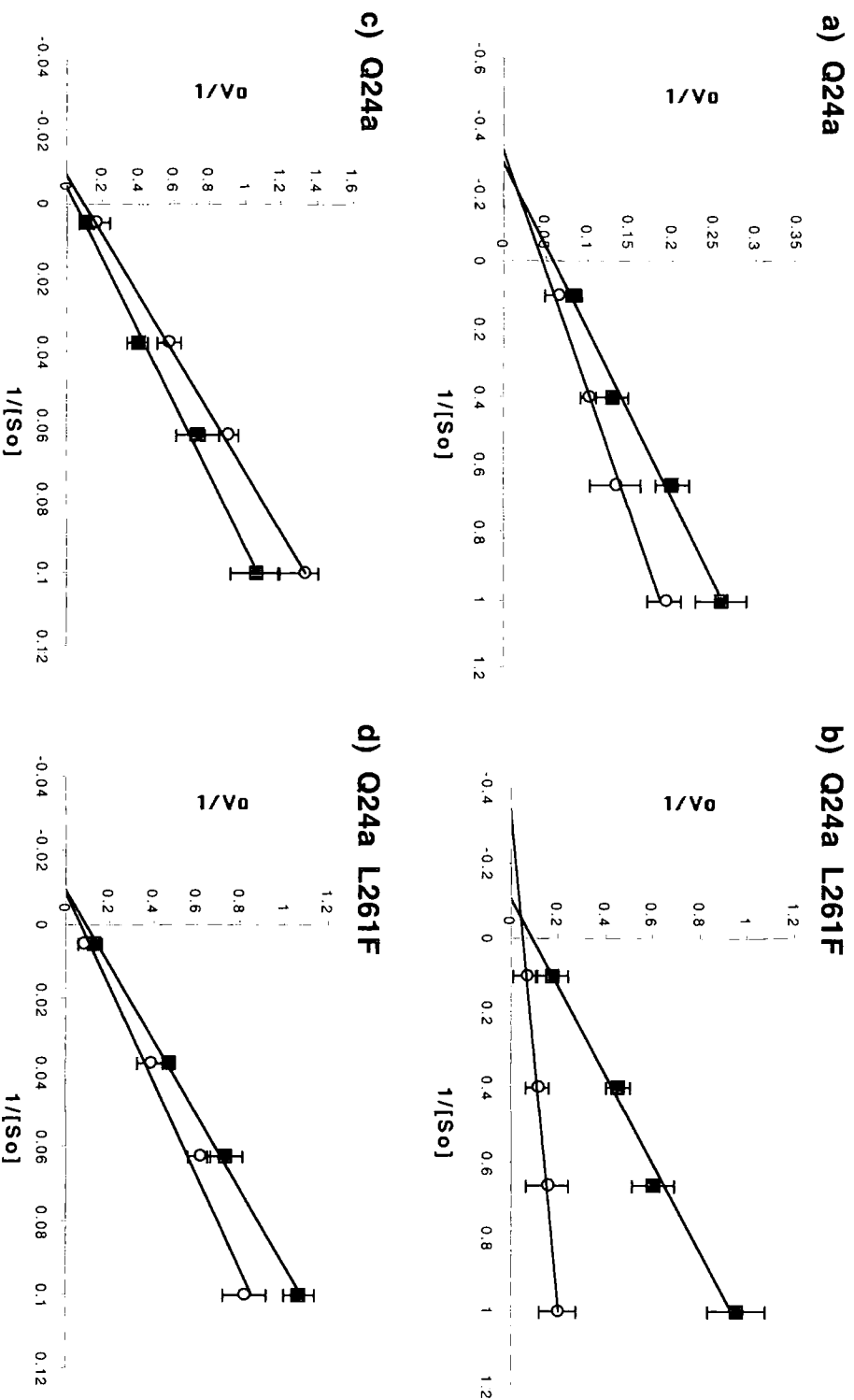


**Figure 5.4 Lineweaver-Burke plots of Q24a and Q24a L261F G3PAT activities.** Assays a) and b) were performed with G3P at 20mM and variable acyl-ACP concentrations. Assays c) and d) were performed at 10  $\mu$ M acyl-ACP and variable G3P concentrations. ■ = 16:0 acyl-ACP and ○ = 18:1 acyl-ACP.  $S_o$  = initial substrate concentration (mM for G3P and  $\mu$ M for acyl-ACP).  $V_o$  = initial reaction velocity in pmol LPA formed per minute. Assays were performed in triplicate and results are presented as mean values  $\pm$  1 standard error measurement.

**Table 5.3 Summary of the kinetic constants for Q24a and Q24a L261F**  
Kms units are uM, Vmax units are pmoles of LPA formed per minute.

	Q24a			Q24a L261F		
	Km G3P	Km acyl-ACP	Vmax	Km G3P	Km acyl-ACP	Vmax
18:1ACP	117	3.01	198	101	2.78	218
16:0ACP	143	3.42	213	151	9.20	101

catalytic rate ( $V_{\max}$ ). This could be due to the difference in shape of the 16:0 and 18:1 acyl chains (discussed in section 5.9).

## **5.6 G3PAT product-inhibition assays**

The catalytic mechanism of soluble G3PAT has been predicted by several groups based on sequence alignments, studies of catalytic motifs via site-directed mutagenesis and, more recently, the elucidation of the structure of G3PAT from squash (Heath and Rock, 1998; Turnbull *et al*, 2001b). However, the catalytic mechanism has not been determined experimentally. If the mechanism of soluble G3PAT were determined it would offer increased information regarding how the substrates are oriented in the active site and which reaction intermediates are formed.

Determination of the binding order and reaction mechanism of G3PAT can be performed via product inhibition assays. In 1914, Michaelis and Pechstein observed that the activity of the enzyme invertase could be inhibited by its two products, fructose and glucose. W.W. Cleland later demonstrated that the types of inhibition observed by each of the substrates in a two substrate reaction, when the levels of the substrates were also varied, could be used to determine the reaction mechanism and order of substrate binding (Cleland, 1963). These studies assume that there is only one active site on the enzyme that can be operative at one time (a reasonable assumption for soluble G3PAT) and compare Michaelis constants (for substrates) and inhibition constants (for products) at different concentrations of a fixed (non-varied) substrate.

Determination of the reaction mechanism will indicate whether catalysis occurs when the enzyme binds both substrates in a single complex (ternary-complex; sequential mechanism) or by binding one substrate, accepting the transferred group and then binding the second substrate for group transfer, i.e. neither of the complete substrates are present at the same time (ping pong; substituted-enzyme mechanism). This would enable one to determine how the substrates bind and to predict which intermediate molecules are present in the active site at the moment of catalysis. Schematic representations of a ternary-complex and a ping-pong reaction mechanism are shown in figures 5.5 and 5.6 respectively. It can be seen that the ternary-complex involves both substrates being present in the active site at once, whilst in the substituted-enzyme reaction mechanism involves the acyl-donor binding, formation of enzyme:acyl complex ('EG' in figure 5.6) and then G3P binding and acyl-transfer to form LPA.

Elucidation of the binding order may facilitate the production of suitable substrate analogues that may be used to probe the G3PAT active site and substrate binding domains. A suitable analogue would still be able to bind to the substrate binding domain(s) but would not undergo catalysis. Crystallisation of such a complex would permit structural data of a G3PAT enzyme with bound substrate to be obtained. Such co-crystals could directly tell us the nature and orientation of the hydrophobic acyl-binding pocket and/or the glycerol-3-phosphate binding pocket, negating the need for computer modelling of substrates into the 3D structure.

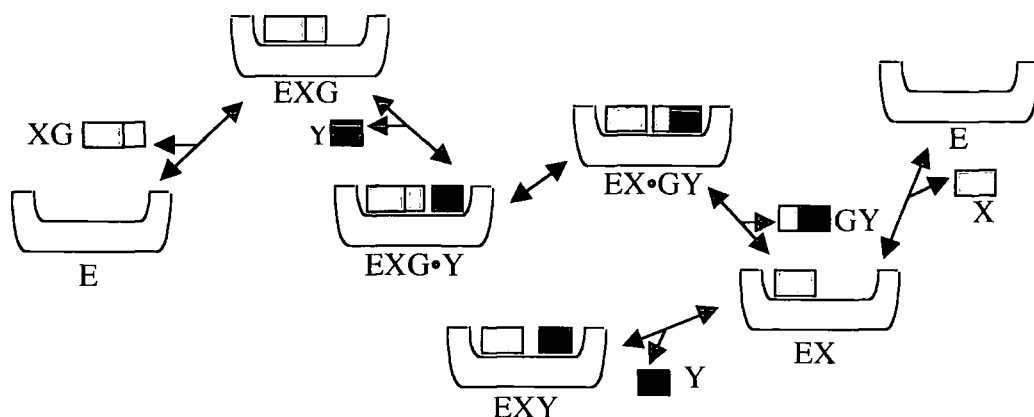


**Figure 5.5 Schematic diagram of a ternary-complex/sequential reaction mechanism.** The acyltransferase reaction is represented as  $XG + Y \rightleftharpoons X + GY$ , where the letter X represents ACP, G represents the acyl group, Y represents G3P and E represents the enzyme, G3PAT. The mechanism shown is a compulsory ordered ternary-complex, with acyl-ACP binding first. However, it is possible that G3P could bind first, or the order could be random. The figure is adapted from 'Fundamentals of Enzyme Kinetics' by Athel Cornish-Bowden, 1995.

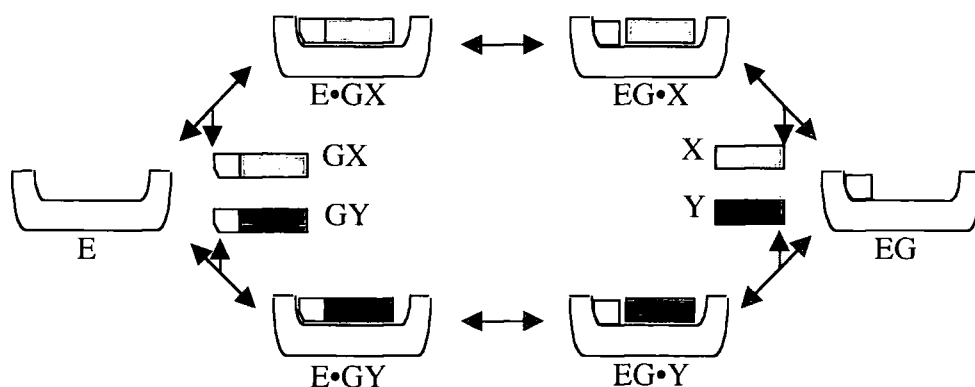


**Figure 5.6 Schematic diagram of a ping-pong/substituted-enzyme reaction mechanism.** As in figure 5.5, the acyltransferase reaction is represented as  $XG + Y \rightleftharpoons X + GY$ . If the reaction were to proceed from left to right, as written, this would be represented as the reaction advancing in a clockwise direction, as shown in the schematic. Neither of the substrates X or Y are present in the active site at the same time. The reaction may be compulsory or random ordered. Non-productive complexes such as EX and EY may also be formed. The figure is adapted from 'Fundamentals of Enzyme Kinetics' by Athel Cornish-Bowden, 1995.

## 5.7 Determination of G3PAT reaction mechanism and binding order

To determine whether G3PAT proceeds via a sequential or ternary complex reaction mechanism, a series of assays using fixed, non-saturating levels of one substrate and varying concentrations of the second substrate were carried out. In the first instance, fixed, non-saturating levels of acyl-ACP (2, 3, 5 and 10  $\mu\text{M}$ ) and varying concentrations of G3P (0.1, 0.3, 1.0 and 3.0 mM) were used. The double reciprocal plots produced from these assays, when analysed by linear regression, showed a series of lines which converge (figure 5.7a). When fixed, non-saturating levels of G3P were used and the concentration of acyl-ACP varied, a similar converging pattern of lines was recorded (figure 5.7b). These patterns indicate that the squash G3PAT reaction occurs via a ternary complex rather than a substituted-enzyme reaction mechanism (Cleland, 1963).

In order to establish whether the G3PAT reaction occurs via a random or compulsory ordered mechanism ACP and LPA, the reaction products, were used as reaction inhibitors. Analysis of the results was performed as by Cleland (1963). When acyl-ACP was varied in the presence of LPA (fig. 5.8B) and G3P varied in the presence of ACP (fig. 5.8C) or LPA (fig. 5.8D), mixed patterns of inhibition were observed in each case. However, when acyl-ACP was varied in the presence of ACP (fig. 5.8A), competitive inhibition was observed. This pattern of inhibition indicates that the mechanism for squash G3PAT is a compulsory-ordered ternary complex with acyl-

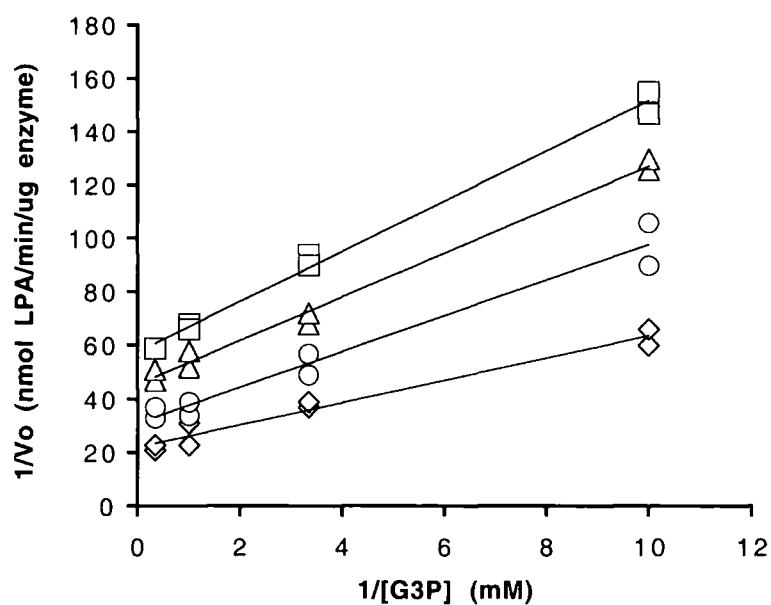


**Figure 5.7a) Determination of squash G3PAT kinetic mechanism.**

Initial velocity was recorded in assays using varying G3P concentrations at fixed, non-saturating concentrations of acyl-ACP ( $2\mu\text{M}$  ( $\leq$ ),  $3\mu\text{M}$  ( $\rho$ ),  $5\mu\text{M}$  (O),  $10\mu\text{M}$  ( $\downarrow$ )). Assays were performed in duplicate. Linear regression shows that the series of lines converge, demonstrating that the enzyme mechanism is sequential rather than substitution.



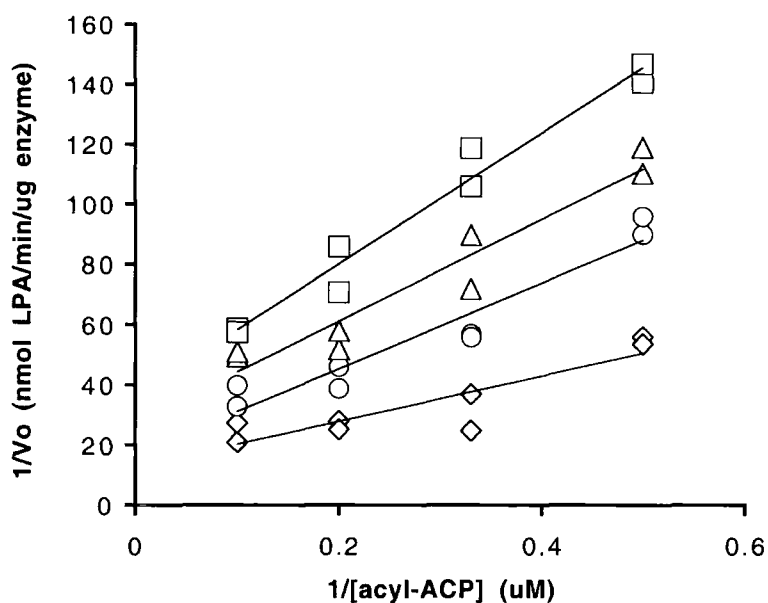
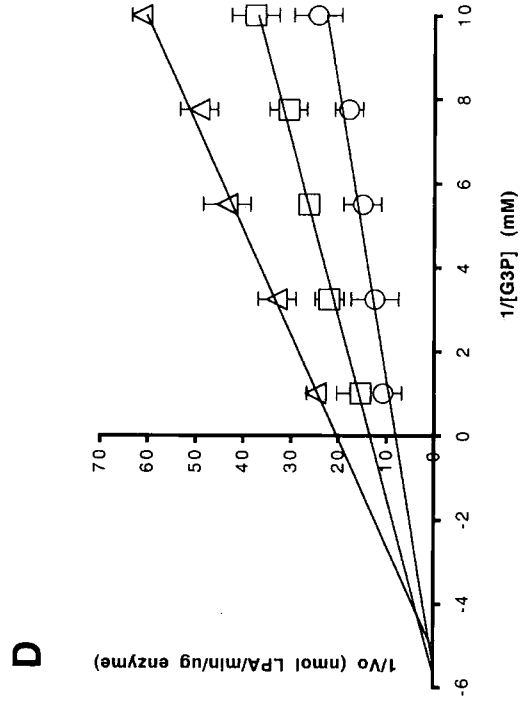
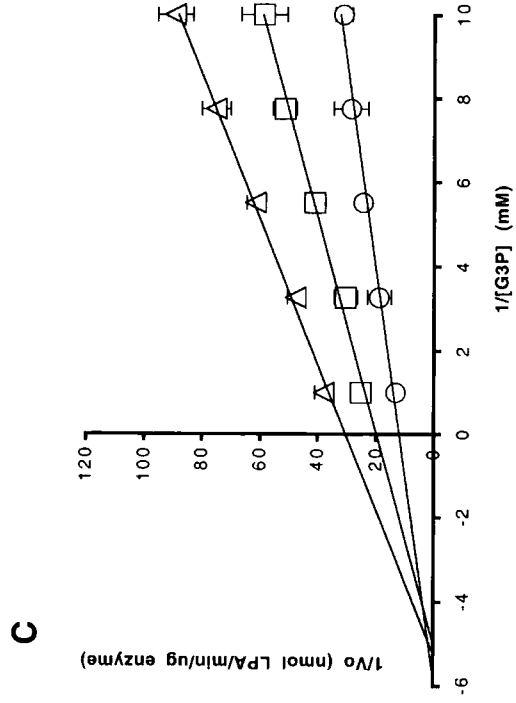
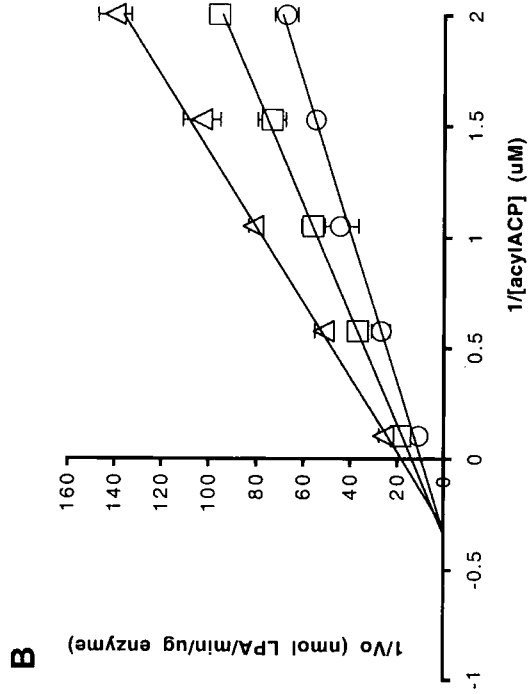
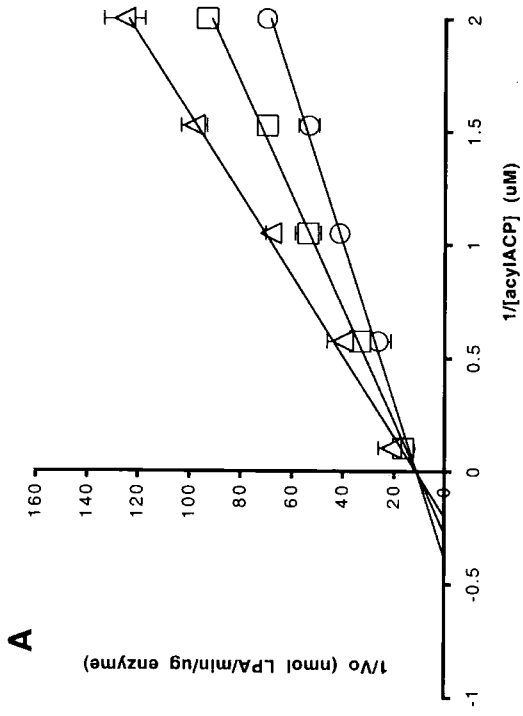


**Figure 5.7b) Determination of squash G3PAT kinetic mechanism.**

Initial velocity was recorded in assays using varying acyl-ACP concentrations at fixed, non-saturating concentrations of G3P (0.1 mM ( $\leq$ ), 0.33 mM ( $\rho$ ), 1.0 mM (O), 3.0 mM ( $\downarrow$ )). Assays were performed in duplicate. Linear regression shows that the series of lines converge, demonstrating that the enzyme mechanism is sequential rather than substitution.

**Figure 5.8 Determination of the order of substrate binding by product inhibition studies.**

Assays were performed with varying concentrations of one substrate at fixed, non-saturating concentrations of the second substrate in the absence of product ( ) and in the presence of 0.2 mM (  $\leq$  ) and 0.4mM (  $\rho$  ) product. The plots are double reciprocal using (A) varying acyl-ACP concentrations at 300  $\mu$ M G3P at different fixed concentrations of ACP; (B) varying acyl-ACP concentrations at 300  $\mu$ M G3P at different fixed concentrations of LPA; (C) varying G3P concentrations at 2  $\mu$ M acyl-ACP at different fixed concentrations of ACP and (D) varying G3P concentrations at 2  $\mu$ M acyl-ACP at different fixed concentrations of LPA. Assays were performed in triplicate and presented as mean values ( $\pm$  1 standard error measurement).



ACP binding first, as competitive inhibition was only observed when acyl-ACP (the acyl-donor) was varied in the presence of ACP. This also implies that LPA is released first, as ACP is the only competitive inhibitor for binding of the next substrate (acyl-ACP).

## **5.8 Substrate binding studies on squash G3PAT**

Following determination of the substrate binding order, direct binding studies were carried out in order to confirm the order of binding. Binding assays were carried out as described in chapter II to assess the binding of each substrate in the absence of the other substrate. Centrifugal micro-concentrators were used to retain the G3PAT enzyme and any bound substrate molecules, above a 30 kDa cut off membrane. Radiolabelled acyl-ACP or G3P substrates (both at 55 Ci/mol) were mixed with pure protein in a ratio of 100 pmoles of substrate to 50 pmoles G3PAT. The enzyme-substrate mixture was equilibrated at room temperature in 250 mM HEPES-OH buffer (pH 8.0) for 10 minutes, prior to centrifugation at 5,000xg for 10 minutes through the 30 kDa cut off membrane. The number of moles of substrate present in the upper and lower compartments (bound and unbound material respectively) was determined by counting in a liquid scintillation counter and used to calculate the molar ratio of substrate which had bound to the G3PAT enzyme, displayed in table 5.4. It was determined that neither substrate was retained by the 30 kDa cut off membrane ('-G3PAT' section of table 5.4). In addition, G3PAT that had been boiled for 5 minutes prior to the binding assay retained (in the upper compartment) less than 2 pmoles and 1 pmole of acyl-ACP and G3P substrates respectively.

**Table 5.4 Differential binding of acyl-ACP and G3P substrates to G3PAT.**

100 pmoles of radiolabelled 18:1-ACP or G3P were incubated with or without 50 pmoles of G3PAT enzyme in the absence of the second substrate and centrifuged through a 30,000 Da molecular weight cut-off membrane. Substrate bound to G3PAT did not pass through the membrane and was retained in the upper compartment. Assays were performed in triplicate and results are presented as mean values  $\pm$  one standard error measurement.

	+ G3PAT		- G3PAT	
	Acyl-ACP	G3P	Acyl-ACP	G3P
total pmoles of substrate in upper compartment	47.4 $\pm$ 0.48	1.01 $\pm$ 0.11	0.11 $\pm$ 0.02	0.09 $\pm$ 0.01
moles of substrate bound per mole of enzyme	0.95 $\pm$ 0.01	0.02 $\pm$ 0.002	n/a	n/a

These data support the findings in section 5.7 - indicating that the substrates do bind in a compulsory order, as acyl-ACP will remain bound in the absence of G3P but not vice versa. This is evidence for a reaction which proceeds with acyl-ACP binding first, in the absence of G3P, with G3P then binding for catalysis to occur.

Binding assays for 18:1 and 16:0-ACP to Q24a and Q24a L261F were additionally performed, under the standard substrate binding assay conditions. Q24a bound 18:1 and 16:0-ACP in molar ratios of  $0.95(\pm 0.01)$  and  $0.90 (\pm 0.02)$  respectively, whilst Q24a L261F bound 18:1 and 16:0-ACP in molar ratios of  $0.92 (\pm 0.02)$  and  $0.82 (\pm 0.02)$ . A slight decrease in the binding of 16:0-ACP is apparent in Q24a L261F, but this assay is less sensitive at detecting a change in  $K_m$  for an individual substrate than conventional kinetic means (compare with table 5.3). However, this it is useful to note that both substrates still bind to the mutant protein under binding-assay conditions.

## 5.9 Discussion

In this study, an examination of the kinetic parameters, reaction mechanism and substrate binding for squash G3PAT and the mutant L261F are presented. The binding constants of 18:1-ACP, 16:0-ACP and G3P have been determined, along with the maximum catalytic velocities with these substrates for a wild type squash G3PAT (Q24a) and a mutated form of the enzyme. The cause of this selectivity change, a single amino acid substitution L261 to F261, has been kinetically characterised. The mutation L261F causes decreased binding affinity for 16:0-ACP substrate, indicated by the elevated  $K_m$  of the mutant (9.2  $\mu\text{M}$ ) compared to 3.4  $\mu\text{M}$  in the wild type. The  $V_{\text{max}}$  with 16:0-ACP substrate is also lower in the mutant, down to 101 (from 213) pmoles LPA formed per minute.

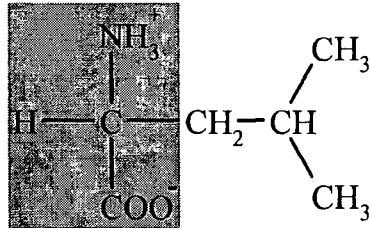
One possibility for the dramatic change in substrate selectivity in the mutant Q24a L261F is that the enzyme conformation has somehow been disturbed due to the amino acid substitution. This may result in a vastly altered catalytic/binding environment (but would be of little practical use in a study of substrate selectivity in this class of enzymes as such a change would be almost impossible to reproduce in other enzyme constructs or enzymes from other species). However, evidence presented here is to the contrary, as an almost identical effect is witnessed when the corresponding residue is mutated in oil palm G3PAT. Furthermore, structural data comparing the 3D structure of Q24a and Q24a L261F indicates that no significant alterations to the folding or 3D structure of the mutant have taken place (chapter 4 - communication from A.P. Turnbull, University of Sheffield). The mutant Q24a L261F has a predicted structure

isomorphous to Q24a. The mutant Q24a L261F has also been shown to bind 18:1-ACP in binding assays (section 5.8) and has a catalytic rate similar to the wild type enzyme. These data indicate that the gross structure of the acyl-binding pocket and ability to bind some substrates have not been significantly altered.

Structural data locates the residue L261 towards the distal end of the acyl binding pocket (figure 4.2), at the opposite end to the phosphopantethenyl linker to the acyl binding protein. This may explain why the mutant has a level of catalytic activity similar to wild type, as the mutation is not in the vicinity of the motif diagnostic for the G3PAT reaction, the H(X)<sub>4</sub>D box (assigned the nomenclature 'Block 1' by Lewin, T.M. *et al*, 1999). Phenylalanine does not appear naturally at this position in any known plant G3PAT sequence and has a side chain that is chemically more hydrophobic and sterically much larger than leucine, as indicated in the schematic representation shown in figure 5.9. It may be the case that the unnatural F residue at position 261 assists the binding of the 'curved' 18:1 acyl chain, but more likely partially blocks the binding of the straight 16:0 acyl chain, resulting in the observed increase in K<sub>m</sub> and drop in V<sub>max</sub> for this substrate compared to the wild type G3PAT. This supposition could be investigated by the creation of 'intermediate' mutants, in which L261 is replaced by residues which are smaller than phenylalanine, for example isoleucine or valine. These results and models derived from them may assist future attempts to determine the exact nature of the acyl binding pocket and the interactions between this domain and the acyl chain.



a) Leucine



b) Phenylalanine

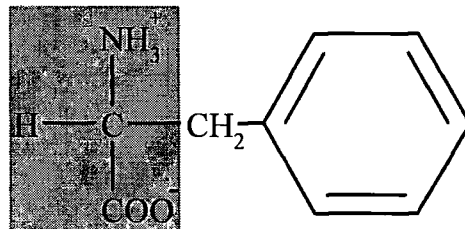


**Figure 5.9 Schematic diagram of the amino acids a) leucine b) phenylalanine.** The boxed area contains the central amino acid unit, the side chain is the part of the molecule extending outside the box.

The G3PAT reaction was found to proceed via a ternary-complex mechanism, not a ping-pong mechanism. Often, a ping-pong mechanism is employed by an enzyme when its two substrates have similar properties and so may occupy the same, or overlapping, space at the active site. However if we consider the substrates involved in the G3PAT reaction it is apparent that they are very different types of molecule. G3P is a small, polar molecule and acyl-ACP is a hydrophobic acyl chain attached to a highly acidic carrier protein. It seems likely that the binding areas for these molecules should be different, bringing the molecules into contact in the vicinity of the H(X)<sub>4</sub>D box. A recently proposed model for G3PAT catalysis (Heath, R.J. and Rock, C.O., 1998) suggests that the invariant histidine in the H4XD box acts as a base, withdrawing a proton from the *sn*-1 hydroxyl group. This would permit the nucleophilic attack on the thioester bond of the acyl-ACP, by the -O<sup>δ-</sup> group at position *sn*-1 (see discussion (chapter 6) and figure 6.1). The invariant aspartate is proposed to act as a 'charge-relay system' to increase the nucleophilicity of the *sn*-1 hydroxyl group of G3P. This proposed scheme fits in with the findings in this chapter, as in a ternary-complex both substrates would be present in the active site at the same moment, enabling one to undergo assisted nucleophilic attack on the other.

This work has been an important step forward in understanding the basis of substrate selectivity in G3PAT enzymes. Squash G3PAT, a non-selective enzyme, and an oleophilic mutant are now kinetically well characterised. The mechanism has been resolved and agrees strongly with an existing hypothetical model for catalysis. Kinetic and ancillary binding studies have determined the order of substrate binding. This

information, combined with an assessment of the range of substrates which G3PAT will utilise (chapter 3), enable better attempts to be made to probe the active site of the enzyme and to obtain enzyme-substrate co-crystals for structural analysis of the fatty acid binding domain. Determination of the 3D structure of G3PAT with bound substrate would eliminate the need for computer modelling and would be an ideal tool for studying the amino acid residues that directly interact with the acyl chain of acyl-ACP substrate. This would assist a rationalised site-directed mutagenesis approach, designed to direct the evolution of the function of G3PAT enzymes using only single amino acid substitutions to strategically 'block' the acyl-binding site a critical points to directly affect the subset of acyl-ACP substrates utilised by the enzyme.

# **Chapter 6**

## **General Discussion**

## 6.1 Discussion

Plant glycerol-3-phosphate acyltransferase has a demonstrated role in the determination of membrane lipid composition, which has proven effects on the overall function of the plant when responding to different environmental stresses, for example chilling temperatures (Murata et al 1992). The molecular mechanisms responsible for substrate selection and the mode of catalysis in acyltransferase enzymes are of interest: an investigation of these parameters in the enzyme *sn*-glycerol-3-phosphate acyltransferase from the chloroplast of squash (*Cucurbita moschata*) has been undertaken.

A critical initial step in an investigation of the molecular mechanisms responsible for substrate selectivity is the development of an assay that can distinguish between selective and non-selective enzyme forms. Chapter 3 reports the optimisation of an existing assay for several purposes. Substrate concentrations and pH have been carefully chosen to be closely approximated to physiological, using values reported in experimental literature backed up with an investigation of a range of assay conditions. The assay has been used to determine the activity level and substrate selectivity of several G3PAT proteins. The assay has also been adapted to permit the determination of kinetic constants for G3PAT proteins, in particular the binding or Michaelis constant ( $K_m$ ) and the maximum reaction velocity ( $V_{max}$ ). These have been performed on a wild type G3PAT protein and a mutant that exhibits altered substrate selectivity following a single amino acid substitution. A method to determine the ratio of acyl-ACP binding to various proteins, specifically BSA and purified recombinant G3PAT has also been developed. This enables an assessment to be made as to whether or not the protein can bind acyl-ACP, and provide a relative

measurement of the strength of this binding (as a ratio of moles of substrate bound per mole of enzyme).

Squash G3PAT will bind and utilise a variety of acyl-ACP and acyl-CoA substrates with acyl-chain lengths as short as 4:0-CoA. This has implications for current approaches to produce co-crystals of squash G3PAT with bound acyl-ACP substrate. If shorter acyl-chain substrates are used by G3PAT, they must still bind correctly for catalysis to occur. Fewer solubility problems are associated with shorter acyl-substrates, which may co-crystallise more easily or be soaked into pre-existing crystals. These data widen the range of possible substrates which can be utilised in such trials. This may help to overcome problems associated with currently used substrates and produce structural information about G3PAT with bound acyl-ACP substrate – direct evidence for the precise location and orientation of substrates in and around the acyl-binding site. Such information would supersede currently used computer models.

The proven effects of BSA in G3PAT assays has led to an investigation of the binding of acyl-ACP substrates to BSA. Assay data and binding experiments indicate that BSA binds both 16:0 and 18:1, but with a differential affinity. This means that proper consideration must be given to BSA levels in any dual-substrate assay of G3PAT activity. In the complete absence of BSA, G3PAT assays work very poorly and low catalysis rates are achieved. This raises questions over the precise function of BSA in the assays. Does the BSA act to increase the local concentration of acyl-ACP/CoA substrates near the G3PAT enzyme? BSA is known to a) bind acyl-ACPs and b) affect the velocity of the G3PAT reaction. Increasing BSA concentration has been shown to increase the rate of acylation

with 16:0-ACP substrate. Is it therefore possible that there is a docking site for BSA on G3PAT? If this is so, it implies that there may be a 'BSA counterpart' in the plastid, responsible for the transfer of acyl-donor substrates to the G3PAT enzyme. ACP may already be fulfilling this role *in vivo*. Future work in this area should seek to isolate, identify and characterise such a protein and study how the acyl-ACP/CoA substrates are transferred, and if the protein can transfer substrate to other acyltransferase enzymes using the same mechanism. It may be possible that G3PAT complexes to FAS *in vivo* and substrate 'channelling' normally occurs.

Structural information on squash G3PAT (Turnbull *et al*, 2001a, b) has led to the creation of several mutant G3PAT proteins, in each of which a single amino acid substitution has been made. Investigation of the catalytic rates and, where possible, determination of substrate selectivity have taken place. The mutations K193S, R235S and R237S result in a total loss of enzyme activity. These residues have previously been proposed to form the glycerol-3-phosphate binding pocket and this data is consistent with that contention.

Structural and biochemical data support the proposal that these proteins remain correctly folded and able to bind the first substrate, acyl-ACP. It appears that the residue H194 may play a subsidiary role in glycerol-3-phosphate binding as the mutation H194S reduces catalytic velocity to 79% of the wild type.

Two residues within the H(X)<sub>4</sub>D box have been mutated, T141 to serine and E142 to alanine. The former mutation was anticipated to have an effect on G3PAT acyl-selectivity, as alignments show it to be a conserved threonine in G3PATs from chilling sensitive (non-selective) species and a conserved serine in chilling tolerant species. However, the

mutation T141S had a surprisingly modest effect on both catalytic activity and substrate selectivity. The mutant protein had a reaction velocity of 106% of wild type and an identical 18:1-ACP/16:0-ACP selectivity of 1.0. Therefore it is likely that this residue is not conserved for the purpose of substrate selectivity. The conversion of the residue E142, conserved in many plant species, to alanine resulted in an enzyme that was fully inactive. The glutamic acid at this position appears to be vital for enzymatic function. Alanine, a relatively small amino acid, would be unlikely to interfere spatially with insertion of substrate into the binding region so perhaps E142 has a catalytic role. It may instead be the case that E142 is responsible for charge-relay around the H139 residue, or the formation of favourable hydrogen bonds with glycerol-3-phosphate. This hypothesis could be investigated further by the creation of a set of mutant proteins in which E142 has been substituted for various different amino acids with one 'characteristic' changed each time. For instance, a substitution for a residue of similar size but opposite or no charge (for example leucine or lysine) could be made, in addition to substitution for a residue with a positive charge but smaller size (for example aspartic acid or asparagine). The effect of substitution for a residue with a hydroxy, sulphur or aromatic containing side chain could also be examined.

One mutation in the acyl-binding pocket has demonstrated that it is possible to alter the substrate selectivity of squash G3PAT with a single amino acid substitution. L261F is a mutation at the distal end of the acyl-binding pocket, farthest from the H(X)<sub>4</sub>D box and G3P binding site. It is possible that the aromatic side chain facilitates preferential binding of the slightly 'bent' 18:1 acyl chain. However it is more likely that this moderately large side chain partially blocks correct insertion of the 'straighter' 16:0 acyl chain, disrupting



normal orientation of the acyl-ACP molecule into the binding pocket (see figure 4.2 for a structural diagram of the acyl-ACP binding pocket). This is reflected in an increased  $K_m$  value for 16:0-ACP, indicating a decreased ability of the mutant enzyme to bind this substrate. This observation has led to the idea that it may be possible to ‘block’ the acyl-binding pocket in strategic places to favour binding of specific acyl groups and disrupt the binding of others. Thus, the substrate selectivity of G3PAT enzymes (and potentially other acyltransferases with similar binding/catalytic sites) could be engineered to preferentially select both acyl chain length and degree of unsaturation.

The G3PAT reaction was determined by kinetic study to proceed via a compulsory ordered ternary complex mechanism. This means that there is a physical (and theoretically ‘isolatable’) intermediate product formed between the two substrates (and enzyme), which quickly rearranges to form the two final reaction products (ACP and LPA) and regenerated G3PAT. This proposed mechanism is in support of a model suggested by Heath and Rock (1998). It also has a general mechanism analogous to serine proteases (in which a histidine/aspartate pair deprotonate the *sn*-1 hydroxyl group of glycerol-3-phosphate, which subsequently undergoes nucleophilic attack on an acyl-substrate) as has been previously suggested (Turnbull *et al* 2001b). The proposed G3PAT reaction mechanism is detailed in the schematic diagram, figure 6.1. The reaction intermediate (ternary complex) is shown in part κ of this schematic.

The order of the compulsory substrate binding for squash G3PAT has been determined. The acyl-ACP substrate was found to bind first, before glycerol-3-phosphate. This finding

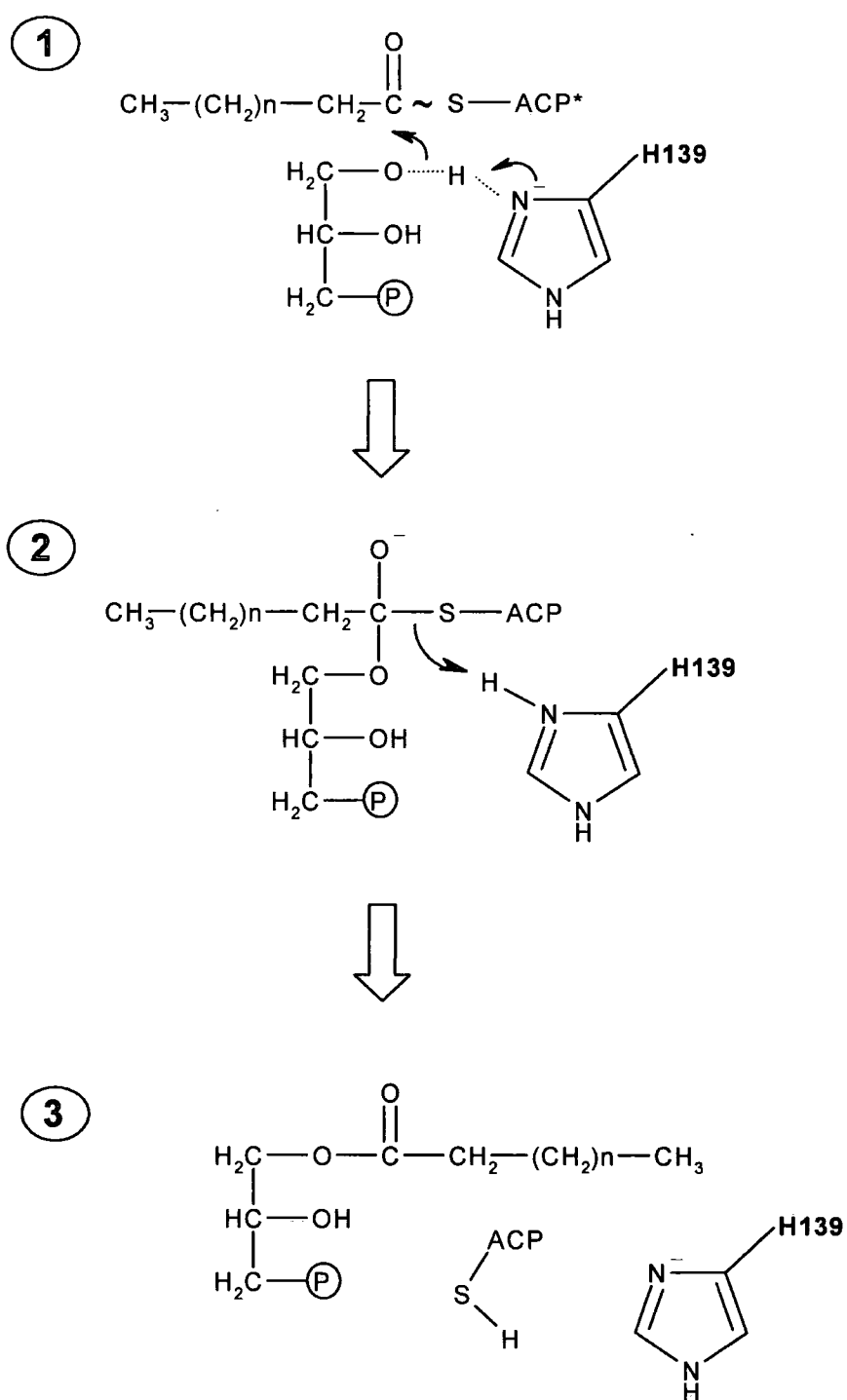


**Figure 6.1** Schematic of the proposed mechanism of squash G3PAT

was substantiated by binding studies using centrifugal filter units with a molecular weight cut-off, which showed that acyl-ACP remained bound to the G3PAT enzyme whereas glycerol-3-phosphate did not. This means that computer models previously generated with palmitoyl-pantothenate as the first-bound substrate were likely to have been more accurate than those with modelled G3P. In addition, enzyme:substrate co-crystals are most likely to be obtained with either acyl-ACP or acyl-CoA substrates, as G3P dissociates from G3PAT more readily. However, co-crystals may be obtained with glycerol-3-phosphate or G3P-based analogues, as these compounds will still have an equilibrium constant with the G3P binding pocket and may bind readily enough if the exogenous concentration is sufficiently high - this assumes that the enzyme 'active-site' does not alter shape after binding of the acyl-ACP molecule to facilitate G3P binding.

This study on G3PAT binding and catalytic motifs and the determination of the reaction mechanism and substrate binding order have increased our understanding of the functional mechanisms central to the G3PAT reaction. The functional relationships elucidated herein may act as a model system with potential application to other acyltransferase systems.

## **6.2 Future work**

The further investigation of residues E142, R170 and L261 via chemical modification or site directed mutagenesis is recommended. These residues are not critical for the acyltransferase reaction but have a demonstrated role in substrate binding. The creation and characterisation of mutants in which these residues are substituted for others will provide increased information on the role of these residues, and how they may be mutated to select some substrate types in preference to others.

Acyl-CoA analogues containing reactive azido groups have previously been used to characterise acyl-binding sites on various proteins (Hach *et al*, 1990; Rajasekharan *et al*, 1993 and Shockey *et al*, 1995). G3PAT has been shown to use azidooleoyl-CoA and -ACP as substrates. The azido group, at position 12, is located at the distal side of the double bond (at position 9) in the 18:1 acyl chain. If covalent binding of this compound to residues in the G3PAT acyl binding pocket was achieved, determination of the spatial orientation of the 18:1 acyl chain within the active site would be possible. Thus the author recommends optimisation of photo-reactive modification of G3PAT with azidooleoyl-CoA and -ACP substrates.

With the structural elucidation of squash G3PAT, it may now be possible to 'direct' the evolution of this enzyme, with the characteristics tailored to produce desirable qualities, for example substrate preference. Rationalisation of the substrate selectivity may be possible, as has been the case with other enzymes (Cahoon *et al*, 1997). A certain amount of 'catalytic plasticity' has been demonstrated in fatty acid modification enzymes (Broun *et al*, 1998) and the same may be true with G3PAT. Increased information about the acyl-binding pocket may enable blocking at strategic points to produce LPA with shortened acyl-chain lengths. It would also be interesting to make the equivalent mutation to L261F in a G3PAT that is already selective for longer, less saturated acyl substrates (for example G3PAT from spinach) to determine if the existing selectivity can be augmented.

The inclusion of BSA in G3PAT assays has a measurable effect on acyl-ACPs with saturated and monounsaturated acyl chains. Increasing BSA concentration has been shown

to increase the rate of acylation with saturated acyl-ACP substrate. This raises the prospect of BSA 'docking' to G3PAT, acyl-ACP, or both. It may be the case that G3PAT complexes to FAS or another protein (the BSA 'counterpart') in the plastid. This could be investigated by chromatography of purified chloroplast lysates on columns containing immobilised FAS components, BSA or G3PAT to see if any novel plastid components have affinity for these proteins.

Several ACP isoforms have been identified in some plants, and there are known differences between ACP from plants and bacteria. Acyltransferase enzymes may have different activities and substrate selectivities with acyl-ACP containing different ACP isoforms. This study has only used ACP from one source (recombinant ACP from *E. coli*) but ACP has been cloned from several plant species. It would be interesting to see how G3PATs from squash (and other species) perform in assays using plant forms of acyl carrier protein.

**Squash glycerol-3-phosphate (1)-acyltransferase - alteration of substrate selectivity  
and identification of arginine and lysine residues important in catalytic activity.**

\*Antoni R. Slabas,<sup>‡</sup> Johan TM. Kroon,<sup>‡</sup> Ted P. Scheirer,<sup>‡</sup> John S. Gilroy,<sup>‡</sup> Matthew  
Hayman,<sup>‡</sup> David W. Rice,<sup>§</sup> Andy P. Turnbull,<sup>§</sup> John B. Rafferty,<sup>§</sup> Tony Fawcett,<sup>‡</sup> and  
William J. Simon<sup>‡</sup>.

<sup>‡</sup> Department of Biological and Biomedical Sciences, University of Durham, Science  
Laboratories, South Road, Durham DH1 3LE, United Kingdom.

<sup>§</sup> The Krebs Institute for Biomolecular Research, Department of Molecular Biology and  
Biotechnology, University of Sheffield, Sheffield S10 2TN, United Kingdom.

Running title: Plant Glycerol-3-phosphate (1)-acyltransferase

\* To whom correspondence should be addressed. Tel +44-191-3743352,  
E.mail: a.r.slabas@durham.ac.uk

**Abbreviations** ACP, acyl carrier protein; BSA, bovine serum albumin; G3PAT, glycerol-  
3-phosphate-acyltransferase; G-3-P, glycerol-3-phosphate; IPTG, isopropyl-1-thio- $\beta$ -  
galactopyranoside; LPA, lysophosphatidic acid; 18:1, oleic acid; 16:0, palmitic acid;

### **Summary**

Glycerol-3-phosphate-1-acyltransferase is a soluble chloroplast enzyme involved in glycerol-lipid biosynthesis associated with chilling resistance in plants [1]. Resistance is associated with higher selectivity for unsaturated acyl substrates over saturated ones. *In vitro* substrate selectivity assays performed under physiologically relevant conditions have been established which discriminate between selective and non-selective forms of the enzyme. A mutation, L261F, in the squash protein, converts it from a non-selective enzyme into a selective one. The mutation lies within 10 Å of the predicted acyl binding site and results in a higher  $K_m$  for 16:0 ACP. Site directed mutagenesis was used to determine the importance of 4 residues, R235, R237, K193 and H194, implicated to be involved in binding of the phosphate group of glycerol-3-phosphate to the enzyme. All the proteins were highly homologous in structure to the wild type enzyme. Mutations in R235, R237 and K193 resulted in inactive enzyme whilst H194 had reduced catalytic activity. The mutant proteins retained the ability to bind stoichiometric quantities of acyl-ACP's supporting the potential role of these residues in G-3-P binding.

## **Introduction**

Glycerol-3-phosphate-1-acyltransferase [G3PAT, [*pls*], EC 2.3.1.15] catalyses the first acylation step in glycerol lipid biosynthesis acylating the *sn*1 position of glycerol-3-phosphate [G-3-P]. Both soluble and membrane bound forms of the enzyme exist [2]. In *E.coli* the enzyme is membrane bound and uses both acyl-ACP and acylCoA as substrates [3]. Plants contain soluble and membrane bound forms of the enzyme, the former being located in the chloroplast and the latter being extra-plastidial [2,4]. Soluble G3PAT has strong substrate selectivity for acyl-ACP over acyl-CoAs consistent with the location of both the enzyme and ACP within the chloroplast [4]. Both selective [4,5,6] and non-selective forms of the enzyme have been isolated from plants [7, and oil palm in this report]. Non-selective enzymes utilise 16:0 and 18:1 substrates at the same rate whilst selective enzymes preferentially incorporate 18:1.

Chilling sensitive plants preferentially incorporate C16 saturated fatty acids at position 1, whilst chilling-resistant plants have a much higher content of unsaturated fatty acids at that position [8]. As a consequence the glycerolipids of chilling-resistant plants are more fluid at lower temperatures and hence less sensitive to chilling damage. Transgenic studies with tobacco using constructs containing selective [*Arabidopsis*] and non-selective [squash-AT2] G3PATs targeted to the chloroplast supported this view [1].



### *Plant Glycerol-3-phosphate (1)-acyltransferase*

G3PAT is nuclear encoded, and import into the chloroplast requires a transit peptide which is removed to give the mature protein. The exact nature of the processing site has not been determined experimentally [9,10]. Transformation experiments performed in tobacco utilising the truncated form of the squash enzyme linked to the RUBISCO transit peptide have demonstrated that this form of the enzyme is both biologically active and non-selective *in vivo* [1].

The primary structure of mature soluble plant G3PAT is highly conserved. Comparison of the amino acid sequences of the putative mature protein from spinach, pea and *Arabidopsis*, all of which show substrate preference for 18:1 over 16:0, reveals that in the mature sequence 199 residues are absolutely conserved between all three of these species. Of these 19 are different in squash, thus it is difficult to identify discrete amino acid residues that could play a major role in determining substrate selectivity.

It is also highly likely, as with the oleate desaturase / hydroxylase [11], that several residues contribute to substrate selectivity and no one residue has a dominating effect.

Determining the nature of the acyl-ACP and glycerol-3-phosphate [G-3-P] binding sites will be of importance as a step in elucidating the mechanism of substrate selectivity of this enzyme. The reaction proceeds via a compulsory ordered ternary complex with acyl-ACP binding before G-3-P [12]. The molecular structure of squash G3PAT has been determined at 1.9 Å resolution [13]. Crystals containing bound substrates could not be

### *Plant Glycerol-3-phosphate (1)-acyltransferase*

obtained, however modelling of the G-3-P and acyl-ACP binding site was performed on the basis of proximity to the conserved H(X)<sub>4</sub>D motif which has been shown to be important in catalysis amongst glycerolipid acyltransferases [14]. From the crystal structure it has been predicted that the phosphate group of G-3-P lies in a positively charged pocket formed by the side chains of two arginine residues R235 and R237, a lysine K193 and a histidine residue H194. The presumptive acyl-ACP site was modelled by maximisation of the substrate contacts with fully conserved residues across the G3PAT family and the positioning of the reactive S of the fatty acid moiety close to the sn1 position of the modelled G-3-P site. This placed the palmitoyl/pantothenate substrate within a deep hydrophobic cleft lined with 14 residues which make van der Waals contacts with the substrate.

We are now in a position to test the predicted models for residues implicated to be important in G-3-P and acyl-ACP binding via site directed mutagenesis. Appropriate assays need to be in place to determine if any change in *in vitro* substrate selectivity occurred, since assaying with a single substrate may mistake change in selectivity with total loss of activity. Assays with G3PAT, in the literature, have been performed under a variety of different conditions, hence we have decided to develop assays pertinent to known physiological conditions. The pH of the stroma in the light is pH 8.0 and pH 7.4 in the dark [15]. Estimates of the concentration of G-3-P vary between 65-90  $\mu$ M in

### *Plant Glycerol-3-phosphate (1)-acyltransferase*

spinach [16] and 450-620 $\mu$ M in *Amaranthus* [17]. Chloroplast acyl-ACP concentration values vary in the literature between 0.6-1.9 $\mu$ M and 0.4-2.0 $\mu$ M for C16:0 and C18:1 acyl ACP respectively [18,19].

In this paper we report on: [1] *in vitro* assays which can distinguish between selective and non-selective G3PATs performed under physiological relevant conditions, [2] the effect of mutation of K193, R235, R237 and H194, proposed to be involved with binding of the phosphate group of G-3-P, on biological activity and acyl-ACP binding, [3] the conversion of non-selective squash enzyme into a selective one by site directed mutagenesis resulting in an alteration of the  $K_m$  for 16:0 ACP. X-ray crystallography has been performed with the protein variants and has shown that the structures are highly homologous to the wild type protein.

## **EXPERIMENTAL PROCEDURES**

### ***Cloning of Oil Palm G3PAT***

A 111 day post anthesis oil palm (*Elaeis guineensis*) mesocarp cDNA library was constructed in the  $\lambda$ ZAPII cloning vector (Stratagene) using the TimeSaver cDNA synthesis kit (Pharmacia) to prepare *EcoRI* flanked double stranded cDNA. A 2043 bp

### *Plant Glycerol-3-phosphate (1)-acyltransferase*

cDNA sequence encoding oil palm G3PAT was isolated from this library by heterologous screening of  $2 \times 10^5$  pfu with a  $^{32}\text{P}$  labelled 1445 bp *EcoRI* cDNA fragment of *Arabidopsis* G3PAT.

### ***Overexpression and Purification of Oil Palm, Arabidopsis and Squash G3PAT in E.coli***

Over-expression of squash (NA4, Q24a, Q17b and JKSQ<sup>+</sup>), *Arabidopsis* (AR1) and oil palm constructs for G3PAT [Figure 1] was carried out using the pET<sup>™</sup> plasmid over-expression system. Typical levels of over-expression of plant G3PAT were 10- 15% of the total *E.coli* proteins.

For substrate selectivity and kinetic analyses recombinant G3PAT was selectively released from the *E.coli* cells by repeated cycles of freezing and thawing in dry ice/ethanol and ice/water [20] and the concentration adjusted to give standard amounts in each assay.

### ***Site Directed Mutagenesis***

Site directed mutations of squash and oil palm G3PAT were generated using the QuickChange<sup>™</sup> site directed mutagenesis kit from Stratagene [21].

### *Plant Glycerol-3-phosphate (1)-acyltransferase*

#### ***Synthesis of Radioactive Acyl-ACPs.***

$^{14}\text{C}$  palmitic and  $^3\text{H}$  oleic acyl-ACPs were synthesised using  $25\text{ }\mu\text{M}$   $^{14}\text{C}$  palmitic or  $^3\text{H}$  oleic acid at a specific activity of 55 Ci/mole and  $33\text{ }\mu\text{M}$  recombinant *E.coli* holo ACP in a reaction catalysed by  $5\text{ }\mu\text{M}$  *E.coli* acyl-ACP synthetase. The reaction was carried out in a total volume of 5.0 ml containing 100 mM Tris-HCl pH 8.0, 400 mM LiCl, 10 mM  $\text{MgCl}_2$ , 2 mM DTT, 5 mM ATP, 1% Triton X100, and proceeded at  $30^\circ\text{C}$  for 10 hours. Following synthesis the radioactive acyl-ACP reaction product was purified away from the other reaction components using anion exchange (Q Sepharose) and hydrophobic interaction (Octyl Sepharose) chromatography.

#### ***Assay for G3PAT Enzymatic Activity.***

Dual substrate specificity assays using radioactive acyl-ACP substrates were carried out using modified reaction conditions of Frentzen *et al*, [7]. Assays were carried out in 250 mM HEPES buffer pH 8.0,  $300\text{ }\mu\text{M}$  G3P, 5.0 mg/ml BSA with  $^{14}\text{C}$  16:0ACP and  $^3\text{H}$  18:1ACP at  $1.1\text{ }\mu\text{M}$  each, in a total volume of  $320\text{ }\mu\text{l}$ . Assays were started with the addition of 200 ng of G3PAT purified protein.  $80\text{ }\mu\text{l}$  aliquots were removed at 0 (before addition of enzyme), 1, 2 and 3 minutes and mixed with  $710\text{ }\mu\text{l}$  of chloroform/ methanol (1:1).  $280\text{ }\mu\text{l}$  of 0.2 M  $\text{H}_2\text{PO}_4$  in 1 M KCl was added to the samples, which were vigorously mixed and the phases separated by centrifugation.

### *Plant Glycerol-3-phosphate (1)-acyltransferase*

250 µl of the lower (LPA containing) layer were removed, dried in a vacuum centrifuge, re-suspended in 280 µl of methanol and mixed with 4 ml Ecoscint A. Samples were counted in a Packard liquid scintillation counter on a  $^{14}\text{C}/^3\text{H}$  dual counting protocol to determine the rate of incorporation of  $^{14}\text{C}$  16:0ACP and  $^3\text{H}$  18:1ACP into LPA. The initial velocities were linear.

### ***Acyl-ACP Binding Assays.***

Binding assays with mutant G3PAT enzymes and acyl-ACP substrates were carried out using a Ultrafree <sup>TM</sup> micro-concentrator (Millipore). 100 pmol of radiolabelled acyl-ACP (18:1ACP) was incubated with 50 pmols of G3PAT enzyme in the absence of the other substrate for 5 minutes in 200 µl 250 mM HEPES buffer pH 8.0. Following incubation the samples were transferred to the concentrator and centrifuged through a 30,000 Mw cut off membrane. The radio-labelled substrate bound to G3PAT was retained by the membrane in the upper compartment of the concentrator. Sample volume in both compartments was readjusted to 200 µl and the sample removed and added to 4 ml Ecoscint A scintillation fluid prior to counting in a Packard liquid scintillation counter. This membrane did not retain acyl-ACPs in the absence of G3PAT.

### *Plant Glycerol-3-phosphate (1)-acyltransferase*

#### ***X-Ray Crystallography.***

X-ray crystallography and modelling of substrates within the structure of squash G3PAT was carried out as described previously [13].

#### ***DNA Sequencing.***

DNA sequencing of all G3PAT constructs was carried out on an Applied Biosystems 377 automated sequencer using forward and reverse primers flanking the position of the G3PAT insert. Primers specific to regions close to mutation sites were also used to confirm the presence of the correct mutation.

#### ***Materials and Chemicals***

General molecular biology reagents and restriction enzymes were obtained from, Boehringer Mannheim or Stratagene. pET expression vectors came from Novagen and competent *E.coli* cells were from Stratagene. Oligonucleotide primers for cloning and mutagenesis reactions were from MWG Biotech.  $^{14}\text{C}$  palmitic and  $^3\text{H}$  oleic acids were supplied by Amersham Pharmacia Biotech. All other reagents were purchased from Sigma or MERCK.

## **RESULTS AND DISCUSSION**

### ***In vitro Substrate Selectivity Assays for Recombinant G3PAT.***

Assays were performed under competitive conditions with two substrates in the reaction mixture, 18:1 and 16:0 acyl-ACP at a concentration of 1.1 $\mu$ M each, which is close to their physiological concentration. Since BSA has routinely been used in assays for G3PAT we chose to include it in these studies. Two different BSA concentrations were used, 0.5 and 5 mg/ml, referred to respectively as low and high. Two different pHs were used, pH 7.4 and pH 8.0, reflecting the pH of the chloroplast in the dark and the light respectively. The G-3-P concentration was 300 $\mu$ M, which is in the physiological range of this substrate.

With the squash enzyme [Figure 2] both reaction velocities are lower at pH7.4 than at pH8.0. At high BSA there is little preference for either 16:0 or 18:1 whilst at low BSA there is a preference for 18:1 over 16:0 which is more marked at the lower pH. At low BSA, in comparison to high BSA, the reaction velocity is lowered for 16:0 and increased for 18:1 resulting in an alteration of the substrate selectivity of the enzyme. Assays conducted with the full-length sequence of the squash enzyme [JSKQ+] in the presence of high BSA and pH 8.0 gave a substrate selectivity of 0.93 which is close to that



### *Plant Glycerol-3-phosphate (1)-acyltransferase*

observed for the truncated enzyme. With the *Arabidopsis* enzyme [Figure 2] similar effects are seen however under all assay conditions the *Arabidopsis* enzyme shows a strong preference for 18:1.

As the physiological concentrations of G-3-P and acyl-ACP could be as high as 2 $\mu$ M for acyl-ACPs and 620 $\mu$ M for G-3-P we conducted further selectivity assays increasing the acyl-ACP and G-3-P concentration at high BSA and pH 8.0. The G-3-P concentration was increased up to 620 $\mu$ M and the acyl-ACP up to a concentration of 2.2 $\mu$ M each.

Assays were conducted with both the squash and *Arabidopsis* enzymes [Table 1].

Doubling the acyl-ACP or G-3-P concentration had little effect on the substrate selectivity. We therefore decided to use 1.1 $\mu$ M of each acyl-ACP, 300 $\mu$ M G-3-P, high BSA and pH 8.0 in all future experimentation.

### ***Mutation of L261 to F Causes Alteration of Substrate Selectivity of both the Squash and Oil palm G3PAT Changing it from a Non-selective Enzyme to an Oleate Selective One.***

In order to prepare large quantities of squash G3PAT, using fermentation, for more extensive crystallization trials we decided to replace the ampicillin selection marker with a kanamycin one. This was to overcome problems with loss of the plasmid due to the expense of maintaining the organism under ampicillin selection in the fermenter. In our

### *Plant Glycerol-3-phosphate (1)-acyltransferase*

cloning strategy we amplified the squash G3PAT cDNA from the plasmid pNA4 via a PCR based protocol using a proof reading taq polymerase [VENT<sup>TM</sup> DNA Polymerase] and inserted it into the pET24a plasmid which contains a kanamycin selection marker. Assays using the dual substrate 16:0/18:1 acyl ACP selectivity assay were performed on selected transformants. It was noticed that G3PAT from one of the transformants showed a preference for 18:1 [Figure 3d] whilst the "wild type" plasmid from which it was derived exhibited no acyl preference [Figure 3a]. Sequencing of the entire coding region for G3PAT in the "mutant" plasmid revealed that two point mutations had occurred during the PCR reactions. These converted L261 and S331 to F and P respectively [Figure 3d]. In order to identify which residue was responsible for this change in substrate selectivity both mutated residues were individually mutated back to the wild type. The L261F enzyme was selective [Figure 3b] whilst the S331P was non-selective [Figure 3c] indicating that a point mutation at 261 converts a non-selective enzyme into a selective one. In order to see if mutation at this residue could result in altered substrate selectivity in other G3PAT enzymes we looked for the corresponding residue in the oil palm G3PAT, which we had recently cloned, and which shows no substrate selectivity. The corresponding residue in oil palm is L352. We mutated this to a F and assayed for substrate selectivity. Mutation of this residue in oil palm caused a similar alteration in substrate selectivity [Figure 3 e + f].

### *Plant Glycerol-3-phosphate (1)-acyltransferase*

Position 261 in the Squash G3PAT structure lies at the end of the deep cleft remote from the H(X)<sub>4</sub>D motif and represents one of 12 residues implicated in binding the fatty acyl substrate [13]. The fact that the structures of the wild type and L261F variant are otherwise identical suggests that differential substrate specificity could arise in part from the large side chain of the phenylalanine residue.

### ***Kinetic Analysis of the L261F and Wild Type Squash Enzymes.***

In order to determine the basis of the alteration in substrate selectivity we performed kinetic analysis on the wild type and mutant enzymes from squash. Assays were performed using acyl-ACP at 10 $\mu$ M each and G-3-P at 20mM at pH 8.0 in the presence of 5mg ml BSA, whilst varying the second substrate concentration. The K<sub>m</sub> and V<sub>max</sub> for both G-3-P and acyl-ACP [Figure 4] are almost identical for the wild type and mutant using 18:1-ACP as substrate, however the K<sub>m</sub> for 16:0 in the mutant was almost 3 times as high [Table 2]. The reaction velocity of both Q24a N-terminally truncated recombinant protein and the Q24a-L261F mutant were determined at 20mM G-3-P and 10 $\mu$ M of both 16:0 and 18:1 ACP [total acyl-ACP concentration 20 $\mu$ M]. The values for 18:1 were similar but were almost half for 16:0 with the mutant, consistent with the mutation being caused by a K<sub>m</sub> effect on 16:0 ACP.

***Mutation of T141 to S Does Not Alter Substrate Selectivity of the Squash Enzyme.***

The H(X)<sub>4</sub>D motif is present in G3PAT and is hypothesised to be involved in metal binding and the D331E mutant of *plsB* in *E.coli* is still capable of binding G-3-P, albeit with an increased *K<sub>m</sub>* of 200μM in comparison to 100μM for the wild type. By analogy with chloramphenicol acetyltransferase [22] it has been argued that the H residue could act as a general base to abstract a proton from the hydroxy group of the acyl acceptor to facilitate nucleophilic attack on the thioester of the acyl donor. It is notable that in all 18:1 selective G3PATs the sequence is HQSEAD whilst in the squash enzyme, which is non-selective, the S is a T(141). The corresponding residue in oil palm is also a T (169). Mutation of T141 to an S in the squash enzyme does not result in any major alteration in substrate selectivity of the protein [Table 3]. It is still fully catalytically active and shows the same substrate preference, indicating that this single residue does not play a major role in determining substrate selectivity.

***Mutation of Residues Predicted to be Involved in G-3-P Binding.***

From the crystal structure it has been predicted that the G-3-P binding site lies in domain 2 of the protein and that the phosphate group lies in a positively charged pocket formed by the side chains of two arginine residues R235, and R237, a lysine K193 and a histidine residue H194 (Figure 5). We mutated each of the four positively charged residues and

*Plant Glycerol-3-phosphate (1)-acyltransferase*

converted them individually to serine residues. The proteins were expressed in *E.coli* at the same level as the wild type protein and were fully soluble. The soluble protein was assayed for biological activity using the standard assay with acyl-ACPs [Table 3]. R235S, R237S and K193S were all inactive, even following incubation times 100 times longer than those normally used. In acyl-ACP binding studies using a spin column, all three inactive enzymes retained their ability to bind stoichiometric quantities of acyl-ACP. The values for nmoles of acyl ACP substrate bound per mole of enzyme were  $0.95 \pm 0.01$ ,  $0.81 \pm 0.03$ ,  $0.91 \pm 0.02$ ,  $0.91 \pm 0.05$  and  $0.90 \pm 0.03$  for Q24a, E142A, K193S, R235S and R237S respectively. Since the reaction proceeds via an ordered ternary complex with acylACP binding first the results are consistent with the three residues being involved in G-3-P binding. The H194S mutant had approximately 80% of the biological activity of the wild type enzyme indicating that this residue is not so critical for binding and catalysis. We also mutated E142 which lies in the H(X)<sub>4</sub>D box to a A. This residue is conserved in all plant G3PAT enzymes. The resultant E142A protein is biologically inactive indicating that it plays an important role in the enzyme. Replacing the E with an A changes the local hydrogen bonding environment close to the presumptive G-3-P binding site and presumably perturbs the structure in such a way that the enzyme is catalytically inactive.

### *Plant Glycerol-3-phosphate (1)-acyltransferase*

High resolution X-ray diffraction data were collected for crystals of the K193S, R235S and R237S mutant enzymes and the three-dimensional structures were solved using molecular replacement methods employing programs from the CCP4 suite (data not shown). Pairwise superposition using the program LSQKAB [23] of the structures of the mutant enzymes with that of the wild type G3PAT structure gave root mean square displacements (rmsd) of C<sub>α</sub> positions ranging between 0.1 Å and 0.3 Å which indicate that the structures of these enzymes are highly homologous. Therefore, the replacement of any of these residues with a serine residue inactivates the enzyme without major perturbation of the three-dimensional structure. Additionally, the structure of the L261F mutant is also highly homologous to the wild type structure with an rmsd of C<sub>α</sub> distances of 0.1 Å.

### ***Overall Implications***

Introduction of *E.coli* [24] and plant *plsB* genes [1], which code for the non-selective enzyme into tobacco has confirmed the importance of the acyl group composition on chilling resistance in plants. Studies using chimeric protein constructs between the pea and the squash enzymes have indicated that the central portion of the enzyme is probably important in substrate selectivity [25]. However these studies have been compromised by the use of non-physiological conditions and substrate analogues.

### *Plant Glycerol-3-phosphate (1)-acyltransferase*

In this study we have developed *in vitro* assays which discriminate between selective and non-selective plant G3PATs. It is interesting to note that BSA which is known to bind fatty acids has a significant effect on this assay prompting us to suggest that chloroplasts may contain an acyl binding protein equivalent to the acyl CoA binding protein present in the cytoplasm [26].

Mutation of a single residue L261F causes major changes in substrate selectivity and from modelling studies this is likely to be due to masking of the hydrophobic cleft. The exact nature of the interactions between the enzyme and fatty acyl substrate awaits further three-dimensional structural data on a binary complex of the enzyme with substrate.

However, the modelling studies combined with the site directed mutagenesis studies presented here have indicated that changing L261 to a phenylalanine residue alters specificity from a non-selective enzyme to one which preferentially incorporates C18:1-ACP. Given that our crystallographic studies reveal no other changes in enzyme structure, the bulky hydrophobic nature of the phenylalanine side chain must alter the shape of the binding pocket so that a lower binding affinity and rate of catalysis is observed with the C16:0 substrate ( $K_m$  3x higher and  $K_{cat}$  50%) whilst the affinity and catalytic rate with the C18:1 substrate remain unchanged compared to the wild type protein.

### *Plant Glycerol-3-phosphate (1)-acyltransferase*

Since knowledge of the active site of the enzyme is important to understand how it functions, we have performed site directed mutagenesis on amino acid residues proposed from modelling studies to be involved in G3P and acyl ACP binding. Our results are consistent with K193, R235 and R237 as residues important in binding the negatively charged phosphate group of G3P.

Clear evidence can not be obtained on the site of acyl ACP binding and this will require further studies either using a catalytically inactive enzyme in order to obtain a suitable enzyme complex or appropriate binding studies using photo-affinity probes. Such studies will be the basis of future work.

### *Acknowledgements*

Matthew Hayman is the recipient of a BBSRC PhD studentship.

Andy P. Turnbull and David W. Rice were supported by a research grant from BBSRC.

John B. Rafferty is a Royal Society-funded Olga Kennard Fellow.

Johan T M. Kroon was supported for part of this work by a grant from MAFF.



**References**

1. Murata, N., Ishizaki-Nishizawa, O., Higashi, S., Hayashi, H., Tasaka, Y., and Nishida, I. (1992) *Nature* 356,710-713.
2. Slabas AR, Hanley Z, Schierer T, Rice D, Turnbull A, Rafferty J, Simon J.W, Brown, A. (2001) *J. Plant Physiol.* 158,505-513.
3. Green, P.R., Merrill, A.H.R., and Bell,R.M. (1981) *J.Biol.Chem.*256,11151-11159.
4. Frentzen, M., Heinz, E., McKeon, T.A., and Stumpf, P.K. (1983) *Eur.J.Biochem.*, 129,629-636.
5. Weber, S., Wolter, F., Buck, F., Frentzen, M., and Heinz, E. (1991) *Plant Mol.Biol.* 17,1067-1076.
6. Nishida, I., Tasaka,Y., Shiraishi, H., and Murata, N. (1993) *Plant.Mol.Biol.* 21,267-277.
7. Frentzen, M., Nishida, I., and Murata, N. (1987) *Plant Cell Physiol.* 28,1195-1201.
8. Murata, N. (1983) *Plant and Cell Physiol.* 24:81-86.
9. Ishizaki, O., Nishida, I., Agata, K., Eguchi, G., and Murata, N. (1988) *FEBS Lett.* 238,424-430.
10. Murata, N., and Tasaka, Y. (1997) *Biochim. Biophys.Acta.* 1348,10-16.
11. Broun P, Shanklin J, Whittle E, Somerville C. (1998) *Science* 282,1315-1317.
12. Hayman, M.W., Fawcett, T and Slabas A.R (2002) *FEBS Letts* 25855; 1-4

*Plant Glycerol-3-phosphate (1)-acyltransferase*

13. Turnbull, A.P., Rafferty, J.B., Sedelnikova, S.E., Slabas, A.R., Schierer, T.P., Kroon, J.T.M., Simon, J.W., Fawcett, T., Nishida, I., Murata, N., and Rice, D. (2001). *Structure* 9,347-353.
14. Heath, R.J., and Rock, C.O. (1998) *J.Bacteriol.* 180,1425-1430.
15. *In Plant Biochemistry and Molecular Biology* (1993)(Lea P.J., and Leegood, R.C Eds) page 30.
16. Sauer, A., and Heise, K.P., (1984) *Z. Naturforsch C* 39 (6): 593-599.
17. Cronan, J.E., Jr and Roughan, P.G. (1987) *Plant Physiol.* 83,676-679.
18. Roughan, G., and Nishida, I. (1990) *Arch. Biochem. Biophys.* 276,38-46.
19. Sol, J., and Roughan, G. (1982) *FEBS Letts.* 146,189-192.
20. Johnson, B.H., and Hecht, M.H. (1994) *Biotechnology* 12,1357-1360.
21. Simon J.W. (2002) *PhD thesis, University of Durham.*
22. Lewin, T.M., Wang, P., and Coleman, R.A. (1999) *Biocemistry* 38:5764-5771.
23. Collaborative Computational Project, Number 4. (1994). The CCP4 suite-Programs for protein crystallography. *Acta Cryst.* D50 760-763.
24. Wolter F.P, Schmidt.R. and Heinz. E. (1992) *EMBO J.* 11 (13): 4685-4692
25. Ferri, S.R., and Toguri, T. (1997) *Arch.Biochim.Biophys.* 337,202-208.
26. Brown AP, Johnson P, Rawsthorne S, Hills MJ. (1998) *Plant Physiol.Biochem.* 36, 629-635.

### Figure Legends

**Figure 1.** Amino acid sequence alignment at the predicted processing sites of G3PATs from *Arabidopsis thaliana* and squash (*Cucurbita moschata*). SQU G3PAT and ARA G3PAT represent the sequences of the full-length precursor G3PATs from squash and *Arabidopsis* respectively. JKSQ+, NA4, Q17b, Q24a and AR1, A17b, A24a are recombinant G3PAT proteins from squash and *Arabidopsis* respectively. The recombinant proteins are N-terminally truncated at predicted processing sites. Bold type depicts amino acids that have been coded for by vector DNA. Arrows indicate predicted processing sites and the symbol # represents amino acids which are not depicted in the figure.

**Figure 2.** *Acyl-ACP selectivity of squash and Arabidopsis G3PAT with varying pH and BSA concentration.* The amount of labelled 1-LPA formed in standard competitive assays was measured. Assays contained 65 ng of purified recombinant squash G3PAT (Q24a) or *Arabidopsis* G3PAT (AR1). Labelled 1-LPA formed in standard competitive assays with labelled 18:1 and 16:0 acyl-ACP thioesters at 1.0  $\mu$ M each and glycerol-3-phosphate at 300  $\mu$ M. Numbers in bold show the ratio of labelled 18:1/16:0 1-LPA formed.

**Figure 3.** *Substrate selectivity of the recombinant squash, oil palm G3PAT and mutant proteins.* Substrate selectivity of squash (a) Q24a, (b) Q24a-L261F, (c) Q24a-S331P (d) Q24a-L261F/S331P, and oil palm (e) JK/OA2.2 and (f) the JK/OA2.2- L352F was measured as incorporation of differently labelled acyl-ACP thioesters into LPA under the standard conditions for the competitive assay described in the materials and methods. ◆ represents 18:1-LPA formation and ○ represents 16:0-LPA formation. The amino acid substitution L352F in the oil palm GPAT is equivalent to the L261F substitution in the Q24a derived squash GPAT proteins.

**Figure 4.** *Kinetic analyses (Michaelis-Menten plots) of squash G3PAT wild type (Q24a) and mutant (Q24a L261F activity.* Assays i + ii were performed with G3P at 20mM and variable acyl-ACP concentrations. Assays iii + iv were performed at 10  $\mu$ M acyl-ACP and variable G3P concentrations. ▲ = 16:0 acyl-ACP and ○ = 18:1 acyl-ACP.

**Figure 5.**

Crystal structure of the predicted glycerol-3-phosphate binding domain of squash G3PAT. The binding site lies in domain 2 of the protein and the phosphate group of the G-3-P lies in a positively charged pocket (arrowed) formed by the side chains of R235, R237, K193 and H194.

**Table 1.** Substrate selectivity assays of squash and *Arabidopsis* G3PAT using varying levels of acyl-ACP and G3P substrates.

Squash G3PAT (Q24a)			
Concentration of each acyl-ACP $\mu\text{M}^1$	[G3P] $\mu\text{M}$	Rates for 18:1/16:0-LPA production in pmol/min	Selectivity <sup>2</sup> (18:1/16:0)
1.1	300	12.4/13.0	0.95
1.1	620	15.6/17.3	0.9
2.2	300	18.2/15.2	1.2
<i>Arabidopsis</i> G3PAT (AR <sub>1</sub> )			
Concentration of each acyl-ACP $\mu\text{M}^1$	[G3P] $\mu\text{M}$	Rates for 18:1/16:0-LPA production in pmol/min	Selectivity <sup>2</sup> (18:1/16:0)
1.1	300	20.1/6.5	3.1
1.1	620	25.9/9.65	2.7
2.2	300	30.1/8.6	3.5

<sup>1</sup>Equimolar mixtures of 18:1 and 16:0ACP were used in the reaction mixture, each at the concentration given.

<sup>2</sup>Selectivity is given as the rate of production of 18:1-LPA divided by the rate of production of 16:0-LPA.

*Plant Glycerol-3-phosphate (1)-acyltransferase*

**Table 2.** Kinetic analysis of squash G3PAT (Q24a) and mutant displaying altered substrate selectivity (Q24a L261F) using acyl-ACP substrates.

Isomeric form	Acyl-ACP	Km acyl-ACP [ $\mu$ M]	Km G-3-P [ $\mu$ M]	Velocity <sup>1</sup> (pmol LPA formed / $\mu$ g G3PAT/ min <sup>-1</sup> )	
				18:1ACP	16:0ACP
Q24a	16:0	3.42	142.6	198	213
	18:1	3.01	117.1		
Q24a L261F	16:0	9.20	150.9	218	101
	18:1	2.78	100.7		

<sup>1</sup>Velocity under conditions close to Vmax. G3P at 20mM. Each acyl-ACP at 10 $\mu$ M.

**Table 3.** Summary of squash G3PAT Q24a mutants created and analysed.

Mutant (based on Q24a numbering)	Activity as % of w.t. (standardised ng of GPAT protein added) <sup>1</sup>	Selectivity (if determined)
Q24a	100 (arbitrary)	1.0
T141S	106	1.0
E142A*	0	
K193S*	0	
H194S	79	0.8
R235S*	0	
R237S*	0	
L261F	90	3.8
S331P	94	1.2
Oil Palm W.t.	100	1.1
Oil Palm L352F	117	3.3

<sup>1</sup>Percentage activity is calculated by assigning the wild type enzyme an activity of 100% and comparing the LPA formed per min (of 18:1 and 16:0-ACP together) against that of the wild type.

\* These assays were performed for up to 100 times the normal incubation time to confirm lack of activity.

*Plant Glycerol-3-phosphate (1)-acyltransferase*

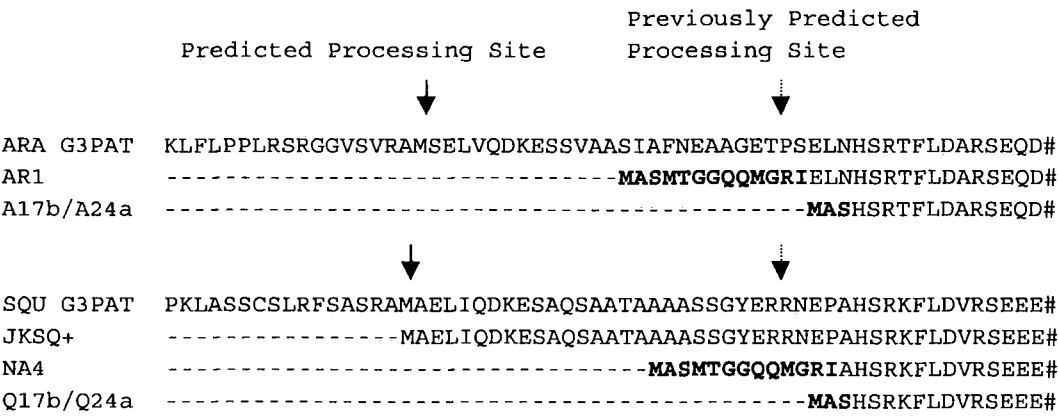


**Figure 1.**



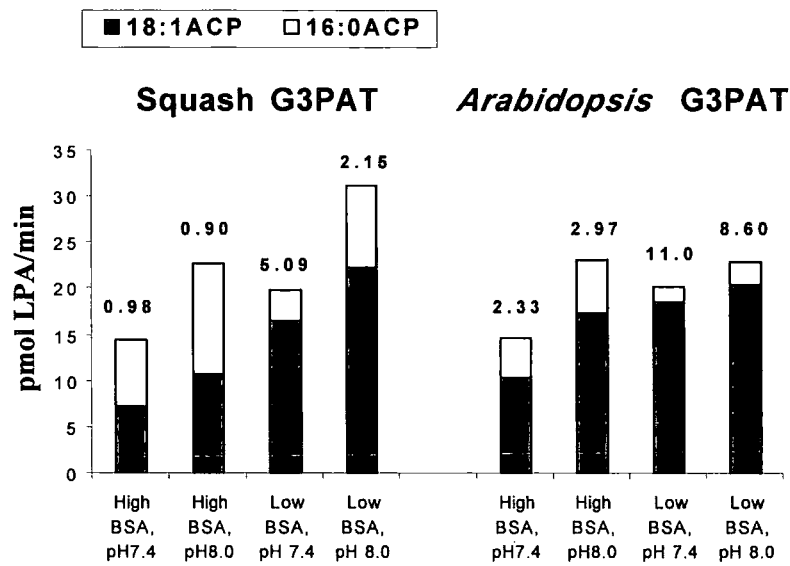
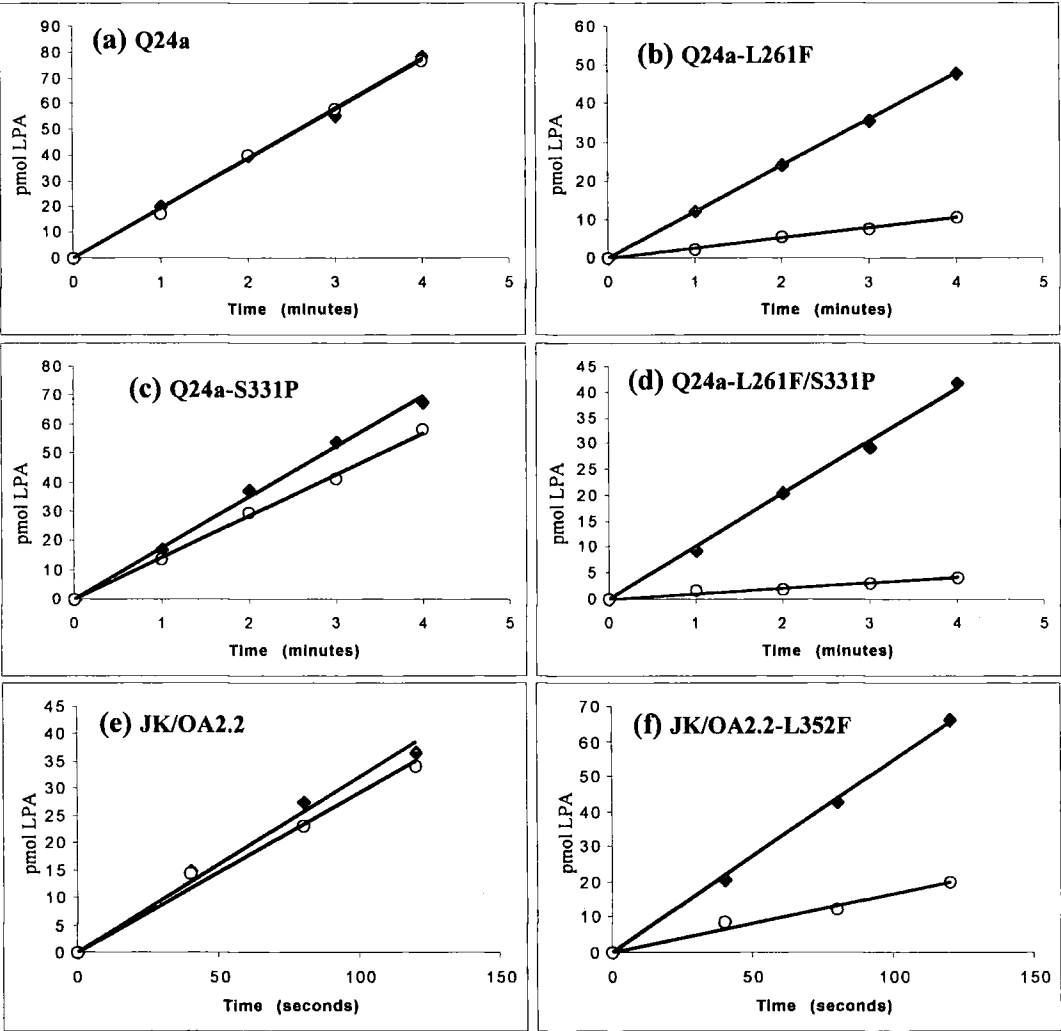


Figure 2.

*Plant Glycerol-3-phosphate (1)-acyltransferase*



**Figure 3.**

*Plant Glycerol-3-phosphate (1)-acyltransferase*

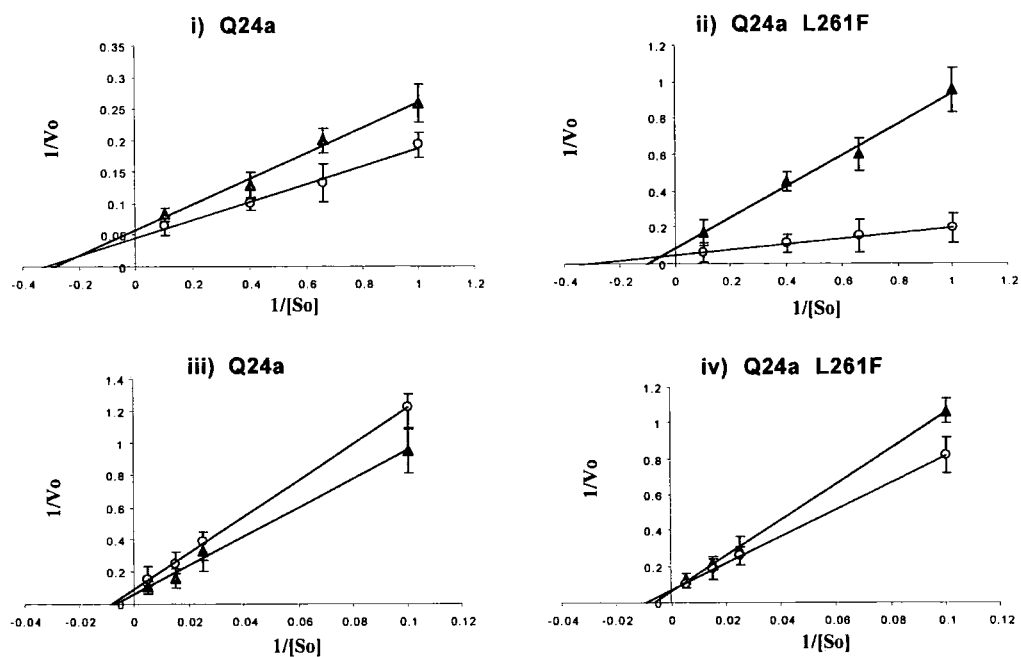


**Figure 4.**

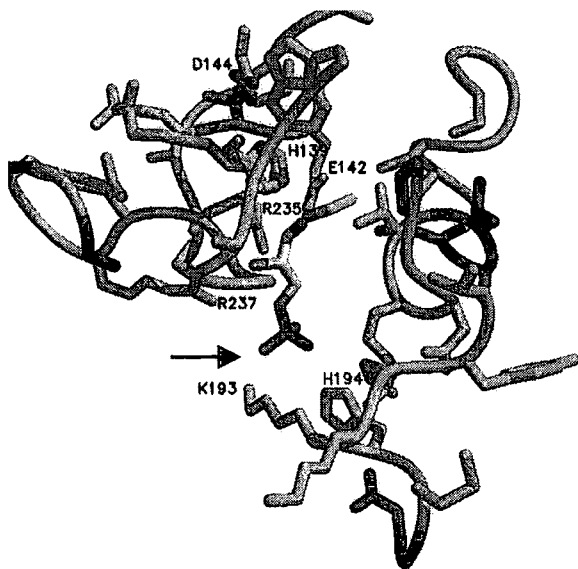


**Figure 5.**

**Appendix 2** - Summary of selectivity assays performed in partnership with Ted Schierer (University of Durham)

Substrate	ACP 18:1/16:0		CoA 18:1/16:0	
Conditions	Squash	Arabidopsis	Squash	Arabidopsis
5.0 mg/ml BSA, pH 7.4	<b>0.98</b> ± 0.03 [7.2/7.4] ±0.15/±0.09	<b>2.33</b> ± 0.15 [10.3/4.4] ±0.22/±0.25	<b>0.77</b> ± 0.03 [5.6/7.3] ±0.61/±0.89	<b>0.93</b> ± 0.02 [12.0/13.0] ±0.73/±1.01
5.0 mg/ml BSA, pH 8.0	<b>0.90</b> ± 0.03 [10.8/12.0] ±0.95/±0.95	<b>2.97</b> ± 0.05 17.3/5.8] ±0.83/±0.24	<b>1.14</b> ± 0.04 [5.1/4.6] ±0.36/±0.33	<b>1.38</b> ± 0.08 [8.7/6.3] ±0.30/±0.59
0.5mg/ml BSA, pH 7.4	<b>5.09</b> ± 0.43 [16.6/3.3] ±0.94/±0.13	<b>11.0</b> ± 0.19 [18.6/1.7] ±0.84/±0.06	<b>1.36</b> ± 0.03 [55.9/41.3] ±4.30/±3.57	<b>1.88</b> ± 0.01 [102.7/54.7] ±6.87/±3.87
0.5 mg/ml BSA, pH 8.0	<b>2.51</b> ± 0.17 [22.3/8.9] ±2.30/±0.78	<b>8.60</b> ± 1.09 [20.5/2.4] ±1.30/±0.23	<b>1.21</b> ± 0.08 [67.9/55.8] ±6.27/±1.86	<b>2.19</b> ± 0.14 [94.7/43.5] ±4.42/±2.91

**Summary of substrate selectivity assays performed on Squash and *Arabidopsis* G3PAT using acyl-ACP and acyl-CoA substrates.**

Values in bold represent the ratio of activity of the enzyme for 18:1ACP over 16:0ACP: if the number is higher than 1 the enzyme has a preference for 18:1 over 16:0. The figures in square brackets show the rate of enzyme activity with each substrate in pmol of LPA formed per minute. Assays were performed in triplicate on two separate occasions and results are presented as mean values  $\pm$  1 standard error measurement. Assays using acyl-CoA substrates presented here were performed jointly by the author and Ted Schierer, University of Durham.

## References

- Altschul, S.F., Gish, W., Miller, W., Myers, E.W., Lipman, D.J. (1990) Basic local alignment search tool. *Journal of Molecular Biology*. **215** pp. 403-410.
- Battey, J.F., Ohlrogge, J.B. (1990) Evolutionary and tissue-specific control of expression of multiple acyl-carrier protein isoforms in plants and bacteria. *Planta*. **180** pp. 352-360.
- Bertrams, M., Heinz, E. (1976) Experiments on enzymatic acylation of *sn*-glycerol-3-phosphate with enzyme preparations from pea and spinach leaves. *Planta* 132 pp. 161-168.
- Bertrams, M., Heinz, E. (1981) Positional specificity and fatty acid selectivity of purified *sn*-glycerol-3-phosphate acyltransferases from chloroplasts. *Plant Physiology*. **68** pp. 653-657.
- Bhat, G.B., Wang, P., Kim, J.H., Black, T.M., Lewin, T.M., Fiedorek, F.T. Jnr., Coleman, R.A. (1999) Rat *sn*-glycerol-3-phosphate acyltransferase: molecular cloning and characterisation of the cDNA and expressed protein. *Biochimica et Biophysica Acta*. **1439** pp. 415-423.
- Bhella, R.S., MacKenzie, S.L. (1994) Nucleotide sequence of a cDNA from *Carthamus tinctoris* encoding a glycerol-3-phosphate acyltransferase. *Plant physiology*. **106** pp. 1713-1714.

Bloch, K., Vance, D. (1977) Control mechanisms in the synthesis of saturated fatty acids. *Annual Review of Biochemistry*. **46** pp. 263-298.

Briggs, S.P., Koziel, M. (1998) Engineering new plant strains for commercial markets. *Current Opinion in Biotechnology*. **9** pp. 233-235.

Broun, P., Shanklin, J., Whittle, E., Somerville, C. (1998) Catalytic plasticity of fatty acid modification enzymes underlying chemical diversity of plant lipids. *Science*. **282** pp. 1315-1317.

Brown, A.P., Brough, C.L., Kroon, J.T.M., Slabas, A.R. (1995) Identification of a cDNA that encodes a 1-acyl-sn-glycerol-3-phosphate acyltransferase from *Limnanthes douglasii*. *Plant Molecular Biology*. **29** pp. 267-278.

Brown, A.P., Coleman, J., Tommey, A.M., Watson, M.D., Slabas, A.R. (1994) Isolation and characterisation of a maize cDNA that compliments a 1-acyl sn-glycerol-3-phosphate acyltransferase mutant of *Escherichia coli* and encodes a protein which has similarities to other acyltransferases. *Plant Molecular Biology*. **26** pp. 211-223.

Browse, J., Somerville, C. (1991) Glycerolipid synthesis – Biochemistry and regulation. *Annual Review of Plant Physiology and Plant Molecular Biology*. **42** pp. 467-506.

Browse, J., Xin, Z.G. (2001) Temperature sensing and cold acclimation. *Current Opinion in Plant Biology*. **4** pp. 241-246.



Cahoon, E.B, Shah, S., Shanklin, J., Browse, J. (1998) A determinant of substrate specificity predicted from the acyl-acyl carrier protein desaturase of developing cat's claw seed. *Plant Physiology*. **117** pp. 593-598.

Cahoon, E.B., Lindqvist, Y., Schneider, G., Shanklin, J. (1997) Redesign of soluble fatty acid desaturases from plants for altered substrate specificity and double bond position. *Proceedings of the National Academy of Sciences of the United States of America*. **94** pp. 4872-4877.

Cleland, W.W. (1963) The kinetics of enzyme-catalysed reactions with two or more substrates or products. *Biochimica and Biophysica Acta*. **67** pp. 104-137.

Coleman, J. (1990) Characterisation of *Escherichia coli* deficient in 1-Acyl-sn-glycerol-3-phosphate acyltransferase activity. *Journal of Biological Chemistry*. **265** pp. 17215-17221.

Cronan, J.E. Jr., Roughan, G. (1987) Fatty acid specificity of the chloroplast sn-glycerol 3-phosphate acyltransferase of the chilling sensitive plant, *Amaranthus lividus*. *Plant Physiology*. **83** pp. 676-680.

Cronin, C.N. (1997) The conserved serine-threonine-serine motif of the carnitine acyltransferases is involved in carnitine binding and transition-state stabilization: A site-directed mutagenesis study. *Biochemical and Biophysical research communications*. **238** pp. 784-789.

Davies, H.M. (1993) Medium chain acyl-ACP hydrolysis activities of developing oilseeds. *Phytochemistry*. **33** pp. 1353-1356.

Dircks, L.K., Ke, J.S., Sul, H.S. (1999) A conserved seven amino acid stretch important for murine mitochondrial glycerol-3-phosphate acyltransferase activity – significance of arginine 318 in catalysis. *Journal of Biological Chemistry*. **274** pp. 34728-34734.

Dörmann, P., Frentzen, M., Ohlrogge, J.B. (1994) Specificities of the acyl-acyl-carrier protein (ACP) thioesterases for octadecanoyl-ACP isomers – identification of a petroselinoyl-ACP thioesterase in *umbelliferae*. *Plant Physiology*. **104** pp. 839-844.

Dörmann, P., Voelker, T.A., Ohlrogge, J.B. (1995) Cloning and expression in *Escherichia coli* of a novel thioesterases from *Arabidopsis thaliana* specific for long-chain acyl-acyl carrier proteins. *Archives of Biochemistry and Biophysics*. **316** pp. 612-618.

Eccleston, V.S., Harwood, J.L. (1995) Solubilisation, partial-purification and properties of acyl-CoA glycerol-3-phosphate acyltransferase from avocado (*Persea americana*) fruit mesocarp. *Biochimica et Biophysica Acta – Lipids and lipid metabolism*. **1257** pp. 1-10.

Fawcett, T., Copse, C.L., Simon, J.W., Slabas, A.R. (2000) Kinetic mechanism of NADH-enoyl-ACP reductase from *Brassica napus*. *FEBS Letters*. **484** pp. 65-68.

Ferri, S.R., Toguri, T. (1997) Substrate specificity modification of the stromal glycerol-3-phosphate acyltransferase. *Archives of Biochemistry and Biophysics*. **337** pp. 202-208.

Frandsen, G.I., Mundy, J., Tzen, J.T. (2001) Oil bodies and their associated proteins, oleosin and caleosin. *Physiol Plant*. **112** pp. 301-307.

Frentzen, M. (1990) Comparison of certain properties of membrane bound and solubilised acyltransferase activities of plant microsomes. *Plant Science*. **69** pp. 39-48.

Frentzen, M. (1993) Acyltransferases and triacylglycerols. In *Lipid Metabolism in Plants*, T.S. Moore Jnr. (Ed.) CRC Press 195-231.

Frentzen, M., Heinz, E., McKeon, T.A., Stumpf, P.K. (1983) Specificities and selectivities of glycerol-3-phosphate acyltransferase and monoacylglycerol-3-phosphate acyltransferase from Pea and Spinach chloroplasts. *European Journal of Biochemistry*. **129** pp. 629-636.

Frentzen, M., Neuberger, M., Joyard, J., Douce, R. (1990) Intraorganelle localisation and substrate specificities of the mitochondrial acyl-CoA *sn*-glycerol-3-phosphate O-acyltransferase and acyl-CoA 1-acyl-*sn*-glycerol-3-phosphate O-acyltransferase from potato tubers and pea leaves. *European Journal of Biochemistry*. **187** pp. 395-402.

Frentzen, M., Nishida, I., Murata, N. (1987) Properties of the plastidial acyl-(acyl-carrier-protein): Glycerol-3-phosphate acyltransferase from the chilling-sensitive plant squash (*Cucurbita moschata*). *Plant Cell Physiology*. **28** pp. 1195-1201.

Frentzen, M., Peterek, G., Wolter, F.P. (1994) Properties and subcellular localisation of a plastidial sn-glycerol-3-phosphate acyltransferase of *Pisum sativum* L. expressed in *Escherichia coli*. *Plant Science*. **96** pp. 45-53.

Fritz, M., Heinz, E., Wolter, F.P. (1995) Cloning and sequencing of a full-length cDNA coding for sn-glycerol-3-phosphate acyltransferase from *Phaseolus vulgaris*. *Plant Physiology*. **107** pp. 1039-1040.

Garg, R., Santha, I.M., Lodha, M.L., Mehta, S.L. (2001) Sequence analysis of a plastidial omega-3 desaturase gene from *Brassica juncea*. *Journal of Plant Biochemistry and Biotechnology*. **10** pp. 13-17.

Guerra, D.J., Ohlrogge, J.B., Frentzen, M. (1986) Activity of acyl carrier protein isoforms in reactions of plant fatty-acid metabolism. *Plant Physiology*. **82** pp. 448-453.

Hach, M., Pedersen, S.N., Børchers, T., Hørjup, P., Knudsen, J. (1990) Determination by photoaffinity labelling of the hydrophobic part of the binding site for acyl-CoA esters on acyl-CoA-binding protein from bovine liver. *Biochemistry Journal*. **271** pp. 231-236.

Hansen, L. (1987) 3 cDNA clones for barley leaf acyl carrier protein-I and protein-III. *Carlsberg research Communications*. **52** pp. 381-392.

Harwood, J.L. (1996) Recent advances in the biosynthesis of plant fatty acids. *Biochimica et Biophysica Acta*. **1301** pp. 7-56.

Harwood, J.L. (1998) Plant lipid biosynthesis: Fundamentals and agricultural applications. Cambridge University Press.

Harwood, J.L., Page, R.A. (1994) In D.J. Murphy, Designer Oil Crops pp. 165-194. Weinheim, VCH.

Hayman, M.W., Fawcett, T., Slabas, A.R. (2002) Kinetic Mechanism and order of substrate binding for sn-glycerol-3-phosphate acyltransferase from squash (*Cucurbita moschata*). *FEBS Letters*. **514** pp. 281-284.

Heath, R.J., Rock, C.O. (1998) A conserved histidine is essential for glycerolipid acyltransferase catalysis. *Journal of Bacteriology*. **180** pp. 1425-1430.

Herman, E.M. (1987) Immuno-gold localisation and synthesis of an oil-body membrane-protein in developing soybean seeds. *Planta*. **172** pp. 336-345.

Hills, M.J., Watson, M.D., Murphy, D.J. (1993) Targetting of oleosins to the oil bodies of oilseed rape (*Brassica napus* L.). *Planta*. **189** pp. 24-29.

Huang, A.H.C. (1992) Oil bodies and oleosins in seeds. *Annual Review of Plant Physiology and Plant Molecular Biology*. **43** pp. 177-200.

Hutchison III, C.A., Phillips, S., Marshall, H.E., Gillam, S., Jahnke, P., Smith, M. (1978) Mutagenesis at a specific position in a DNA sequence. *Journal of Biological Chemistry*. **253** pp. 6551-6560.

Ishizaki, O., Nishida, I., Agata, K., Eguchi, G., Murata, N. (1988) Cloning and nucleotide sequence of cDNA for the plastid glycerol-3-phosphate acyltransferase from squash.

*FEBS*. **238** pp. 424-430.

Jackowski, S., Jackson, P.D., Rock, C.O. (1994) Sequence and function of the AAS gene in *Escherichia coli*. *Journal of Biological Chemistry*. **269** pp. 2921-2928.

Jackowski, S., Jackson, P.D., Rock, C.O. (1994) Sequence and function of the aas gene in *Escherichia coli*. *Journal of Biological Chemistry*. **269** pp. 2921-2928.

Jaworski, J.G., Post-Beittenmiller, D., Ohlrogge, J.B. (1993) Acetyl-acyl carrier protein is not a major intermediate in fatty acid biosynthesis in spinach. *European Journal of Biochemistry*. **213** pp. 981-987.

Johnson, B.H., Height, M.H. (1994) Recombinant proteins can be isolated from *Escherichia coli* cells by repeated cycles of freezing and thawing. *Bio-technology*. **12** pp. 1357-1360.

Johnson, T.C. Schneider, J.C., Somerville, C. (1992) Nucleotide sequence of acyl-acyl carrier protein glycerol-3-phosphate acyltransferase from Cucumber. *Plant Physiology*. **99** pp. 771-772.

Jones, A., Davies, H.M., Voelker, T.A. (1995) Palmitoyl-acyl carrier protein (ACP) thioesterase and the evolutionary origin of plant acyl-ACP thioesterases. *Plant Cell*. **7** 359-371.

Joyard, J., Douce, R. (1977) Site of synthesis of phosphatidic acid and diacylglycerol in spinach chloroplasts. . *Biochimica and Biophysica Acta*. **486** pp. 273-285.

Kennedy, E. (1961) Biosynthesis of complex lipids. *Fed. Proc.* **20** 934-941.

Kiegle, E., Moore, C.A., Haseloff, J., Tester, M.A., Knight, M.R. (2000) Cell-type-specific calcium responses to drought, salt and cold in the *Arabidopsis* root *Plant Journal*. **23** pp. 267-278.

Kroon, J.T.M. (2000) Molecular studies on plant glycerol-3-phosphate acyltransferase. *Thesis*. University of Durham, U.K.

Lacey, D.J., Hills, M.J. (1996) Heterogeneity of the endoplasmic reticulum with respect to lipid synthesis in developing seeds of *Brassica napus* L. *Planta*. **199** pp. 545-551.

Lamb, R.G., Fallon, H.J. (1972) Inhibition of monoacylglycerophosphate formation by chlorophenoxyisobutyrate and –benzalbutyrate. *Journal of Biological Chemistry*. **247** pp. 1281-1287.

Lamppa, G., Jacks, C. (1991) Analysis of 2 linked genes coding for the acyl carrier protein (ACP) from *Arabidopsis thaliana* (columbia). *Plant Molecular Biology*. **16** pp. 469-474.

Lassner, M.W., Levering, C.K., Davies, H.M., Knutzon, D.S. (1995) Lysophosphatidic acid acyltransferase from Meadowfoam mediates insertion of erucic acid at the sn-2 position of triacylglycerol in transgenic rapeseed oil. *Plant physiology*. **109** pp. 1389-1394.

Lea, P.J., Leegood, R.C. (Editors) (1993) In Plant Biochemistry and Molecular Biology, page **30**.

Leonard, J.M., Knapp, S.J., Slabaugh, M.B. (1998) A cuphea beta-ketoacyl-ACP synthase shifts the synthesis of fatty acids towards shorter chains in *Arabidopsis* seeds expressing cuphea FatB thioesterases. *Plant Journal*. **13** pp. 621-628.

Lewin, T.M., Wang, P., Coleman, R.A. (1999) Analysis of amino acid motifs diagnostic for the sn-glycerol-3-phosphate acyltransferase reaction. *Biochemistry*. **38** pp. 5764-5771.

Lightner, V.A., Larson, T.J., TAILLEUR, P., KANTOR, G.D., RAETZ, C.R., BELL, R.M., MODRICH, P. (1980) Membrane phospholipid synthesis in *Escherichia coli*. Cloning of a structural gene (plsB) of the sn-glycerol-3-phosphate acyltransferase. *Journal of Biological Chemistry*. **255** pp. 9413-9420.

Liu, J.M., Chen, S.N., Yan, B., Huang, X.Q., Yang, M.Z. (1999) Cloning and sequencing of the cDNA (accession no. AF090734) coding for glycerol-3-phosphate acyltransferase from *Vicia faba*. *Plant Physiology*. **120** p. 934.



Machida, Y., Bergeron, R., Flick, P., Bloch, K. (1973) Effects of cyclodextrins on fatty acid synthesis. . *Journal of Biological Chemistry*. **248** pp. 6246-6247.

Maisonneuve, S., Bessoule, J.J., Lessire, R., Delseny, M., Roscoe, T.J. (2000) Mutagenesis of a plastidial lysophosphatidic acid acyltransferase. *Biochemical Society Transactions*. **28** pp. 961-964.

Manaf, A.M., Harwood, J.L. (2000) Purification and characterisation of acyl-CoA: glycerol-3-phosphate acyltransferase from oil palm (*Elaeis guineensis*) tissues. *Planta*. **210** pp. 318-328.

Mancha, M. and Stymne, S. (1997) Remodelling of triacylglycerols in microsomal preparations from developing castor bean (*Ricinus communis* L) endosperm *Planta* **203** pp. 51-57.

McKeon, T.A., Stumpf, P.K. (1982) Purification of the steroyl acyl carrier protein desaturase and the acyl-acyl carrier protein thioesterases from maturing seeds of safflower. *Journal of Biological Chemistry*. **257** pp. 2141-2147.

Mikolajczyk, S., Brody, S. (1990) *De novo* fatty-acid synthesis mediated by acyl-carrier protein in *Neurospora crassa* mitochondria. *European Journal of Biochemistry*. **187** pp. 431-437.

Millar, A.A., Kunst, L. (1997) Very long chain fatty acid biosynthesis is controlled through the expression and specificity of the condensing enzyme. *Plant Journal*. **12** pp. 121-131.

Mishra, S., Kamisaka, Y. (2001) Purification and characterisation of thiol-reagent-sensitive glycerol-3-phosphate acyltransferase from the membrane fraction of an oleaginous fungus. *Biochemical Journal*. **355** pp. 315-322.

Monroy, A.F., Sangwan, V., Dhindsa, R.S. (1998) Low temperature signal transduction during cold acclimation: protein phosphates 2A as an easy target for cold-inactivation. *Plant Journal*. **13** pp. 653-660.

Murata, N. (1983) Molecular species composition of phosphatidylglycerols from chilling-sensitive and chilling-resistant plants. *Plant Cell Physiology*. **24** pp. 81-86.

Murata, N., Ishizaki-Nishizawa, O., Higashi, S., Hayashi, H., Tasaka, Y., Nishida, I. (1992) genetically engineered alteration in the chilling sensitivity of plants. *Nature*. **356** pp. 710-713.

Murata, N., Sato, N., Takahashi N., Hamazaki, Y. (1982) Compositions and positional distributions of fatty acids in phospholipids from leaves of chilling-sensitive and chilling-resistant plants. *Plant and Cell Physiology*. **23** pp. 1071-1079.

Murata, N., Tasaka, Y. (1997) Glycerol-3-phosphate acyltransferase in plants. *Biochimica et Biophysica Acta*. **1348** pp. 10-16.

Murphy, D.J. (1994) Biogenesis, function and biotechnology of plant storage lipids.

*Progress in Lipid Research*. **33** pp. 71-85.

Murphy, D.J., Cummins, I. (1989) Biosynthesis of seed storage products during embryogenesis in rapeseed, *Brassica napus*. *Journal of Plant Physiology*. **135** pp. 63-69.

Napier, J.A., Michaelson, L.V. (2001) Towards the production of pharmaceutical fatty acids in transgenic plants. *Journal of the Science of Food and Agriculture*. **81** pp. 883-888.

Napier, J.A., Michaelson, L.V., Stobart, A.K. (1999) Plant desaturases: harvesting the fat of the land. *Current Opinion in Plant Biology*. **2** pp. 123-127.

Napier, J.A., Stobart, A.K., Shrewry, P.R. (1996) The structure and biosynthesis of plant oil bodies: the role of the ER membrane and the oleosin class of proteins. *Plant Molecular Biology*. **31** pp. 945-956.

Nishida, I., Frentzen, M., Ishizaki, O., Murata, N. (1987) Purification of isometric forms of acyl-[acyl-carrier-proteins]:glycerol-3-phosphate acyltransferase from greening squash cotyledons. *Plant Cell Physiology*. **28** pp. 1071-1079.

Nishida, I., Murata, N. (1996) Chilling sensitivity in plants and cyanobacteria: The crucial contribution of membrane lipids. *Annual Review of Plant Physiology and Plant Molecular Biology*. **47** pp. 541-568.

Nishida, I., Sugiura, M., Enju, A., Nakamura, M. (2000) A second gene for acyl-(acyl-carrier protein): glycerol-3-phosphate acyltransferase in squash, *Cucurbita moschata* cv, shirogizuka, codes for an oleate-selective isozyme: Molecular cloning and purification studies. *Plant and Cell Physiology*. **41** pp. 1381-1391.

Nishida, I., Tasaka, Y., Shiraishi, H., Murata, N. (1993) The gene and the RNA for the precursor to the plastid-located glycerol-3-phosphate of *Arabidopsis thaliana*. *Plant Molecular biology*. **21** pp. 267-277.

Ohlrogge, J.B., Jaworski, J.G. (1997) Regulation of fatty acid synthesis. *Annual Review of Plant Physiology and Plant Molecular Biology*. **48** pp. 109-136.

Page, R.A., Okada, S., Harwood, J.L. (1994) Acetyl-CoA carboxylase exhibits strong flux control over lipid-synthesis in plants. *Biochimica et Biophysica Acta*. **1210** pp. 369-372.

Perry, H.J., Bligny, R., Gout, E., Harwood, J.L. (1999) Changes in Kennedy pathway intermediates associated with increased triacylglycerol synthesis in oil-seed rape. *Phytochemistry*. **52** pp. 799-804.

Plieth, C., Hansen, U.P., Knight, H., Knight, M.R. (1999) Temperature sensing by plants: the primary characteristics of signal perception and calcium response. *Plant Journal*. **18** pp. 491-497.

Pollard, M.R., Anderson, L., Fan, C., Hawkins, D.J., Davies, H.M. (1991) A specific acyl-ACP thioesterase implicated in medium-chain fatty acid production in immature

cotyledons of *Umbellularia californica*. *Archives of Biochemistry and Biophysics*. **284** pp. 306-312.

Post-Beittenmiller, D., Hlousekradojcic, A., Ohlrogge, J.B. (1989) DNA-sequence of a genomic clone encoding an arabidopsis acyl carrier protein (ACP). *Nucleic Acids Research*. **17** p. 1777.

Post-Beittenmiller, D., Jaworski, J.G., Ohlrogge, J.B. (1990) *In vivo* pools of free and acylated carrier proteins in Spinach. *Journal of Biological Chemistry*. **266** pp. 1858-1865.

Post-Beittenmiller, D., Jaworski, J.G., Ohlrogge, J.B. (1991) *In vivo* pools of free and acylated acyl carrier proteins in spinach. *Journal of Biological Chemistry*. **266** pp. 1858-1865.

Rajasekharan, R., Mariani, R.C., Shockey, J.M., Kemp, J.D. (1993) Photoaffinity labelling of Acyl-CoA oxidase with 12-Azidooleoyl-CoA and 12-[(4-Azidosalicyl)amino]dodecanoyl-CoA. *Biochemistry*. **32** pp. 12386-12386.

Ray, T. K. and Cronan, J. E. Jr. (1976) Activation of long chain fatty acids with acyl carrier protein: Demonstration of a new enzyme, acyl–acyl carrier protein synthetase in *Escherichia coli*. *Proc. Natl. Acad. Sci. USA* **73** pp. 4374–4378).

Rock, C.O., Cronan, J.E. Jr. (1979) Solubilisation, purification and salt activation of acyl-acyl carrier protein synthetase from *Escherichia coli*. *Journal of Biological Chemistry*. **254** pp. 7116-7122.

Rock, C.O., Garwin, J.L. (1979) Preparative enzymatic synthesis and hydrophobic chromatography of acyl-acyl carrier protein. *Journal of Biological Chemistry*. **254** pp. 7123-7128.

Rock, C.O., Garwin, J.L., Cronan, J.E. Jnr. (1981) Preparative enzymatic synthesis of acyl-acyl carrier protein. *Methods in Enzymology*. **72** pp. 397-403.

Roughan, P.G. (1997) Stromal concentrations of coenzyme A and its esters are insufficient to account for rates of chloroplast fatty acid synthesis: evidence for substrate channelling within the chloroplast fatty acid synthase. *Biochemical Journal*. **327** pp. 267-273.

Roughan, P.G., Ohlrogge, J.B. (1996) Evidence that isolated chloroplasts contain an integrated lipid-synthesising assembly that channels acetate into long-chain fatty acids. *Plant Physiology*. **110** pp. 1239-1247.

Roughan, P.G., Slack, C.R. (1982) Cellular organisation of glycerolipid metabolism. *Annual Review of Plant Physiology*. **33** pp. 97-132.

Roughan, P.G., Slack, R. (1984) Glycerolipid synthesis in leaves. *TIBS*. pp.383-387.

Russell, G.C., Guest, J.R. (1991) Site-directed mutagenesis of the lipoate acetyltransferase of *Escherichia coli*. *Proceedings of the Royal Society of London series B – Biological sciences*. **243** pp. 155-160.

Safford, R., Windust, J.H.C., Lucas, C., Desilva, J., James, C.M., Hellyer, A., Smith, C.G., Slabas, A.R., Hughes, S.G. (1988) Plastid-localised seed acyl-carrier protein of *Brassica napus* is encoded by a distinct nuclear multigene family. *European Journal of Biochemistry*. **174** pp. 287-295.

Sambrook, J., Fritsch, E.F., Maniatis, T. (1989) Molecular cloning – A laboratory manual. 2<sup>nd</sup> Edition. *Cold Spring Harbour Laboratory Press*.

Sarimento, C., Ross, J.H.E., Murphy, D.J. (1997) Expression and subcellular targeting of a soybean oleosin in transgenic rapeseed. Implications for the mechanism of oil-body formation in seeds. *Plant Journal*. **11** pp. 783-796.

Sauer, A., Heise, K.P. (1983) The influence of the glycerol-3-phosphate level in the stroma space on lipid synthesis of intact chloroplasts. *Z. Naturforsch.* **38c** pp. 399-404.

Sauer, A., Heise, K.P. (1984) Control fatty acid incorporation into chloroplast lipids in vitro. *Z. Naturforsch.* **39c** pp. 593-599.

Scherer, D.E., Knauf, V.C. (1987) Isolation of a cDNA clone for the acyl carrier protein-I of spinach. *Plant Molecular Biology*. **9** pp. 127-134.

Shanklin, J. (2000) Overexpression and purification of the *Escherichia coli* inner membrane enzyme acyl-acyl carrier protein synthase in active form. *Protein Expression and Purification*. **18** pp. 355-360.

Shin, D.H., Paulauskis, J.D., Moustaid, N., Sul, H.S. (1991) Transcriptional regulation of P90 with sequence homology to *E.coli* glycerol-3-phosphate acyltransferase. *Journal of Biological Chemistry*. **266** pp. 23834-23839.

Slabas, A.R., Fawcett, T. (1992) The biochemistry and molecular biology of plant lipid biosynthesis. *Plant Molecular Biology*. **19** pp. 169-191.

Soll, J, Roughan, G. (1982) Acyl-acyl carrier protein pool sizes during steady-state fatty acid synthesis by isolated spinach chloroplasts. *FEBS Letters*. **146** pp. 189-192.

Somerville, C., Browse, J. (1991) Plant lipids – Metabolism, mutants and membranes. *Science*. **252** pp. 80-87.

Somerville, C., Browse, J. (1996) Dissecting desaturation: plants prove advantageous. *Trends in Cell Biology*. **6** pp. 148-153.

Stobart, A.K., Stymne, S., Shrewry, P.R., Napier, J. (1998) In J.L. Harwood, Plant lipid biosynthesis: Fundamentals and agricultural applications. pp. 223-245. Cambridge University Press.

Stumpf, P.K. (1994) A retrospective view of plant lipid research. *Progress in Lipid Research*. **33** pp. 1-8.

Suh, M.C., Schultz, D.J., Ohlrogge, J.B. (1999) Isoforms of acyl carrier protein involved in seed-specific fatty acid synthesis. *Plant Journal*. **17** pp. 679-688.



Taylor, D.C., Barton, D.L., Giblin, E.M., MacKenzie, S.L., van den Berg, C.G.J., McVetty, P.B.E. (1995) Microsomal lysophosphatidic acid acyltransferase from a *Brassica oleracea* cultivar incorporates erucic acid into the sn-2 position of seed triacylglycerols. *Plant physiology*. **109** pp. 409-420.

Theimer, R.R., Wanner, G., Anding, G. (1978) Isolation and biochemical properties of two types of microbody from *Neurospora crassa* cells. *Cytobiologie*. **18** pp. 132-144.

Thomashow, M.F. (1999) Plant cold tolerance: freezing tolerance genes and regulatory mechanisms. *Annual Review of Plant Physiology and Plant Molecular Biology*. **50** pp. 571-599.

Thoyts, P.J.E., Millichip, M.I., Stobart, A.K., Griffiths, W.T., Shewry, P.R., Napier, J.A. (1995) Expression and in vitro targeting of a sunflower oleosin. *Plant Molecular Biology*. **29** pp. 403-410.

Tillman, T.S., Bell, R.M. (1986) Mutants of *Saccharomyces cerevisiae* defective in sn-glycerol-3-phosphate acyltransferase. *Journal of Biological Chemistry*. **261** pp. 9144-9146.

Turnbull, A.P., Rafferty, J.B., Sedelnikova, S.E., Slabas, A.R., Schierer, T.P., Kroon, J.T.M., Nishida, I., Murata, N., Simon, J.W., Rice, D.W. (2002a) Crystallization and preliminary X-ray analysis of the glycerol-3-phosphate 1-acyltransferase from squash (*Cucurbita moschata*). *Acta Crystallographica*. **57** pp. 451-453.

Turnbull, A.P., Rafferty, J.B., Sedelnikova, S.E., Slabas, A.R., Schierer, T.P., Kroon, J.T.M., Simon, J.W., Fawcett, T., Nishida, I., Murata, N., Rice, D.W. (2002b) Analysis of the structure, substrate specificity and mechanism of squash glycerol-3-phosphate 1-acyltransferase. *Structure*. **9** pp. 347-353.

Turnham, E., Northcote, D.H. (1982) The use of acetyl-CoA carboxylase activity and changes in wall composition as measures of embryogenesis in tissue cultures of oil palm (*Eleis guineensis*). *Biochemical Journal*. **208** pp. 323-332.

Turnham, E., Northcote, D.H. (1983) Changes in the activity of acetyl-CoA carboxylase during rapeseed formation. *Biochemical Journal*. **212** pp. 223-229.

Tzen, J.T.C., Cao, Y.Z., Laurent, P., Ratnayake, C., Huang A.H.C. (1993) Lipids, proteins and structure of seed oil bodies from diverse species. *Plant Physiology*. **101** pp. 267-276.

Vick, B., Beavers, H. (1977) Phosphatidic acid synthesis in castor bean endosperm. *Plant Physiology*. **59** pp. 459-469.

Vogel, G., Browse, J. (1996) Cholinephosphotransferase and diacylglycerol acyltransferase – substrate specificities at a key branch point in seed lipid metabolism. *Plant Physiology*. **110** pp. 923-931.

Volpe, J.J., Vagelos, P.R. (1973) Saturated fatty acid biosynthesis and its regulation. *Annual Review of Biochemistry*. **42** pp. 21-60.

Wallis, J.G., Browse, J. (2002) Mutants of *Arabidopsis* reveal many roles for membrane lipids. *Progress in Lipid Research*. **41** pp. 254-278.

Weber, S., Wolter, F.P., Buck, F., Frentzen, M., Heinz, E. (1991) Purification and cDNA sequencing of an oleate-selective acyl-ACP:sn-glycerol-3-phosphate acyltransferase from pea chloroplasts. *Plant Molecular Biology*. **17** pp. 1067-1076.

Wood, H.G., Barden, R.E. (1977) Biotin enzymes. *Annual Review of Biochemistry*. **46** pp. 385-413.

Xin, Z.G., Browse, J. (1998) *eskimo* 1 mutants of *Arabidopsis* are constitutively freezing tolerant. *Proceedings of the National Academy of Sciences of the United States of America*. **95** pp. 7799-7804.

Xin, Z.G., Browse, J. (2000) Cold comfort farm: the acclimation of plants to freezing temperatures. *Plant Cell Environment*. **23** pp. 893-902.

Yokoi, S., Higashi, S., Kishitani, S., Murata, N., Toriyama, K. (1998). Introduction of the cDNA for *Arabidopsis* glycerol-3phosphate acyltransferase (GPAT) confers unsaturation of fatty acids and chilling tolerance of photosynthesis on rice. *Molecular Breeding*. **4** pp. 269-275.

Zou, J.T., Katavic, V., Giblin, E.M., Barton, D.L., MacKenzie, S.L., Keller, W.A., Hu, X., Taylor, D.C. (1997) Modification of seed oil content and acyl composition in the brassicaceae by expression of a yeast sn-2 acyltransferase gene. *Plant Cell*. **9** pp. 909-923.

